ANNUAL REPORT

NOVEMBER 1993

Innovative Processing of Composites for Ultra-High Temperature Applications

by

Reza Abbaschian
Department of Materials Science and Engineering
University of Florida
Gainesville, Florida

Sponsored by: The Advanced Research Projects Agency

Monitored by: The Office of Naval Research

ARPA Grant No. N00014-91-J-4075

BOOK I OF III

Executive Summary

The overall objective of this program was to provide a fundamental understanding of the processing science and technology necessary to fabricate ceramic-matrix, intermetallic-matrix, and metal-matrix composites with superior mechanical properties in high temperature and oxidizing environments. The composites are intended for use as structural materials for advanced aerospace applications at temperatures exceeding 1200°C (2200°F).

In order to accomplish the program objective, interactive research groups were established in three key area of (a) Fiber Fabrication, (b) Coatings and Infiltration, and (c) Composite Fabrication. The objective of the fiber fabrication group was to develop new fibers which have superior strength and toughness at high temperatures and in oxidizing environments. The research effort focused on the development of two types of fibers: (1) glass-free mullite-based fibers, and (2) oxygen-free silicon carbide fibers. The coatings program had two primary objectives: (1) to control the characteristics of matrix/reinforcing phase interfaces (e.g., to control chemical reactions and bonding at a matrix/fiber interface) and (2) to develop coatings that will improve the oxidation resistance of metal-matrix and intermetallic-matrix composites. Coatings methods utilized included chemical vapor deposition, sol-gel processing, and solution coating with polymeric precursors to ceramics.

The composite fabrication group investigated various methods to incorporate reinforcing phases (i.e., fibers, whiskers, and particulates) into ceramic-, metal-, and intermetallic-matrices. Processing methods investigated included colloidal processing, chemical vapor infiltration, reactive hot-compaction and *in situ* coating, and microwave sintering. The objectives were not only to utilize innovative processing techniques, but also to develop an improved scientific understanding of processing-microstructure relationships in composites fabrication.

This annual report consists of seven sections compiled in three books as described below:

Book I

Section 1 Processing and Properties of Silicon Carbide Fibers
Principal Investigators: C.D. Batich
M.D. Sacks

Section 2 Processing of Mullite Composite Fibers
Principal Investigators: A.B. Brennan
J.H. Simmons

Section 3 Chemical Vapor Deposition (CVD) and Chemical Vapor Infiltration (CVI)
Principal Investigator: T. Anderson

Book II

Section 1 Processing and Properties of Intermetallic Matrix Composites
Principal Investigator: R. Abbaschian

Section 2 Mechanical Alloying of $MoSi_2$
Principal Investigator: M.J. Kaufman

Book III

Section 1 Processing of Ceramic Matrix Composites
Principal Investigator: M.D. Sacks

Section 2 Processing of $BaO\text{-}Al_2O_3\text{-}2SiO_2$ Fibers.
Principal Investigator: D.E. Clark

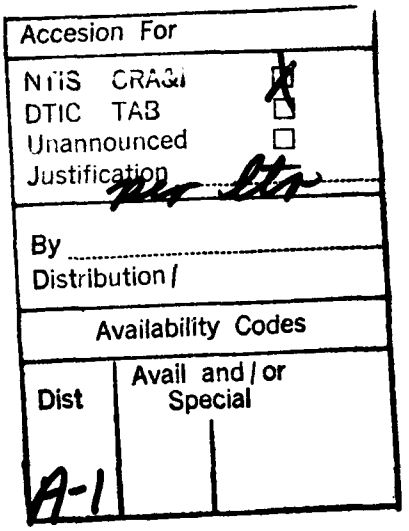

BOOK I

Section 1

Processing and Properties

of

Silicon Carbide Fibers

Principal Investigators: C.D. Batich
M.D. Sacks

Processing and Properties of Silicon Carbide Fibers

Principal Investigators: C.D. Batich
M.D. Sacks

Objectives

The two overall objectives of this program are as stated last year and remain the same:

(1) To develop and characterize high performance, SiC fibers (designated "UF fibers") which have improved thermomechanical properties compared to commercially available SiC fibers and which are suitable for use in ceramic-matrix composites for high temperature ($>1300°C$) structural applications.

(2) To establish related R&D programs with industrial partners which will result in (i) process scale-up to provide sufficient quantities of high performance, multifilament fiber tows and weaves to fully evaluate fiber properties and (ii) to allow the fabrication of composite test panels and (iii) commercialization of UF SiC fibers in ≤ 5 years.

Research Summary

The properties and preparation of the basic fiber have been discussed in several earlier reports and publications. Our most detailed and broad paper on the fibers has been accepted for publication this year in "Composites Science and Technology." This paper discusses background, unique properties methods of preparation, and has an extensive bibliography. A copy of the preprint is attached. In addition, the basic patent has now been issued on the process (US #5,171,722,December 15, 1992). A copy is attached. A related divisional patent application including additional claims has been allowed (U.S. Patent Application Serial No. 07/886,805) and a final divisional application is under review. An additional application has been prepared covering new fibers with substantially different additives and is being modified prior to submission. Objective (1) has clearly been realized to a large extent and efforts to extend that work continue.

We have found two avenues to reach objective (2) - a relationship with industrial partners. The approaches emphasize highest achievable modulus and separately highest achievable temperature stability under the HSCT/EPM and IHPTET programs respectively. Both of these phase I projects are in progress and initial results are very promising.

Research during this last year has included characterization of our existing UF fiber process and product as well as exploring novel variations from this robust and consequently highly

adaptable process.

Fractographic analysis (with Dr. Jack Mecholsky) has shown a clear relationship between mirror radius and tensile strength as expected. The data support a room temperature fractography very similar to Nicalon® fibers. Essentially all flaws occur on the surface suggesting that process improvements will yield stronger fibers. Scale-up is expected to lower the number of these flaws.

Stoichiometry changes have been accomplished by changes in the spinning dope. We have been able to improve high temperature stability significantly but only modest changes in modulus have so far been achieved.

12/16/92

To be published in Composites Science and Technology

POLYMER-DERIVED SILICON CARBIDE FIBERS WITH LOW OXYGEN CONTENT AND IMPROVED THERMOMECHANICAL STABILITY

William Toreki, Christopher D. Batich, Michael D. Sacks, Mohamed Saleem, Guang J. Choi, and Augusto A. Morrone, Department of Materials Science and Engineering, University of Florida, Gainesville, FL 32611

ABSTRACT

Continuous silicon carbide fibers ("UF fibers") with low oxygen content (~1-2 wt%) were prepared in a range of diameters (~8-50 μm) by dry spinning of organosilicon polymer solutions and subsequent pyrolysis of the polymer fibers. Room temperature mechanical properties were similar to commercially-available Nicalon™ fibers, as average tensile strengths ≈3 GPa were obtained for some batches with fiber diameters in the range of ~10 μm. Furthermore, UF fibers showed significantly better thermomechanical stability compared to Nicalon™, as indicated by lower weight losses, lower specific surface areas, and improved strength retention after heat treatment at temperatures up to 1700°C. The structure and composition of UF fibers were also characterized using scanning electron microscopy, transmission electron microscopy, X-ray diffraction, Auger depth profiling analysis, neutron activation analysis, and atomic absorption.

Keywords: Fibers, Silicon Carbide, Polymer, Polycarbosilane, Thermomechanical Properties

INTRODUCTION

There has been considerable interest in fiber-reinforced ceramic-matrix composites (CMC's) for high temperature structural applications since Yajima et al.[1,2] first developed continuous silicon carbide fibers with fine diameter and high tensile strength. CMC's with high strength and high fracture toughness at elevated temperatures have been developed by combining Nicalon™ SiC fibers (Nippon Carbon Co., Tokyo, Japan) with a variety of matrix materials, including glasses, glass-ceramics, and crystalline ceramics.[3-7] Despite the impressive properties achieved, there is still a need for SiC fibers with improved thermomechanical properties. The mechanical properties of Nicalon™ fibers often deteriorate at (or below) the temperatures required for processing CMC's, as well as below the maximum useful temperatures for many of the ceramic matrix materials used in structural applications. Thermal degradation of Nicalon™ fibers is highly dependent upon atmosphere, but significant weight losses can occur at temperatures as low as 1200°C and decreases in tensile strength can occur at temperatures below 1000°C.[7-15] Studies have shown that these effects are associated with the presence of oxygen (~8-15 wt%) and excess carbon in the fibers. Carbothermal reduction reactions (i.e., between carbon and siliceous material) lead to the evolution of volatile species (primarily CO and SiO) which results in large weight losses, formation of porosity, and the growth of SiC grains and other strength-degrading flaws in the fiber microstructure.[7-15]

Nicalon™ fibers are prepared by melt spinning of a low-molecular-weight organosilicon polymer (i.e., polycarbosilane). As-spun fibers are then heated at low temperature (~150-200°C) in air in order to cure (cross-link) the polymer. This treatment prevents the fibers from re-melting during the subsequent pyrolysis step (in which the polymer is converted at higher temperatures to a SiC-rich ceramic). However, curing in air also leads to the high oxygen content in Nicalon fibers. To produce fibers with improved thermomechanical stability, alternative processes for fabricating SiC fibers with minimal oxygen "contamination" have been investigated.[16-22]

Frechette et al.[16] produced stoichiometric polycrystalline SiC fibers with low oxygen content by using a process which is a hybrid of polymer melt spinning and ceramic powder/liquid extrusion. SiC particles and molten organic polymer were mixed, extruded through a spinneret, and wound on a rotating drum to form "green" fibers. This was followed

by "binder burnout" (i.e., pyrolysis of the organic polymer) and subsequent sintering of the SiC "powder compact" at high temperatures (>1900°C). The sintered fibers had high relative density (i.e., minimal residual porosity) and an ~1-2 μm average grain size. The fibers had average tensile strengths at room temperature in the range ~1.0-1.2 GPa and the strength level was maintained after heat treatment at 1550°C. A related process for producing polycrystalline SiC fibers with low oxygen content was developed by Silverman et al.[17] Fibers were produced using concentrated SiC particle slurries prepared with xylene as the liquid media and polycarbosilane (PC) as a binder. Mixtures were extruded through a spinneret and subsequently heat treated to pyrolyze the PC and to sinter (at 2000°C) the fibers to high relative density (>99%). The fiber tensile strength and strength retention after heat treatment were similar to that reported by Frechette et al.[16] The average elastic modulus was ~380 GPa, i.e., only slightly below the value for bulk polycrystalline SiC samples.

Despite the excellent thermal stability, there are several limitations associated with the powder processing routes utilized by Frechette et al. and Silverman et al. to produce SiC fibers. First, since the starting particle sizes for the SiC powders are relatively large (i.e., average sizes on the order of ~0.5 μm), the grain sizes in the sintered fibers are also relatively large (i.e., compared to those observed in polymer-derived fibers). This, in turn, limits the maximum tensile strength that can be achieved. Second, powder processing routes currently have a lower limit of ~25 μm for the fiber diameter,[16,17] i.e., ~10 μm larger than Nicalon.™ The larger fiber diameter and lower strength of the fibers (e.g., compared to Nicalon™) limit the flexibility and, hence, weavability of the fibers. Consequently, there is still considerable interest in using organosilicon polymers as precursors for the development of SiC fibers with low oxygen content.[18-22]

Lipowitz et al.[18,19] developed stoichiometric, polycrystalline SiC fibers using polycarbosilane and methylpolydisilylazane polymers. Fibers were melt spun, cross-linked, and heat treated at temperatures above 1600°C in argon in order to react excess carbon and oxygen in the fibers. As noted earlier, PC-derived fibers normally become very weak and develop a porous, large-grained microstructure during this type of heat treatment. However, Lipowitz et al. incorporated "sintering additives" (unspecified chemistry) in the polymer which allowed fibers to retain their integrity (and fine grain size) during the carbothermal reduction reactions

discussed earlier. The resulting fibers had fine diameter (8-10 μm), high relative density, small average grain sizes (in the range ~0.03-0.5 μm, depending on the Si:C ratio), low oxygen content (<0.1%), high tensile strength (up to 2.6 GPa), high elastic modulus (up to 420 GPa), and good strength retention after high temperature (1800°C) heat treatment in argon. The key limitation in this process was apparently a difficulty in producing continuous fibers. Although details were not provided, the authors indicated that further developments in rapid cross-linking technology were needed, as well as improvements in the fiber spinnability and green strength.

Takeda et al.[20,21] have reported the development of low-oxygen-content (0.4 wt%), fine diameter (~15 μm) SiC fibers. These fibers are prepared in a similar manner as Nicalon™ (i.e., by melt spinning of PC), except that cross-linking is accomplished by electron beam irradiation (i.e., instead of using oxidation). The high temperature stability of the fibers increased dramatically as the oxygen content of the fibers decreased. Fibers with 0.4 wt% oxygen retained high strength (~2.4 GPa) and high modulus (~250 GPa) after heat treatment at 1500°C in argon. The main drawback of this method is that cross-linking of the polymer by electron beam irradiation is a slow and costly processing step.

The present authors have also fabricated PC-derived SiC fibers (designated "UF fibers") with low oxygen content (~2 wt%) and good thermal stability.[22] In contrast to the melt spinning techniques used by Takeda et al. and Lipowitz et al., UF fibers are prepared using a solution-based fiber spinning process. In this paper, more detailed information is provided on the processing, structure, and properties of these fibers.

EXPERIMENTAL METHODS

Synthesis and Processing

Polycarbosilane (PC) was synthesized by pressure pyrolysis of polydimethylsilane (Huls, Bristol, PA) in a stainless steel autoclave (model 4651, Parr Instrument Co., Moline, IL) under a nitrogen atmosphere. PC's with controlled average molecular weight (in the range ~1,000-12,000*) were produced by varying the pyrolysis temperature and time. The PC was purified

* Molecular weight distributions were determined by size exclusion chromatography with UV detection at 254 nm. Measurements were carried out using 500 and 5000 Å Phenogel™ columns (Phenomenex, Torrance, CA), polystyrene standards, and THF as the solvent.

by dissolving the reaction product in chloroform, filtering the solutions, and subsequently precipitating the PC in an excess of acetone. The product was vacuum dried at ~60°C and stored under vacuum in a desiccator.

Control over molecular weight (MW) was a key requirement for successfully producing PC fibers by solution processing. PC's with low MW (e.g., <5,000) were highly soluble in common organic solvents (e.g., toluene, hexane, chloroform, etc.), but useful fibers could not be produced because the polymer melted during subsequent heat treatment. (Furthermore, there is low ceramic yield after pyrolysis of low-molecular-weight PC's.) In contrast, high-molecular-weight PC's (e.g., >10,000) did not melt during heat treatment, but the polymer solubility was too low to prepare useful fiber spinning solutions. Therefore, fibers were spun using intermediate-molecular-weight PC's (~5,000-10,000) which not only enabled preparation of highly concentrated solutions (e.g., typically ~50 wt%), but also allowed fibers to be pyrolyzed without melting. The latter consideration is particularly important because it allows the formation of fibers without introducing an oxidative curing step. Thus, any oxygen present in the pyrolyzed fibers results from impurities in the starting materials and/or contamination due to exposure to oxygen or water vapor during the various processing steps.

Several additives were found to be effective in improving the spinnability of the PC solutions and the strength of as-spun fibers. These included vinylic polysilazane (MW ≈ 50,000) and polyisobutylene (MW ≈ 50,000). The former polymer was prepared according to procedures described in detail previously,[23] while the latter polymer was commercially available (Vistanex®, Exxon Chemical Co., Houston, TX). The mixed polymer solutions were passed through a 2-4 μm glass frit filter to remove insoluble material (e.g., particulate impurities, polymer "microgel" particles, etc.) Some solutions were also passed through 0.1 or 0.2 μm PTFE filters. After filtration, solutions were concentrated on a rotary evaporator at ~60°C until ~50 wt% solvent remained. Rheological characteristics of the spinning solution were determined using a cone-plate viscometer (Model HBT, Brookfield Engineering Laboratories, Inc., Stoughton, MA).

Fibers were formed at room temperature by extruding the polymer solutions through

stainless steel spinnerets (~70 or ~120 μm diameter orifices) under nitrogen pressure. Three to five filaments were extruded simultaneously in most experiments. Continuous "green" fibers were collected by winding on a rotating drum which was placed approximately 30 cm below the spinneret. A range of fiber diameters were produced by varying the spinneret orifice size, nitrogen pressure, winding speed, and solution viscosity. After fiber spinning, batches (typically a few grams) were cut from the drum (~15-20 cm lengths) and heat treated in a tube furnace to pyrolyze the polymeric fibers to a SiC-containing ceramic. Most of the samples were heated at ~0.5°C/min to 150°C, then ~3.5°C/min to 1000°C, followed by a hold of 1 h at 1000°C. It was determined later that higher heating rates could be used without any adverse effect on fiber properties, so the schedule was changed to ~1°C/min to 150°C and ~7°C/min to 1000°C. The pyrolysis atmosphere was nitrogen, argon, or argon with a small amount of hydrogen (~1-2%). Fibers with controlled diameters in the range of ~8-50 μm were produced after pyrolysis.

Fiber Characterization

Weight loss behavior of green and pyrolyzed fibers was determined by thermal gravimetric analysis, TGA (Model TGA-7, Perkin-Elmer, Norwalk, CT; Model STA-409, Netzsch Co., Exton, PA). Specific surface areas of heat-treated fibers were determined by the BET method using nitrogen or krypton gas adsorption measurements (Model ASAP 2000, Micromeritics, Atlanta, GA). Fibers were also examined by scanning electron microscopy, SEM (Model JSM-6400, JEOL, Tokyo, Japan) and transmission electron microscopy, TEM (Model 200 CX, JEOL).

Elemental compositions of carbosilane polymers and heat-treated fibers were determined by outside analytical laboratories (IRT Corp., San Diego, CA; Radio-Analytical Services, University of Kentucky, Lexington, KY; Galbraith Laboratories Inc., Knoxville, TN) using neutron activation analysis (for oxygen, nitrogen, and silicon), atomic absorption (for silicon), and LECO combustion analysis (for carbon, hydrogen, and nitrogen). Phase analysis of heat-treated fibers was carried out by X-ray diffraction, XRD, (Model APD 3720, Philips Electronic Instruments Co., Mt. Vernon, NY) using Ni-filtered CuKα radiation.

Compositional analyses of individual pyrolyzed fibers were also carried out by scanning Auger microprobe (SAM) analysis (model PHI 660, Perkin Elmer Corp., Eden Prairie, MN). Fibers were mounted horizontally and a 10 kV electron beam (30 nA) was focused on a small area ($<0.01\ \mu m^2$) on the center portion of the fiber surface. A detailed survey spectrum (10 scans) was collected over the entire kinetic energy range (50-2050 eV). The analyzed surface was then etched by sputtering for 6 sec with an Ar^+ ion beam; this was followed by re-analysis of the same fiber area, but only over the spectral regions for C, Si, and O. This process was repeated in rapid sequence (5 scans for each analysis) for an extended period ($\sim$18 min total sputtering time) in order to obtain a depth profile for the fiber elemental composition. The results were corrected for relative atomic sensitivities and displayed as atomic percentage vs. sputtering time. (The sputter rate was adjusted to correspond to approximately 100Å per minute for a tantalum oxide standard.) After depth profiling was completed, a detailed survey spectrum (10 scans) of the fiber interior was collected.

Fiber tensile strengths were determined at room temperature according to ASTM procedure D-3379.[24] Both green and pyrolyzed fibers were tested. In addition, pyrolyzed fibers were tested after additional heat treatments in the range 1200-1700°C (0.5-2.0 h) in argon or argon/1-2% hydrogen atmospheres. Individual fibers were attached to paper tabs using an epoxy adhesive and loaded in tension (0.5 mm/min crosshead speed) until failure using a mechanical testing apparatus (Model 1122, Instron Corp., Canton, MA). The gage length was 25 mm and at least 8 fibers (but usually 10-15) were tested for each batch. To calculate tensile strengths, fiber diameters were determined using an optical microscope equipped with a micrometer in the eyepiece. Rupture strains and elastic modulus values were obtained from the stress-strain data collected during the strength measurements. Modulus values were calculated without any corrections for the compliance of the mechanical testing system.

Fiber tensile strengths were also measured at elevated temperatures at the High Temperature Materials Laboratory at Oak Ridge National Laboratory. Individual fibers with a 178 mm gage length were mounted directly in pneumatic grips. Measurements were made in air at 1400°C.

RESULTS AND DISCUSSION

As noted earlier, successful formation of fibers required both control over the PC molecular weight and the use of spinning aids. In addition, it was necessary to control the polymer/solvent ratio in the spinning solution in order to prepare useful fibers. If the polymer solution had a large excess of solvent, fibers did not maintain their shape after exiting the spinneret and it was not possible to form continuous fibers. With a smaller excess of solvent, continuous fibers were formed but they would stick together on the wind-up drum (i.e., due to insufficient solvent evaporation during the time period between exiting the spinneret and winding on the drum.) In contrast, if polymer solutions were too concentrated (solvent deficient), it was difficult to extrude the solutions through the spinneret (i.e., due to the high viscosity). This tended to produce discontinuous brittle fibers with rough surfaces. In the appropriate range of solvent/polymer concentrations, fibers could be spun continuously for periods up to ~ 20 min. (The primary cause of interruptions in spinning was gas bubbles in the polymer solutions. These bubbles developed mostly from entrainment of gas during preparation and mixing of the polymer solutions, but also possibly from nitrogen introduced during the extrusion of the solutions through the spinneret. In some cases, the continuous spinning time was only limited by the amount of polymer solution contained in the reservoir in the spinneret head.) The spinning solutions showed slightly shear thinning rheological flow behavior with a typical viscosity on the order of 25 Pa • s at a shear rate of 40 s^{-1}. Figure 1 shows typical plots of shear stress vs. shear rate and viscosity vs. shear rate for solutions used in fiber spinning. The measurements were made by first increasing the shear rate from 1 to 40 s^{-1} and then decreasing the shear rate back to 1 s^{-1}. Solutions showed negligible thixotropy under these measuring conditions.

Stress-strain measurements were carried out on green fibers (as-spun) and fibers heated at 400°C for 0.5 h. The green fibers had an average tensile strength of ~ 20 MPa and average rupture strain of ~ 1.0%.* The fibers showed only elastic deformation before failure. In contrast, the 400°C-pyrolyzed fibers exhibited considerable plastic deformation. The average

* These results were obtained on fibers with sufficient handling strength to be tested. However, many fibers failed during preparation for testing, so the reported values may not be representative of the true average mechanical properties.

tensile strength increased to ~45 MPa and the average rupture strain increased to ~4%. Hasegawa et al.[26] observed similar mechanical properties for oxidatively-cured PC-derived fibers (i.e., Nicalon™-type) heated at 400°C for 1 h in nitrogen or in vacuum.

Figure 2 shows TGA results for unpyrolyzed fibers that were heated at a rate of 20°C/min in flowing argon to 950°C. The ceramic yield (~80 wt%) is relatively high, especially compared to yields (~60 wt%) reported for low-molecular-weight PC's (such as used in melt spinning of Nicalon™-type fibers).[25,26] In fact, the ceramic yield for the UF fibers is comparable to values reported for *oxygen-cured* PC fibers.[15,26] The high yield, in combination with the observation that the polymers do not melt during heat treatment, suggest that the intermediate-molecular-weight PC's prepared in this study have significantly greater intramolecular branching and ring structure development compared to low-molecular-weight PC's.

Pyrolyzed fibers (750-1200°C) have a visual appearance similar to Nicalon™ (i.e., black color). SEM observations of a 1000°C-pyrolyzed sample (Fig. 3) show fibers have round cross-sections and relatively smooth surfaces. Fracture surfaces (Fig. 3) have a glassy appearance which reflects the fact that the pyrolyzed fibers consist of weakly crystalline, extremely fine-grained β-SiC and amorphous carbon. Electron diffraction on a 1200°C-pyrolyzed sample shows a ring pattern (Fig. 4A) which corresponds to the three strongest reflections in β-SiC (111, 220, and 311). The TEM bright field image in Figure 4B shows that the crystal domains in this sample are only on the order of a few nanometers. These microstructural features are similar to those observed in Nicalon™ fibers heated at relatively low temperatures ($\leq$1200°C).[8,9,15]

Figure 5 shows a plot of average tensile strength (at room temperature) vs. fiber diameter for various UF fiber batches pyrolyzed at 1000°C in nitrogen. The strength decreases with increasing fiber diameter. (This effect is usually attributed to the increased probability of encountering strength-limiting flaws as the fiber diameter increases.[27] It has also been reported that large-diameter fibers may develop large processing flaws,[27] but this possibility was not investigated for UF fibers.) Figure 5 shows that some UF batches with fiber diameters in the range of ~10 μm had average tensile strengths ≈3 GPa. (Individual fiber strengths exceeding 5 GPa were obtained in a few cases.) Figure 5 also shows tensile strengths for Nicalon™ fibers

(reported by the manufacturer and measured at UF*). Data reported by Yajima et al. on Nicalon™-type fibers is also included.[1,27] It is evident from Fig. 5 that the 1000°C-pyrolyzed UF fibers and Nicalon™ fibers have very similar tensile strengths at room temperature. Some of the scatter in the tensile strengths for UF fibers may be attributed to the fact that experimental conditions were deliberately varied during the development of the process (e.g., polymer molecular weight, spinning solution viscosity, solution filtration procedure, gas pressure and winding speed during fiber fabrication, etc.) The variations in strength may also reflect the difficulty in rigorously controlling processing conditions because of the small batch sizes (i.e., a few grams) used in most experiments.

Figure 6 shows a comparison of TGA data obtained for Nicalon™ fibers and UF fibers. The UF fibers used in this experiment were initially pyrolyzed (from the green state) at 750°C for 1 h in nitrogen. As-received Nicalon fibers were given the same heat treatment prior to the TGA experiment. The weight loss was then monitored (Fig. 6) as the fibers were heated in argon at 10°C/min to 1550°C and then held for 1 hour at temperature. UF fibers lost only ~3 wt% during this treatment, while the Nicalon™ fiber lost ~25 wt%. (The latter value is consistent with the weight loss reported for Nicalon™ in other studies.[11,21]) As discussed earlier, the large weight loss in Nicalon™ is associated with the high oxygen content of the fiber, as siliceous material reacts with excess carbon to form oxygen-containing volatile products (primarily CO and SiO). In contrast, the relatively low weight loss observed for the UF fibers can be attributed to the absence of such reactions due to the low oxygen content (i.e., since fibers were prepared without an oxidative cross-linking step).

The low oxygen content of UF fibers was confirmed by neutron activation analysis (NAA). Table 1 shows that UF fibers have been produced with oxygen contents in the range ~1.1-2.6 wt%, while Nicalon™ fibers have oxygen contents in the range of 10-15 wt%.** (The range of oxygen contents listed in Table 1 for the UF fibers represents analyses on 12 separate batches which were pyrolyzed at 1000°C. Nine of these batches had oxygen contents ≤1.9 wt%.) Other elemental analyses (Table 1) show that UF and Nicalon™ fibers have

---

* Lot No. AP-018001, Ceramic Grade, Nippon Carbon Co., Tokyo, Japan.

** According to the manufacturer (see Table 1), Ceramic Grade (CG) Nicalon™ fibers have ~10 wt% oxygen. In this study, however, the NAA analysis on two lots (AP-018001 and 093) gave oxygen contents of 15 and 13.5 wt%, respectively.

similar Si, N, and H contents. These results indicate that the UF fiber has an excess of carbon, i.e., in comparison to both Nicalon™ fibers and stoichiometric SiC.*

It should be emphasized that the oxygen present in UF fibers is *not* deliberately incorporated (i.e., to effect polymer cross-linking), but results from unintentional contamination during processing. NAA showed that the starting material for polymer synthesis (i.e., polydimethylsilane) contained only ~0.3-0.4 wt% oxygen. However, analysis of several PC batches showed that oxygen contents increased to levels in the range ~0.3-1.3 wt%, presumably due to exposure to ambient air during the synthesis and purification steps and during storage. Oxygen contamination also occurred during fiber spinning and pyrolysis because most fiber batches were (i) spun and wound in the ambient air atmosphere and (ii) pyrolyzed in an ungettered furnace using standard-grade nitrogen or argon (≥99.995% purity, ~5-20 ppm O_2). Due to the large amount of surface area created when fine-diameter fibers are formed, the oxygen contamination picked up during spinning, winding, and pyrolysis is concentrated near the surfaces of the fibers. This was shown by scanning Auger microprobe (SAM) depth profiling analysis on 1000°C-pyrolyzed UF fibers with relatively low overall oxygen content (~1.9 wt% as determined by NAA). Figure 7 shows survey scans obtained from the fiber surface (i.e., before sputtering) and fiber interior (i.e., after sputtering to a depth of approximately 180 nm). The results show that there is a very large oxygen content at the fiber surface (Fig. 7A), while no oxygen signal is observed in the spectrum from the fiber interior (Fig. 7B). The atomic concentration depth profiles of Si, C, and O for this fiber are given in Fig. 8.** It is evident

---

* The carbon content (~42 wt%) listed in Table 1 for UF fibers was determined by difference, i.e., 100% minus the combined concentrations for Si, O, N, and H. Combustion analysis (LECO method) on UF fibers consistently gave lower carbon contents (~37 wt%) than the value listed in Table 1. However, these results were considered unreliable since oxidative combustion of the UF fibers was probably incomplete under the experimental conditions used in the measurements. In contrast, analysis of the carbon content by the combustion method is considered reliable for Nicalon™ because the fibers degrade more rapidly at elevated temperatures. The development of porosity and high specific surface area in heat-treated Nicalon™ fibers (see Figs. 11 and 12) is expected to accelerate the oxidative combustion reaction rate. In fact, the carbon content determined by the LECO method is in good agreement with the value reported by the manufacturer. Furthermore, the concentrations of Si, C, O, N, and H total to ~100% for the Nicalon™ fibers.

** Based on the atomic sensitivities, magnitude of the C and Si signals, and signal-to-noise ratio, it is estimated that the limit of detection for oxygen for the survey scan shown in Fig. 7B is ~1 at%. The apparently high oxygen levels (~3 at%) in the fiber interior in Fig. 8 are attributed to higher background noise (i.e., lower oxygen signal-to-noise ratios), as data was collected for shorter scanning times compared to the survey scan. Thus, the oxygen levels in Fig. 8 should not be taken as precise quantitative measurements.

that the oxygen content is significantly higher in the outer several hundred angstroms of the fiber.

At high levels of surface oxygen contamination, UF fibers undergo the same type of carbothermal reduction reactions observed in Nicalon,™ i.e., reactions occur between excess carbon and siliceous (Si-O containing) material near the fiber surface. Figure 9 shows SEM micrographs of an oxygen-contaminated UF fiber sample which was initially pyrolyzed in a nitrogen atmosphere (ungettered furnace) to 1000°C and subsequently heat treated to 1500°C in argon. Growth of some large grains and roughening of the surface is evident. This type of degradation can be avoided by exercising greater control over the spinning and pyrolysis atmospheres so that less exposure to oxygen and water vapor occurs during processing. For example, in order to lower the oxygen partial pressure during pyrolysis, heat treatment was carried out in an argon/1-2% hydrogen atmosphere in some experiments. Figure 10 shows SEM micrographs of a sample pyrolyzed to 1200°C (for 1 h) in argon/1-2% hydrogen and subsequently heated to 1600°C (for 1 h) in argon. The fibers show no evidence of degradation reactions, as their appearance is similar to the 1000°C-pyrolyzed sample shown in Fig. 3. This can be contrasted to the appearance of Nicalon™ fibers which degrade extensively after heat treatment at 1600°C in argon (Fig. 11).

Even in samples with high levels of oxygen contamination, degradation of UF fibers is confined to a region near the surface (i.e., the region with more than a few percent oxygen). This was evident from SEM observations of the fiber interior (e.g., see Fig. 9B). It was also illustrated using gas adsorption surface area measurements. When degradation reactions occur (and volatile reaction products are eliminated), the fibers develop porosity and the specific surface area increases. If the degradation is limited to a surface region, only moderate increases in specific surface area are observed. Figure 12 shows plots of specific surface area as a function of heat treatment temperature for Nicalon™ and UF fibers. Nicalon™ fibers show a sharp increase in specific surface area above 1200°C, reaching ~25 m^2/g at 1600°C. This is consistent with the microstructural observations shown in Fig. 11 and the large weight loss observed by TGA (Fig.6). In contrast, UF fibers show more gradual increases in specific surface area. For a fiber batch (UF-94) with high oxygen contamination at the surface, the specific surface area increased from ~0.2 m^2/g after pyrolysis at 1000°C in nitrogen to ~2.5

m^2 after subsequent heat treatment at 1600°C in argon. However, a fiber batch (UF-127) with lower surface oxygen contamination shows almost no change in specific surface area during heat treatment, i.e., the values were ~0.5 m^2/g after pyrolysis in argon/1-2% hydrogen at 1000°C and ~0.8 m^2/g after further heat treatment in argon at 1600°C.*

Based on the TGA (Fig. 6), SEM (Figs. 9-11), and specific surface area (Fig. 12) results, it is not surprising that UF fibers showed superior thermomechanical properties compared to Nicalon™ fibers. Figure 13 shows average tensile strength values for UF and Nicalon™ fibers that were heat treated in the range 1000-1700°C in an argon atmosphere.** The data labeled "UF-80" were collected from a single lot of fibers. The results are considered representative of some of the first UF fiber batches that were prepared with low overall oxygen content (~2 wt%), but *without* taking steps to control surface oxygen contamination. In comparison with Nicalon™, UF-80 fibers show considerably higher strengths at heat treatment temperatures above 1300°C. For example, after 1.0 h at 1400°C, UF-80 fibers have an average tensile strength of ~1.2 GPa compared to only ~0.3 GPa for Nicalon™.*** Furthermore, the UF-80 fibers retained substantial strength (~0.9 GPa) after heat treatment at 1700°C (1.0 h), while the Nicalon™ fibers were too weak to be tested.

Figure 14 shows a comparison of average tensile strengths for batch UF-80 with data obtained on a more recently prepared batch (UF-127). Figure 14 also shows data for samples designated "UF - highest strength." This data represents the highest average strength values obtained from ~15 fiber lots that were processed between lots UF-80 and UF-127. Significant improvements in average strength values are noted in batches prepared more recently. The maximum average strengths were ~3.3 GPa and ~2.2 GPa for 1000°C and 1500°C heat-treated fibers, respectively. (The maximum strengths for individuals fibers in these batches

---

* The initial surface area (1000°C-pyrolyzed sample) for the fiber with lower surface oxygen contamination is probably larger than the corresponding sample with higher surface oxygen contamination (~0.5 vs. ~0.2 m^2/g) because the fiber diameter is smaller (i.e., ~11 vs. ~23 μm).

** Heat treatment times were 1.0 h except that the 1300°C Nicalon™ sample was heated for 2.0 h and the 1500°C UF-80 and Nicalon™ samples were heated for 0.5 h.

*** The results in Fig. 13 for Nicalon™ fibers heated to high temperatures (e.g., ≥1400°C) are probably not representative of the true average strengths because the values reported were determined on fibers that had sufficient handling strength to be tested. However, many fibers failed during preparation for testing. Thus, true average strengths for the Nicalon™ fibers are probably less than indicated in Fig. 13.

exceeded 5 GPa and 3.5 GPa, respectively.)

The precise reason(s) for the increased tensile strengths in more recent UF fiber batches are not known. However, there are two factors which may be responsible, at least in part, for the effect:

(1) The procedure for filtering the spinning solutions was improved. The polymer solution used to prepare UF-80 was passed only through a 2-4 μm glass filter, while the solutions used to prepare fiber batches with highest strength (including UF-127) were also filtered through 0.1 μm PTFE. Therefore, the size and concentration of strength-limiting defects in the latter fiber batches were probably reduced due to more effective removal of impurity particles, polymer "microgel" particles, etc. from the spinning solutions.

(2) The partial pressure of oxygen used during pyrolysis of the high strength batches (including UF-127 fibers) was lower, so the fibers probably had less surface oxygen contamination. Based on the SEM (Figs. 9 and 10) and specific surface area (Fig. 12) results described earlier, this should lead to improved strength retention after heat treatment (especially at temperatures $\geq$1400°C).

There are probably other factors which contribute to the observed variations in tensile strength values, including batch-to-batch variations in the characteristics of the polymer (e.g., molecular weight distribution) and the spinning solution (e.g., polymer concentration, rheological properties, etc.). As noted earlier, it was difficult to rigorously control these variables because of the small batch sizes (i.e., typically a few grams) prepared in this study.

Rupture strains and elastic modulus values were also determined from the stress-strain measurements on pyrolyzed and heat-treated fibers. Figure 15 shows average rupture strains as a function of heat treatment temperature for Nicalon™ and UF fibers (batches 80 and 127). Nicalon™ and UF fibers heated at 1000°C show similar rupture strains (~1.5%). This result suggests that UF fibers would have good weavability (i.e., comparable to Nicalon™) since the fibers also have high tensile strength and fine diameter.

At higher heat treatment temperatures, Nicalon™ fibers showed a more rapid decrease in rupture strains compared to UF fibers (Fig. 15). This is not surprising considering the large decrease in tensile strength for Nicalon™ above 1300°C (Fig. 13). Figure 15 also shows that UF-80 and UF-127 fibers have similar rupture strains despite significant differences in tensile strength. This can be attributed to the higher elastic modulus of UF-127 fibers, as shown in Fig. 16.

Figure 16 shows plots of elastic modulus vs. heat treatment temperature for Nicalon™ and UF fibers. Data is included for the UF-80 and UF-127 fibers, as well as the UF fiber

batches having the highest average elastic modulus values. Nicalon™ fibers show a large decrease in modulus after heat treatment above 1300°C. This presumably reflects the formation of porosity in the fibers as weight loss occurs at high temperatures. In contrast, UF fibers show either small increases (UF-80) or nearly constant (UF-127) modulus values with increasing heat treatment temperature, reflecting the improved thermal stability compared to Nicalon.™

The reason(s) for the large differences in modulus between the various UF fiber batches are not known. XRD analysis did not reveal any significant differences in the degree of crystallization (i.e., amount of β-SiC). (XRD patterns were virtually identical for UF-80 and UF-127 samples heated to 1600°C.) Preliminary analysis by SAM depth profiling indicates that the carbon content may be somewhat lower for batch UF-127, but more data (quantitative elemental analysis) is needed to confirm this.

It should be noted that both Nicalon™ and UF fibers have relatively low elastic modulus values compared to stoichiometric polycrystalline SiC. As discussed earlier in regards to Fig. 4, PC-derived fibers develop an amorphous, carbon-rich structure after low temperature pyrolysis.[8,9,15] The fibers retain a substantial amount of amorphous carbon during heat treatment at higher temperatures in inert atmospheres. Phase development in UF fibers is similar to that observed in Nicalon.™ Figure 17 shows typical XRD diffraction patterns for UF fibers after pyrolysis at 750°C and after subsequent heat treatments in the range 1000-1600°C. The patterns are very similar to results reported for Nicalon™-type fibers, except that peaks associated with silica are absent in UF fibers due to their low oxygen content.[8,9,15] The β-SiC peaks progressively narrow and increase in intensity as the heat treatment temperature is increased. TEM results are consistent with the XRD data in that the size of the β-SiC grains was observed to increase with increasing temperature. However, it is unclear if the amount of crystalline SiC is also increasing (i.e., relative to amorphous, carbon-rich material). It was originally believed that the small increase in elastic modulus for UF-80 fibers indicated an increase in the amount of crystalline SiC.* However, UF-127 fibers show similar changes in

* The largest elastic modulus for UF-80 fibers is observed in the 1700°C-heat treated sample. This may be due to the increased importance of the reaction between carbon and siliceous (Si-O containing) material at higher temperatures. In this case, the volume fraction of SiC would increase as oxygen and excess carbon are eliminated (i.e., as volatile species such as CO and SiO.)

the XRD patterns (i.e., increased β-SiC peak intensities), yet no increase in elastic modulus is observed with increasing heat treatment temperature (Fig. 16). (As noted earlier, UF-80 and UF-127 fibers heat treated at 1600°C in argon show essentially identical XRD patterns.) Despite the high content of amorphous carbon-rich material, UF fibers have relatively good thermomechanical stability in an air atmosphere. For example, after 1.0 hour heat treatments in air at 1400 and 1500°C, the average tensile strengths (at room temperature) for three different lots of UF fibers were in the range of ~1.3-1.7 GPa and ~1.2-1.4 GPa, respectively. In addition, a UF fiber batch* tested at 1400°C in air had an average tensile strength of ~1.1 GPa (178 mm gage length). In contrast, Nicalon™ fibers tested under identical conditions had a strength of only ~0.7 GPa.

A TGA experiment showed that UF fibers (initially pyrolyzed at 1000°C) gained ~1.5 wt% when heated in air at 10°C/min to 1550°C and subsequently held for 1 hour at temperature. NAA showed that the oxygen content in this particular sample increased from ~2.6 wt% (as-pyrolyzed) to ~5.5 wt% (after oxidation treatment). It is presumed that the oxygen weight gain is greater than the overall weight gain due to an oxidation reaction that forms silicon dioxide (non-volatile) and carbon monoxide (volatile), i.e., a reaction such as:

$$SiC_{x(s)} + (1+\tfrac{x}{2})O_{2(g)} \Rightarrow SiO_{2(s)} + xCO_{(g)}\uparrow$$

Characterization of the fibers by electron microscopy and SAM depth profiling would be helpful in understanding the oxidation mechanism. A more detailed investigation of the thermochemical and thermomechanical stability of UF fibers in highly oxidizing environments is planned.

CONCLUSION

Continuous silicon carbide fibers (designated "UF fibers") with low oxygen contents (~1-2 wt%), small diameters, and high tensile strengths were prepared by dry spinning of novel organosilicon polymer solutions and subsequent pyrolysis of the as-spun fibers. By controlling several key polymer and solution characteristics, a process with the following advantages was developed: (1) fiberizing solutions had excellent spinnability, (2) green and

---

* This batch was initially pyrolyzed at 1250°C in nitrogen, i.e., prior to testing at high temperature.

partially-pyrolyzed fibers had good mechanical properties, (3) green fibers could be directly pyrolyzed to a ceramic without melting, i.e., the process was carried out without an oxidative or irradiative cross-linking step, (4) a high ceramic yield was obtained after pyrolysis, and (5) fibers with smooth surfaces and round cross-sections could be produced with a range of diameters (~8-50 μm).

UF fibers showed excellent thermomechanical stability in comparison to commercially-available Nicalon™ fibers, as indicated by lower weight losses, lower specific surface areas, and improved strength retention after heat treatment at elevated temperatures. This was attributed to the relatively low oxygen content for UF fibers (i.e., compared to Nicalon™). Scanning Auger microprobe analysis showed that the residual oxygen in UF fibers was concentrated near the fiber surfaces, apparently due to contamination from atmospheric oxygen and water vapor during the spinning and pyrolysis operations. In samples with high levels of surface oxygen contamination, reaction between siliceous (Si-O containing) and carbon-rich materials resulted in some surface degradation of the fibers after high temperature ($\geq$1500°C) heat treatment. Fibers with improved thermomechanical stability were produced by reducing the partial pressure of oxygen during pyrolysis. SEM observations and specific surface area measurements showed that surface degradation reactions were greatly inhibited in fibers with lower oxygen contamination.

As observed in other PC-derived ceramics, heat-treated UF fibers have a carbon-rich, weakly-crystalline structure. This resulted in relatively low elastic modulus, even after heat treatment at temperatures up to 1700°C. Ongoing investigations are being directed toward the development of fully-crystalline, stoichiometric silicon carbide fibers with higher elastic modulus, while still retaining high tensile strength and excellent thermomechanical stability.

ACKNOWLEDGEMENT

The authors gratefully acknowledge B.J. Madana and E.J. Serrano of the University of Florida (UF) for assistance in room temperature mechanical property measurements, E. Lambers of UF for assistance in the SAM measurements, and M. Jenkins of Oak Ridge National Laboratory for assistance in high temperature strength measurements. This work was supported by the Defense Advanced Research Projects Agency under Contract Nos. MDA 972-88-J-1006 and N00014-91-J-4075.

REFERENCES

1. S. Yajima, J. Hayashi, M. Omori, and K. Okamura, "Development of a Silicon Carbide Fiber with High Tensile Strength," Nature, 261 683-685 (1976).
2. S. Yajima, K. Okamura J. Hayashi, and M. Omori, "Synthesis of Continuous SiC Fibers with High Tensile Strength," J. Am. Ceram. Soc., 59 324-327 (1976).
3. K. Prewo and J. Brennan, "High-Strength Silicon Carbide-Fiber-Reinforced Glass Matrix Composites," J. Mater. Sci., 15 [2] 463-468 (1980).
4. J. Brennan and K. Prewo, "Silicon Carbide Fiber Reinforced Glass-Ceramic Matrix Composites Exhibiting High Strength and Toughness," J. Mater. Sci., 17 2371-2383 (1982).
5. K.M. Prewo, J. J. Brennan, and G.K. Layden, "Fiber Reinforced Glasses and Glass-Ceramics for High Performance Applications," Am. Ceram. Soc. Bull., 65 [2] 305-313, 322 (1986).
6. P.J. Lamicq, G.A. Bernhart, M.M. Dauchier, and J.G. Mace, "SiC/SiC Composite Ceramics," Am. Ceram. Soc. Bull., 65 [2] 336-338 (1986).
7. "Fiber Reinforced Ceramic Composites: Materials, Processing, and Technology," edited by K.S. Mazdiyasni, Noyes Publications, Park Ridge, NJ (1990).
8. T. Mah, N.L. Hecht, D.E. McCullum, J.R. Hoenigman, H.M. Kim, A.P. Katz, H. Lipsitt, "Thermal Stability of SiC Fibres (Nicalon)," J. Mater. Sci., 19 [4] 1191-1201 (1984).
9. G. Simon and A.R. Bunsell, "Mechanical and Structural Characterization of the Nicalon Silicon Carbide Fibre," J. Mater. Sci., 19 [11] 3649-3657 (1984).
10. T.J. Clark, R.M. Arons, J.B. Stamatoff, and J. Rabe, "Thermal Degradation of Nicalon SiC Fiber," Ceram. Eng. Sci. Proc., 6 [7-8] 576-578 (1985).
11. M.H. Jaskowiak and J.A. DiCarlo, "Pressure Effects on the Thermal Stability of Silicon Carbide Fibers," J. Am. Ceram. Soc., 72 [2] 192-197 (1989).
12. D.J. Pysher, K.C. Goretta, R.S. Hodder, Jr., and R.E. Tressler, "Strengths of Ceramic Fibers at Elevated Temperatures," J. Am. Ceram. Soc., 72 [2] 284-288 (1989).
13. B.A. Bender, J.S. Wallace, and D.J. Schrodt, "Effect of Thermochemical Treatments on the Strength and Microstructure of SiC Fibers," J. Mater. Sci. 26 970-976 (1991).
14. S.M. Johnson, R.D. Brittain, R.H. Lamoreaux, and D.J. Rowcliffe, "Degradation Mechanisms of Silicon Carbide Fibers," Comm. Am. Ceram. Soc., 71 [3] C-132 -C-135 (1988).
15. Y. Hasegawa, "Synthesis of Continuous Silicon Carbide Fibre. Part 6. Pyrolysis Process of Cured Polycarbosilane Fibre and Structure of SiC Fibre," J. Mater. Sci., 24 1177-1190 (1989).
16. F. Frechette, B. Dover, V. Venkateswaran, and J. Kim, "High Temperature Continuous Sintered SiC Fiber for Composite Applications", Ceram. Eng. Sci. Proc., 12 [7-8] 992-1006 (1991).
17. L.A. Silverman, W.D. Hewett, Jr., T.P. Blatchford, and A.J. Beeler, "Silicon Carbide Fibers From Slurry Spinning", J. Appl. Polymer Sci.: Applied Polymer Symposium 47 99-109 (1991).
18. J. Lipowitz, J.A. Rabe, and G.A. Zank, "Polycrystalline SiC Fibers from Organosilicon Polymers," Ceram. Eng. Sci. Proc., 12 [9-10] 1819-1831 (1991).

19. J. Lipowitz, J.A. Rabe, and G.A. Zank, "Crystalline SiC Fibers from Organosilicon Polymers," proceedings of the HITEMP REVIEW 1991, NASA Lewis Research Center, Cleveland, OH, 1991.

20. M. Takeda, Y. Imai, H. Ichikawa, and T. Ishikawa, "Properties of the Low Oxygen Content SiC Fiber on High Temperature Heat Treatment", Ceram. Eng. Sci. Proc., 12 [7-8] 1007-1018 (1991).

21. M. Takeda, Y. Imai, H. Ichikawa, T. Ishikawa, N. Kasai, T. Suguchi, and K. Okamura "Thermal Stability of the Low Oxygen Content Silicon Carbide Fibers Derived from Polycarbosilane," Ceram. Eng. Sci. Proc., 13 [7-8] 209-217 (1992).

22. Wm. Toreki, G.J. Choi, C.D. Batich, M.D. Sacks, and M. Saleem, Ceram. Eng. Sci. Proc., 13 [7-8] 198-208 (1992).

23. Wm. Toreki, C.D. Batich, M.D.Sacks, and A.A. Morrone, "Synthesis and Applications of a Vinylsilazane Preceramic Polymer," Ceram. Eng. Sci. Proc., 11 (9-10) 1371-1386 (1990).

24. "Test Method for Tensile Strength and Young's Modulus for High Modulus Single Filament Materials," ASTM Designation D3379, American Society for Testing and Materials, Philadelphia, PA.

25. "New Product Information - Polycarbosilane," product bulletin, Dow Corning Corp., Midland, MI (1989).

26. Y. Hasegawa, M. Iimura, and S. Yajima, "Synthesis of Continuous Silicon Carbide Fibre. Part 2. Conversion of Polycarbosilane Fibre into Silicon Carbide Fibres," J. Mater. Sci., 15 720-728 (1980).

27. K.J. Wynne and R.W. Rice, "Ceramics via Polymer Pyrolysis," Ann. Rev. Mater. Sci., 14 297-324 (1987).

FIGURE CAPTIONS

Figure 1: Plots of (A) shear stress vs. shear rate and (B) viscosity vs. shear rate for a typical UF fiber spinning solution.

Figure 2: TGA plot for "green" (as-spun) UF fibers heated in argon to 950°C at 20°C/min.

Figure 3: Scanning electron micrographs of 1000°C-pyrolyzed UF fibers.

Figure 4: (A) TEM electron diffraction pattern and (B) TEM bright field image of 1200°C-pyrolyzed UF fibers.

Figure 5: Plots of average tensile strength vs. fiber diameter for different batches of UF fibers. Data are also shown for Nicalon™ fibers.

Figure 6: Weight loss behavior for UF fibers (top) and Nicalon™ fibers (bottom) heated in argon to 1550°C at 10°C/min and then held for 1 hour at temperature.

Figure 7: Scanning Auger microprobe survey scans at the (A) surface and (B) interior of a 1000°C-pyrolyzed UF fiber.

Figure 8: Scanning Auger microprobe depth profiles of the O, Si, and C atomic concentrations for the same fiber as in Fig. 7.

Figure 9: Scanning electron micrographs of UF fibers with relatively high surface oxygen contamination after heat treatment at 1500°C for 1 h in argon. Growth of large grains and degradation reactions occur at the fiber surface.

Figure 10: Scanning electron micrographs of UF fibers with relatively low surface oxygen contamination after heat treatment at 1600°C for 1 h in argon. The fibers have a similar appearance to the 1000°C-pyrolyzed fibers shown in Fig. 3.

Figure 11: Scanning electron micrograph of Nicalon™ fiber after heat treatment at 1600°C for 1 h in argon.

Figure 12: Plot of specific surface area vs. heat treatment temperature for UF fibers and Nicalon™ fibers. Values are given for UF-127 fibers (lower surface oxygen contamination) and UF-94 fibers (higher surface oxygen contamination).

Figure 13: Plots of average tensile strength vs. heat treatment temperature for UF-80 fibers and Nicalon™ fibers.

Figure 14: Plots of average tensile strength vs. heat treatment temperature for UF 80 and UF-127 fibers and for UF fiber batches with the highest average strengths. For clarity, the error bars (± one standard deviation) are not included for the highest strength data points.

Figure 15: Plots of average rupture strain vs. heat treatment temperature for UF fibers and Nicalon™ fibers. Values for UF fibers are given for batch nos. 80 and 127.

Figure 16: Plots of average elastic modulus vs. heat treatment temperature for UF fibers and Nicalon™ fibers. Values for UF fibers are given for batch nos. 80 and 127 and for the batches with the highest average elastic moduli. For clarity, the error bars (± one standard deviation) are not included for the highest modulus data points.

Figure 17: X-ray diffraction patterns for UF fibers after heat treatment at the indicated temperatures.

TABLE 1. ELEMENTAL ANALYSIS

Sample	O (wt%)	Si (wt%)	C (wt%)	N (wt%)	H (wt%)
UF Fiber	1.1-2.6†	55†,‡	42▼	1-2▲,†	<0.5▲
Nicalon	13.5-15†	55‡	29▲	<0.5▲	<0.5▲
Nicalon*	10	58	31		

---

* Reported by manufacturer
† Determined by neutron activation analysis
‡ Determined by atomic absorption
▲ Determined by LECO combustion method
▼ Determined by difference

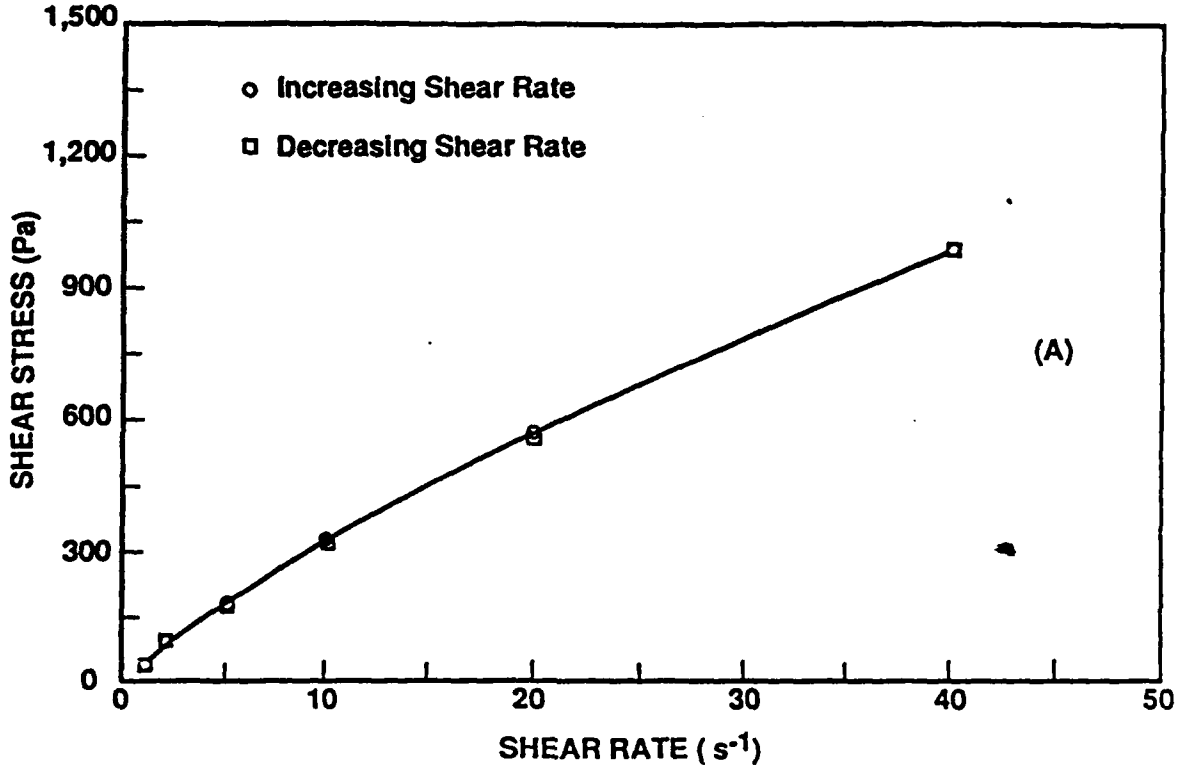
1,500
1,200
900
600
300
0
SHEAR STRESS (Pa)
Increasing Shear Rate
Decreasing Shear Rate
(A)
0
10
20
30
40
50
SHEAR RATE (s-1)

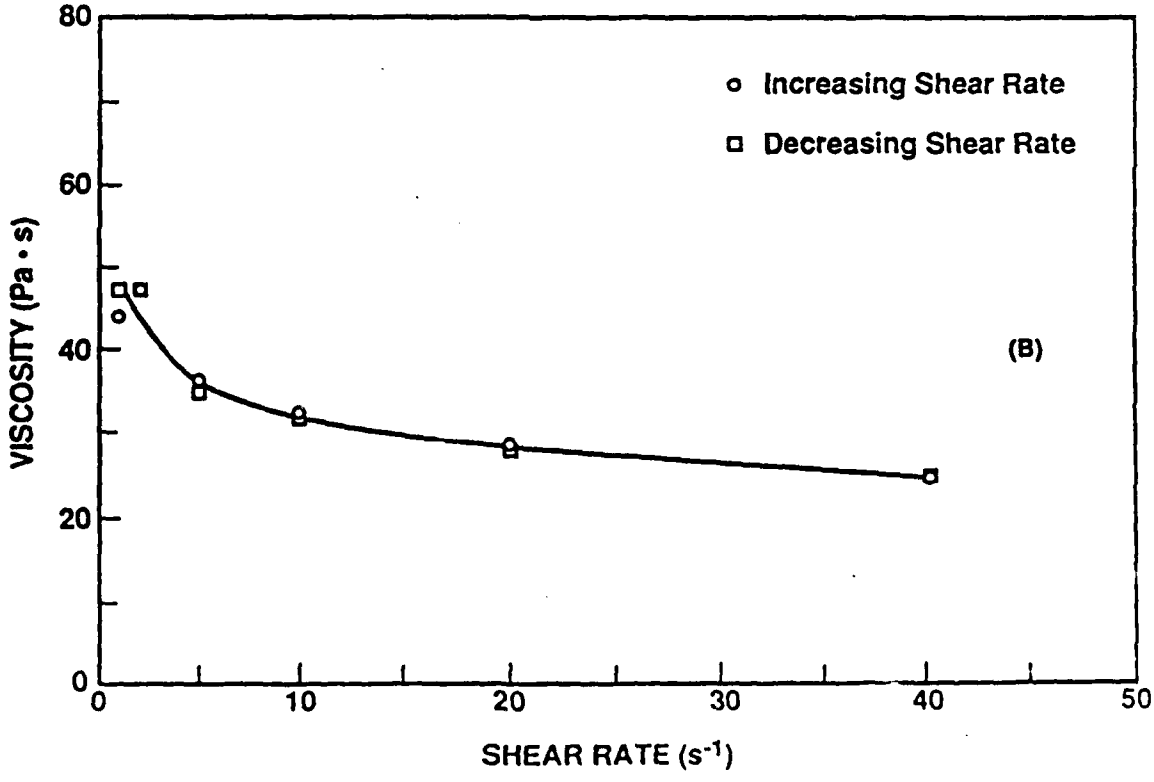
80
60
40
20
0
VISCOSITY (Pa • s)
Increasing Shear Rate
Decreasing Shear Rate
(B)
0
10
20
30
40
50
SHEAR RATE (s-1)

Figure

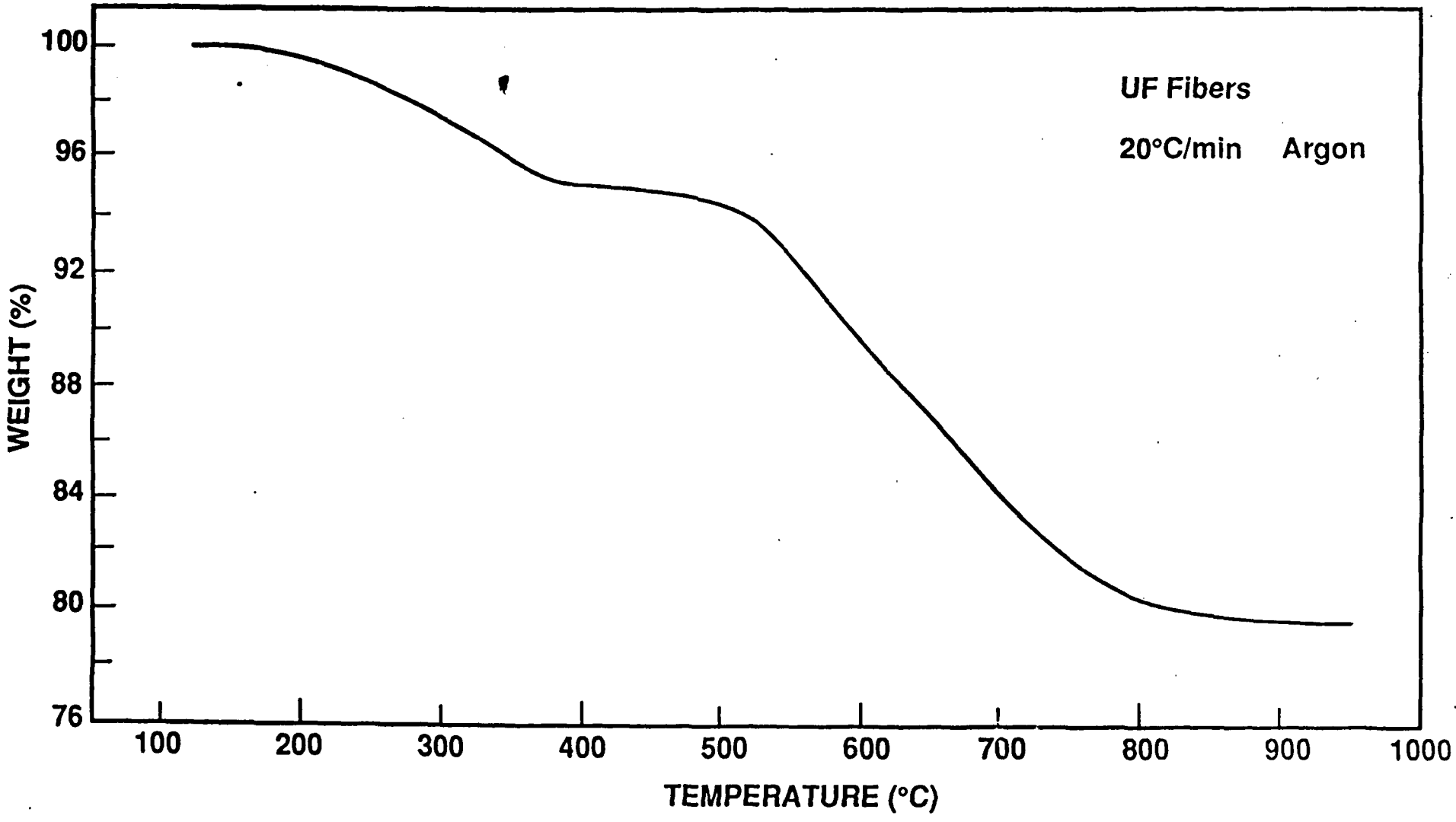
UF Fibers
20°C/min Argon
WEIGHT (%)
100
96
92
88
84
80
76
100
200
300
400
500
600
700
800
900
1000
TEMPERATURE (°C)

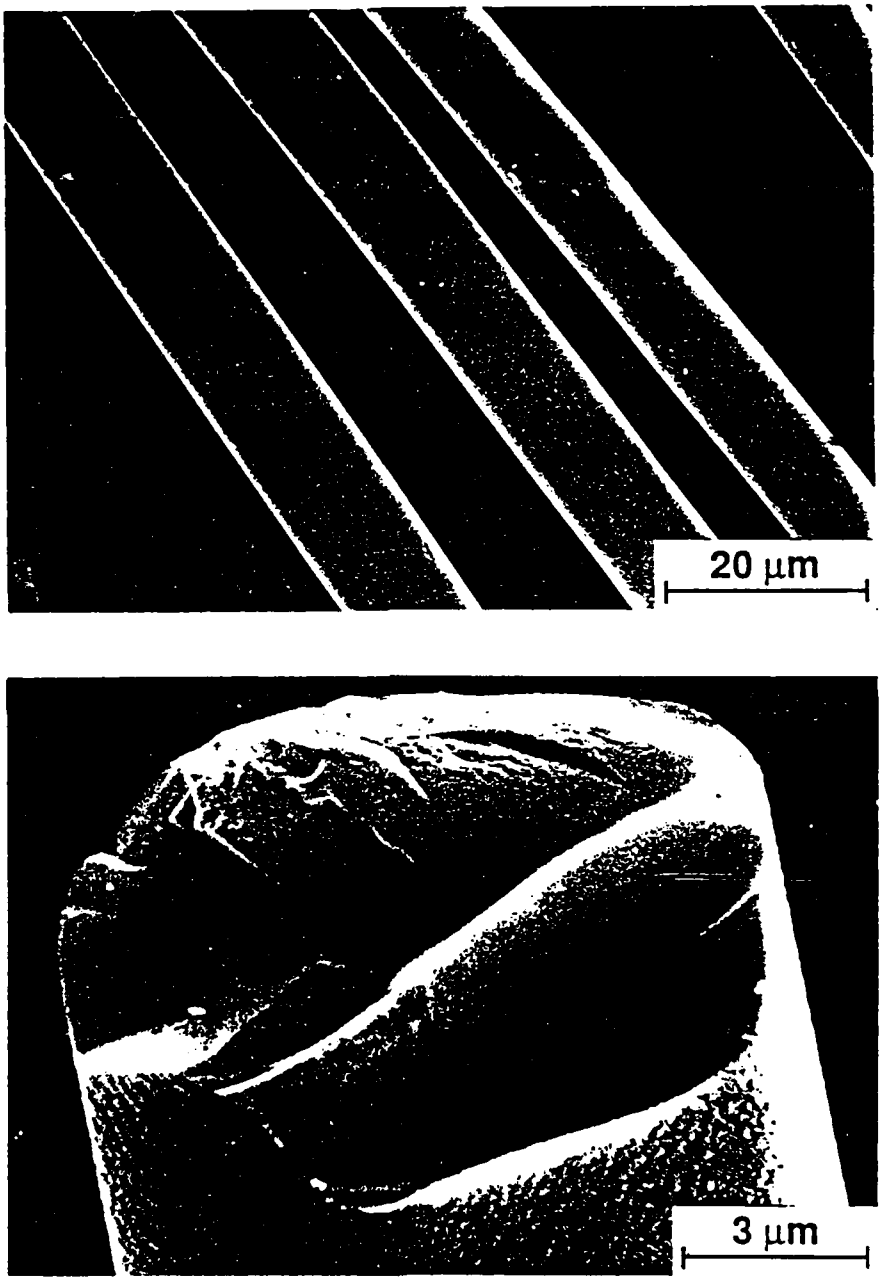
20 µm
3 µm

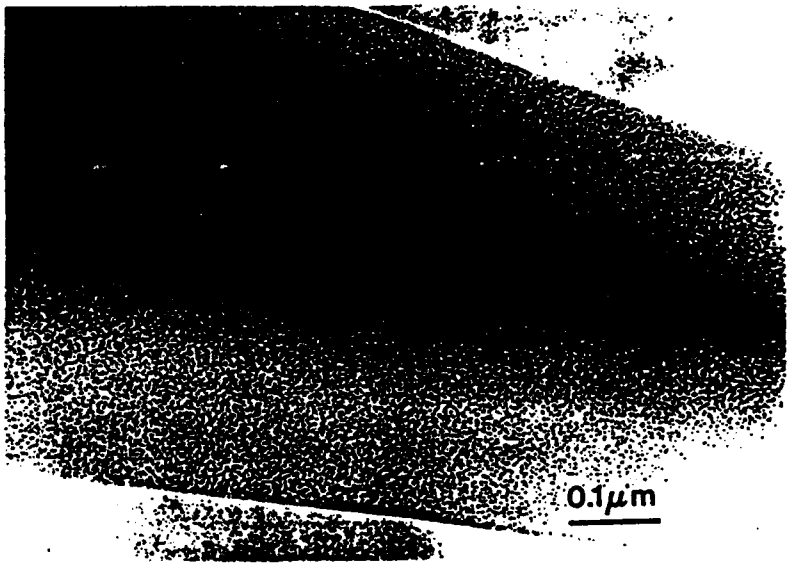
0.1μm

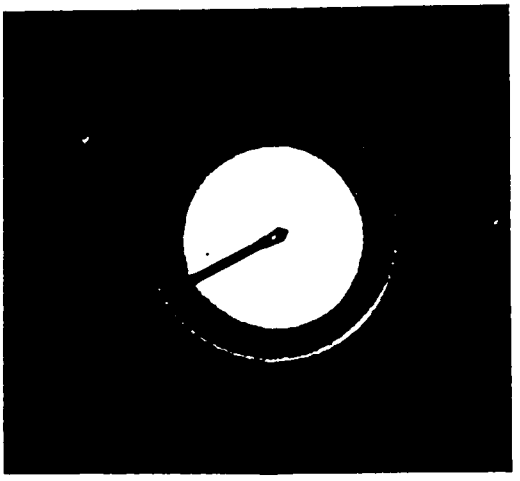

Figure 5

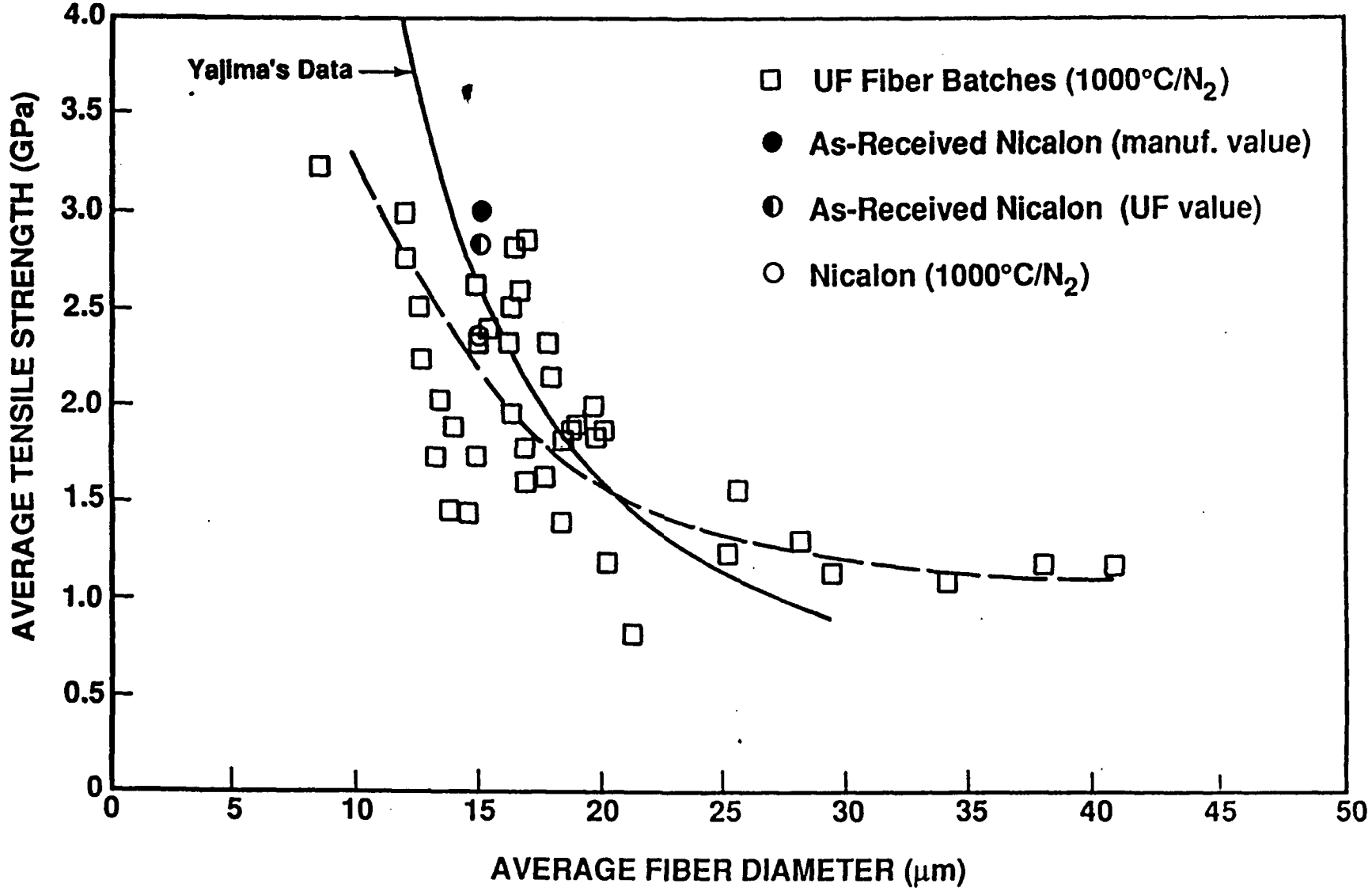
Yajima's Data
UF Fiber Batches (1000°C/N2)
As-Received Nicalon (manuf. value)
As-Received Nicalon (UF value)
Nicalon (1000°C/N2)
AVERAGE TENSILE STRENGTH (GPa)
AVERAGE FIBER DIAMETER (μm)
0
0.5
1.0
1.5
2.0
2.5
3.0
3.5
4.0
0
5
10
15
20
25
30
35
40
45
50

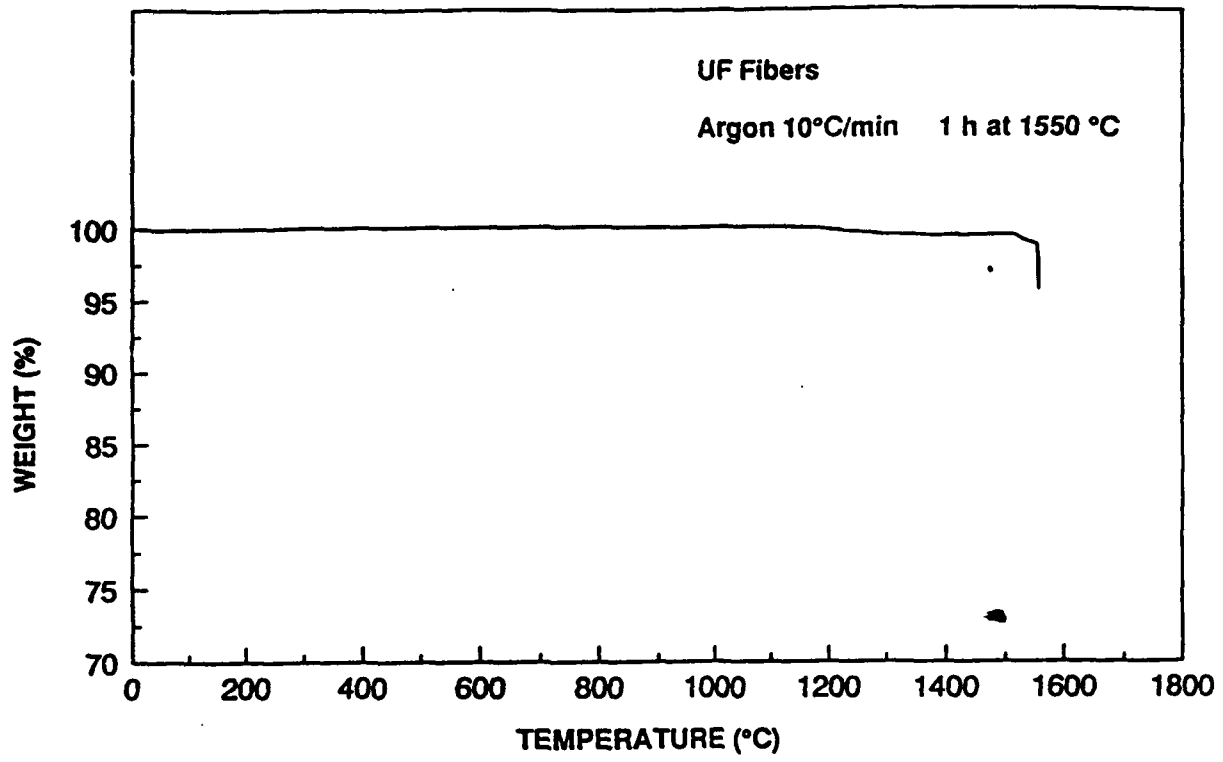
UF Fibers
Argon 10°C/min 1 h at 1550 °C
WEIGHT (%)
100
95
90
85
80
75
70
0
200
400
600
800
1000
1200
1400
1600
1800
TEMPERATURE (°C)

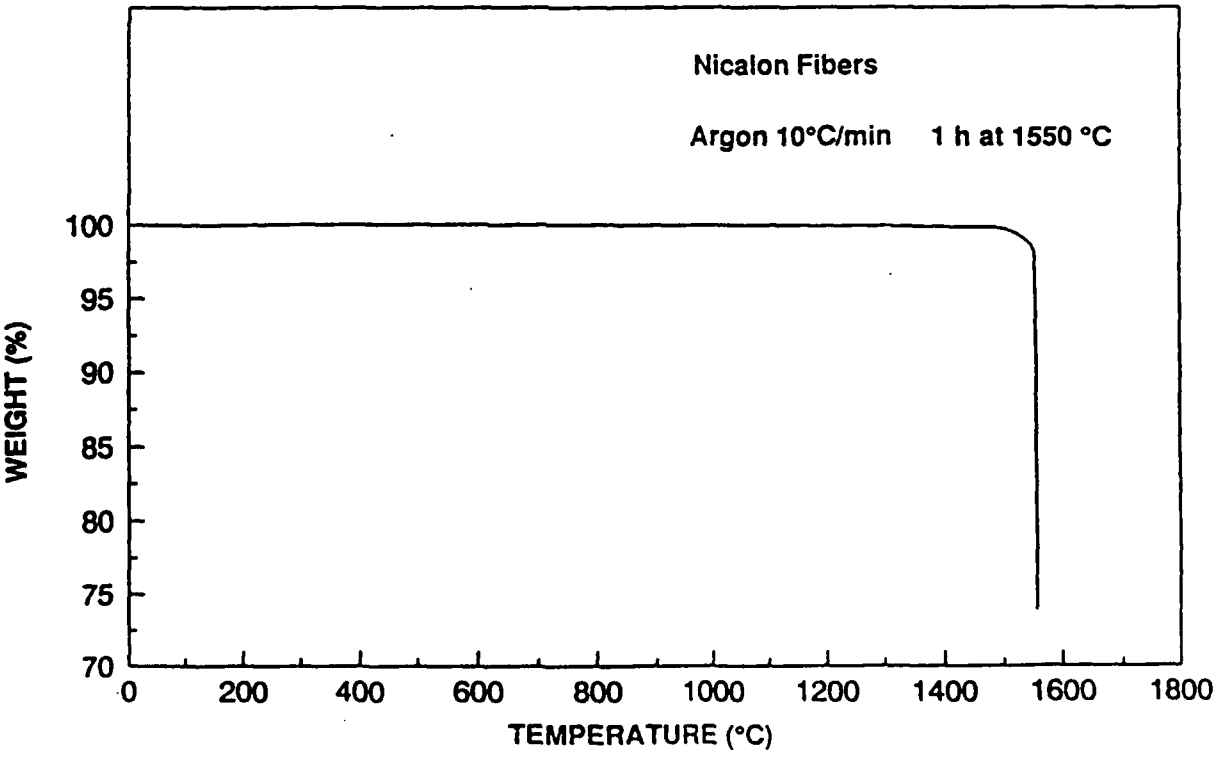
Nicalon Fibers
Argon 10°C/min 1 h at 1550 °C
WEIGHT (%)
100
95
90
85
80
75
70
0
200
400
600
800
1000
1200
1400
1600
1800
TEMPERATURE (°C)

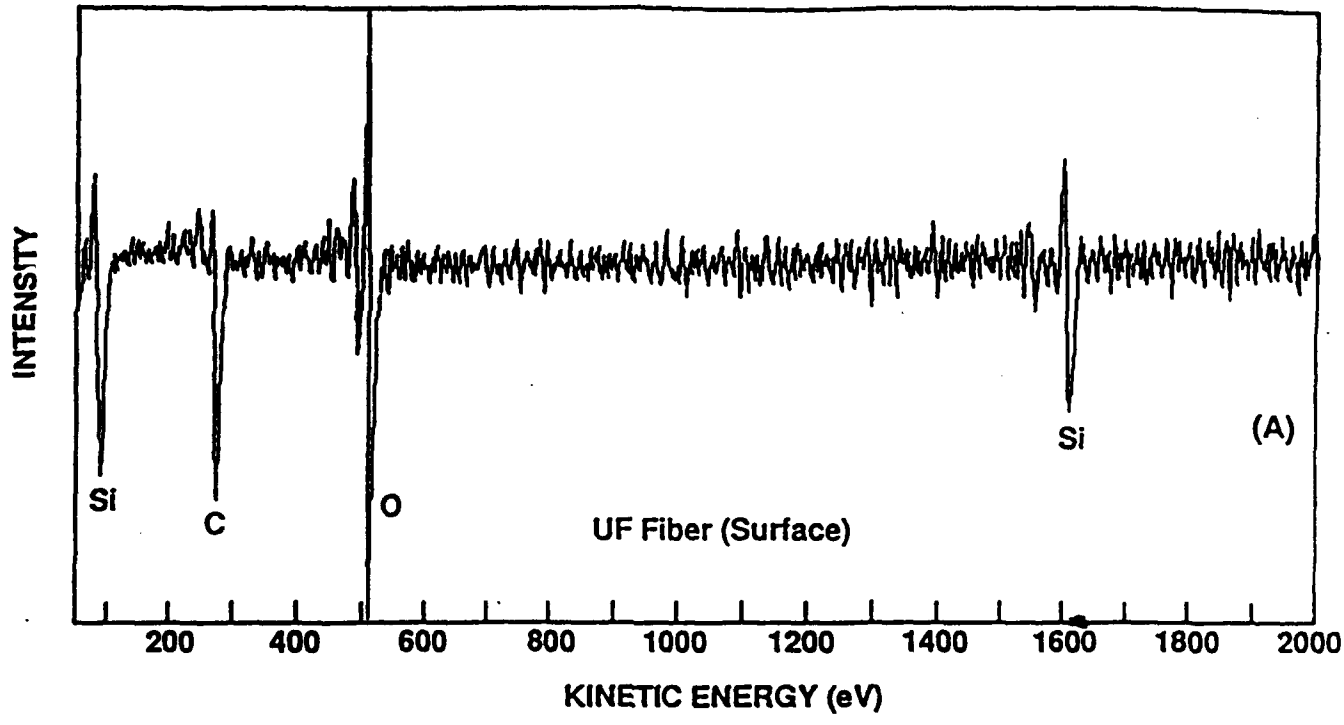
INTENSITY
Si
C
O
Si
(A)
UF Fiber (Surface)
200
400
600
800
1000
1200
1400
1600
1800
2000
KINETIC ENERGY (eV)

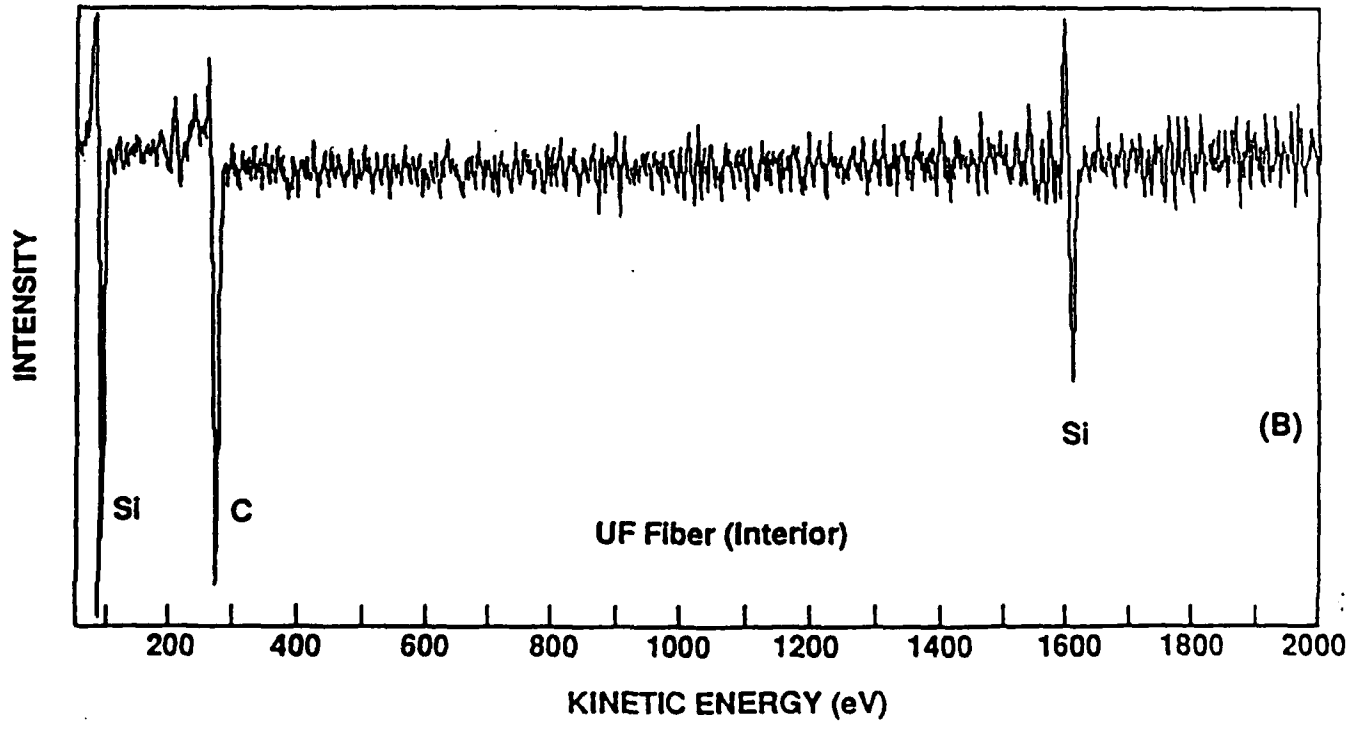
INTENSITY
Si
C
Si
(B)
UF Fiber (Interior)
200
400
600
800
1000
1200
1400
1600
1800
2000
KINETIC ENERGY (eV)

Figure 1

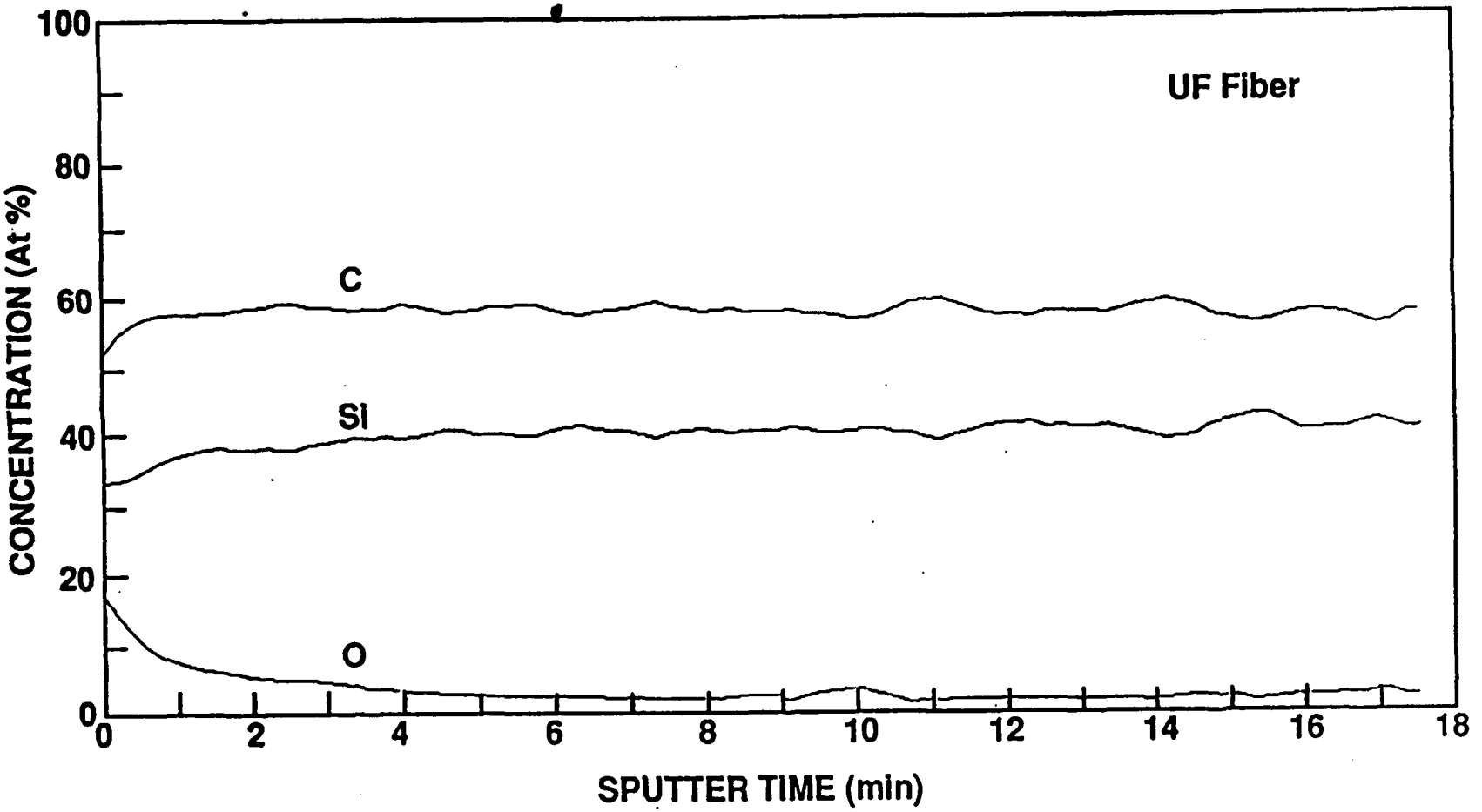
UF Fiber
CONCENTRATION (At %)
SPUTTER TIME (min)
C
Si
O
100
80
60
40
20
0
0
2
4
6
8
10
12
14
16
18

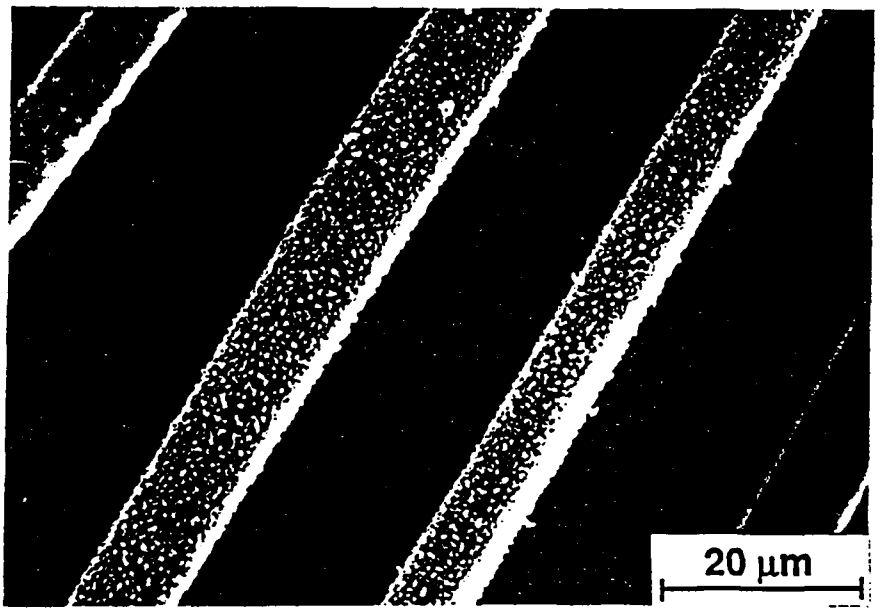
20 µm

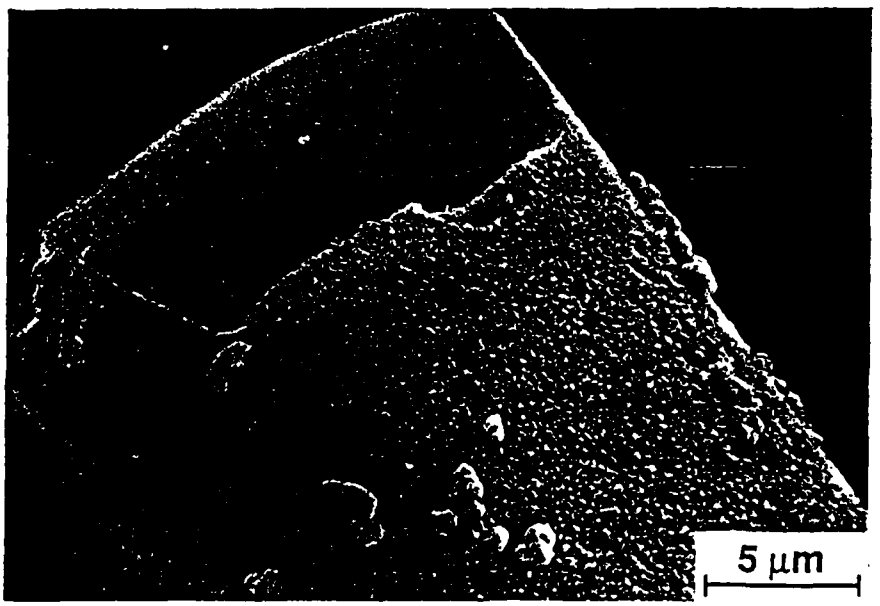
5 µm

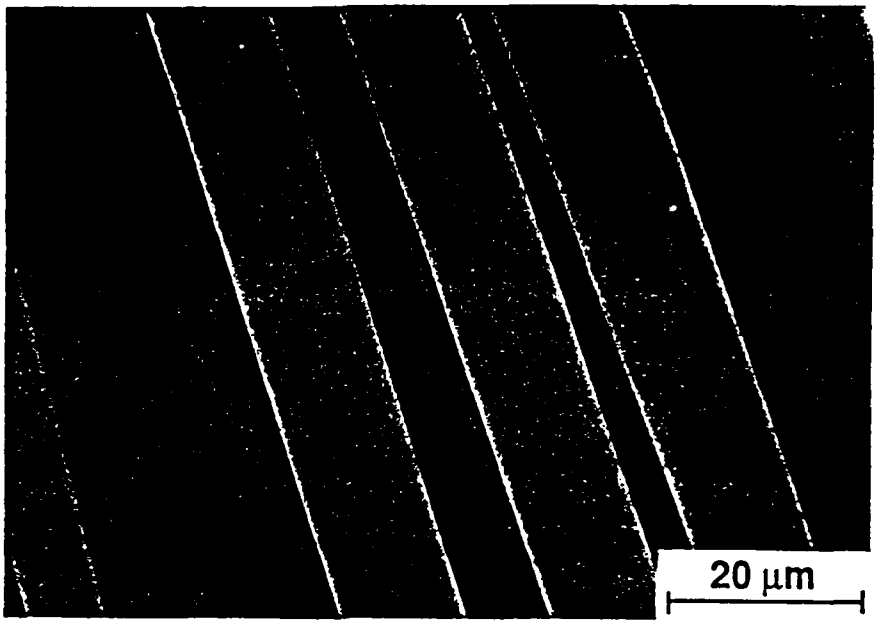
20 µm

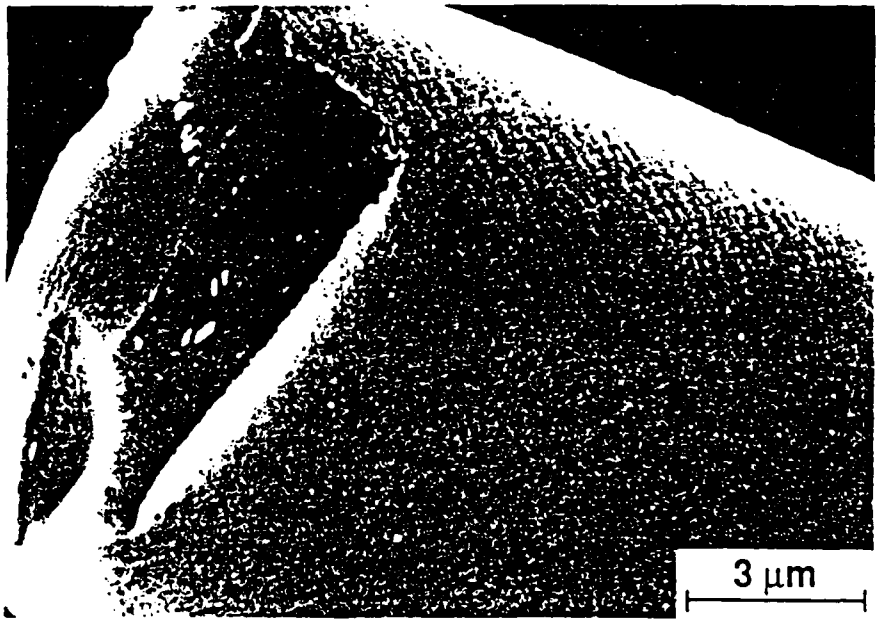
3 µm

Nicalon™ 1600°C in Argon

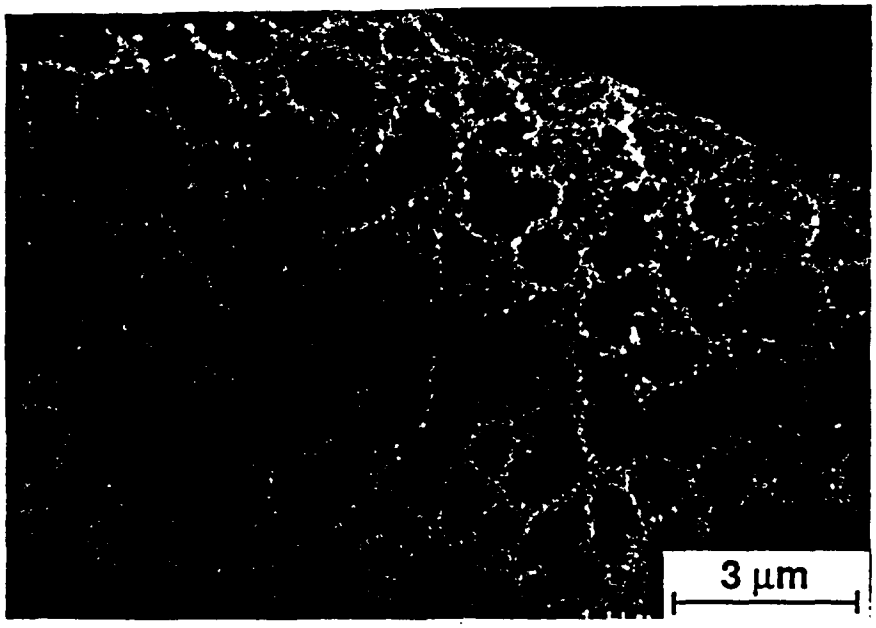

Figure 12

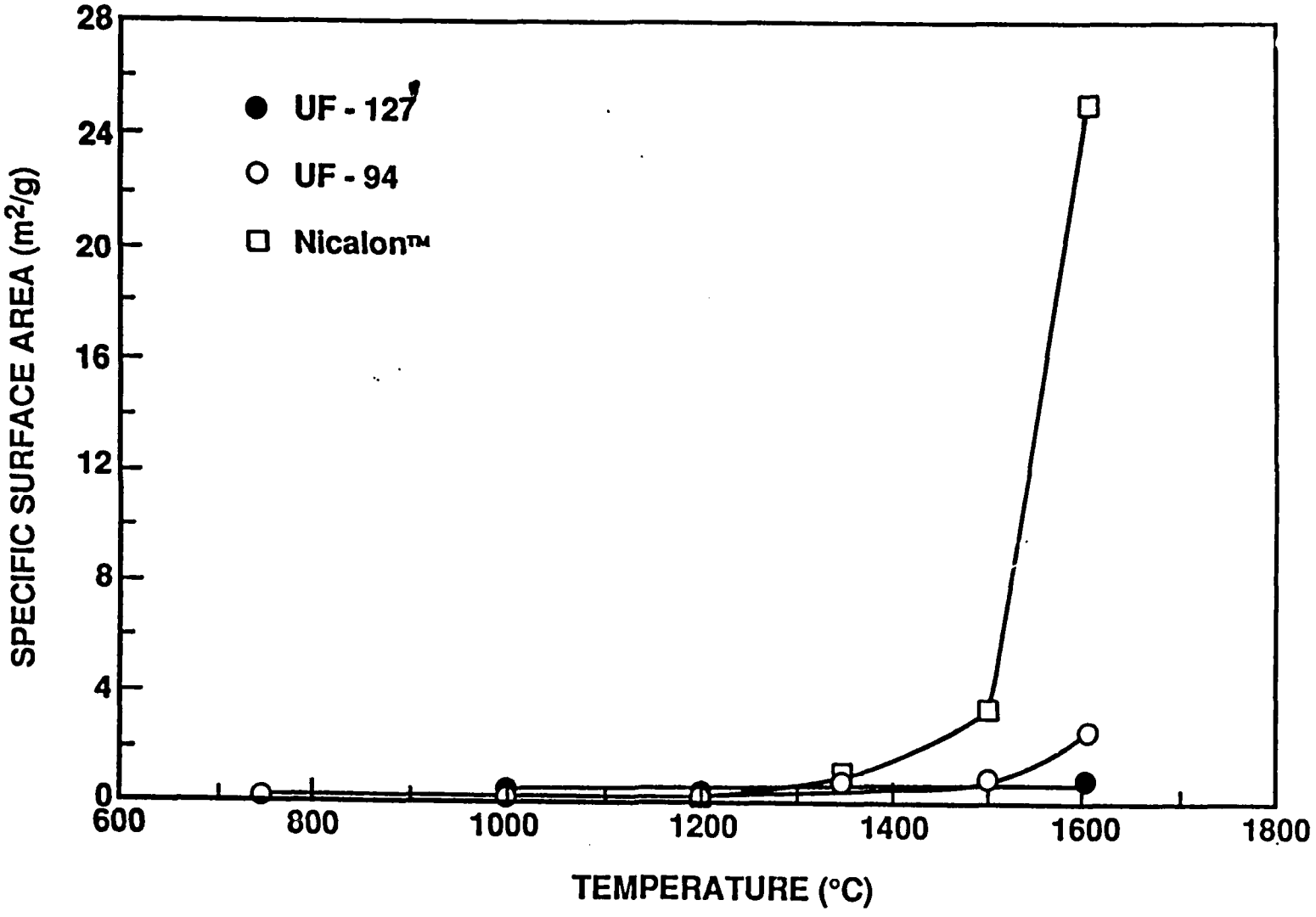
28
24
20
16
12
8
4
0
SPECIFIC SURFACE AREA (m²/g)
UF - 127
UF - 94
Nicalon™
600
800
1000
1200
1400
1600
1800
TEMPERATURE (°C)

Figure 1:

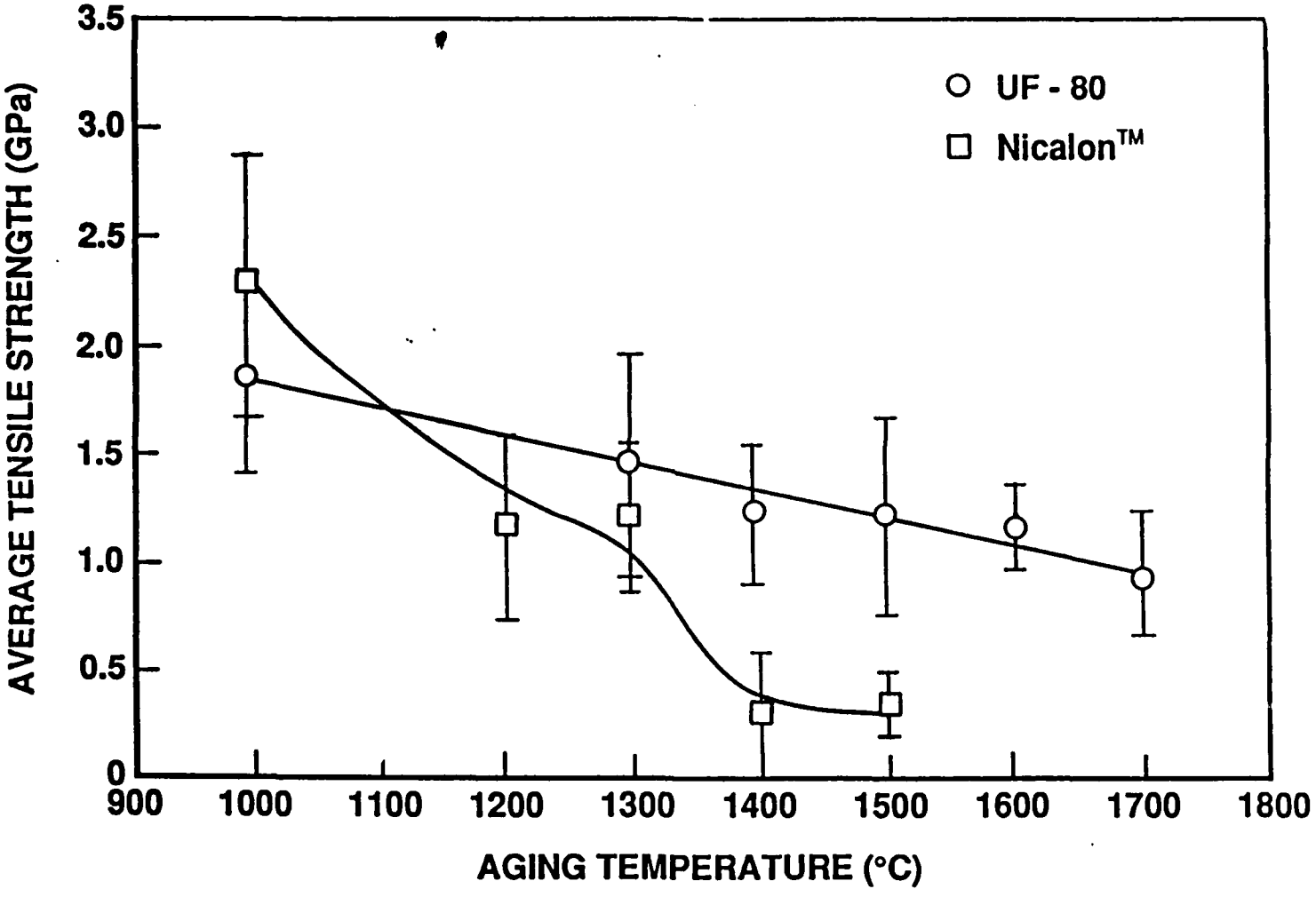
AVERAGE TENSILE STRENGTH (GPa)
3.5
3.0
2.5
2.0
1.5
1.0
0.5
0
900
1000
1100
1200
1300
1400
1500
1600
1700
1800
AGING TEMPERATURE (°C)
UF - 80
Nicalon™

Figure 14

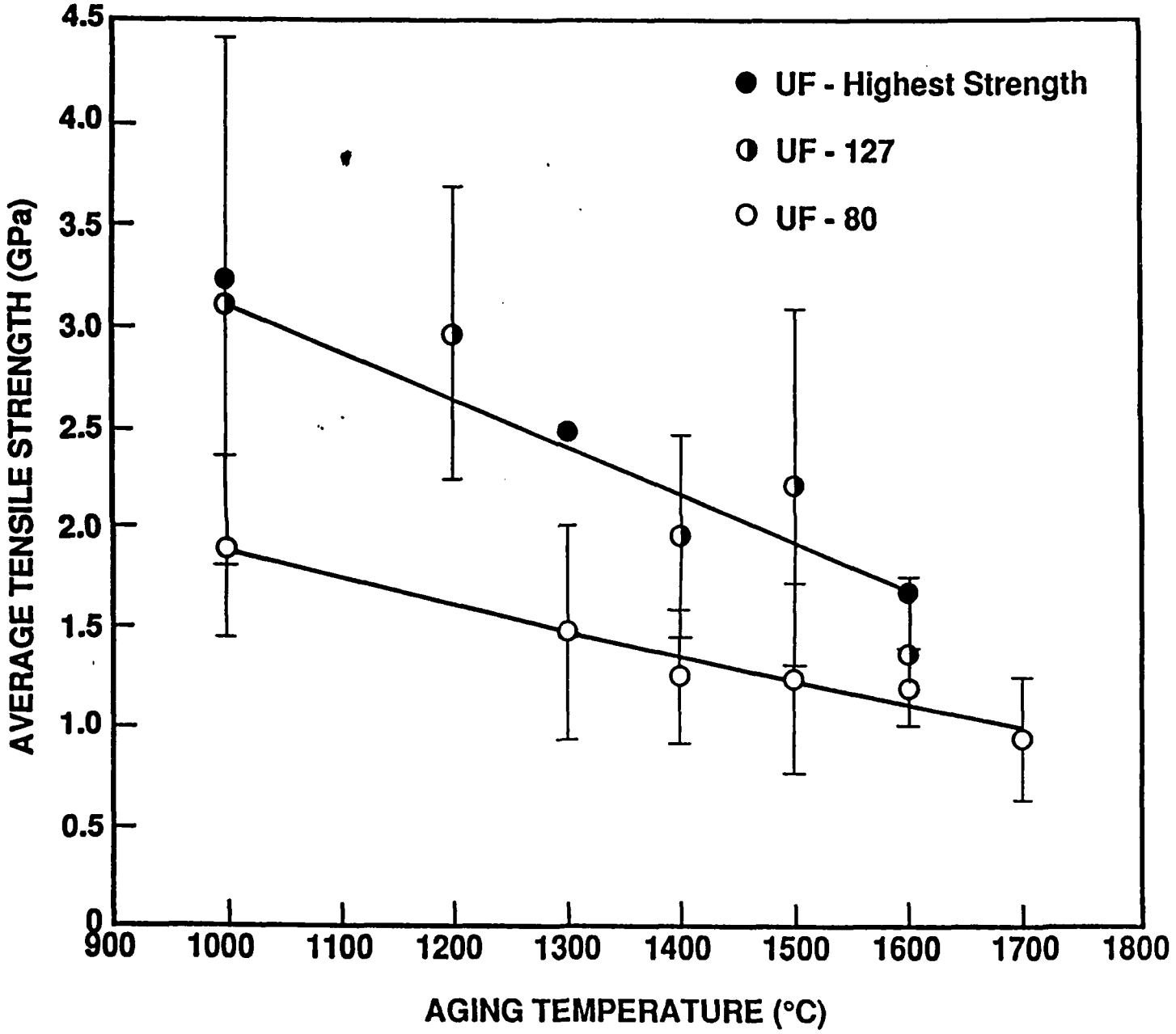
AVERAGE TENSILE STRENGTH (GPa)
4.5
4.0
3.5
3.0
2.5
2.0
1.5
1.0
0.5
0
900
1000
1100
1200
1300
1400
1500
1600
1700
1800
AGING TEMPERATURE (°C)
UF - Highest Strength
UF - 127
UF - 80

Figure 1:

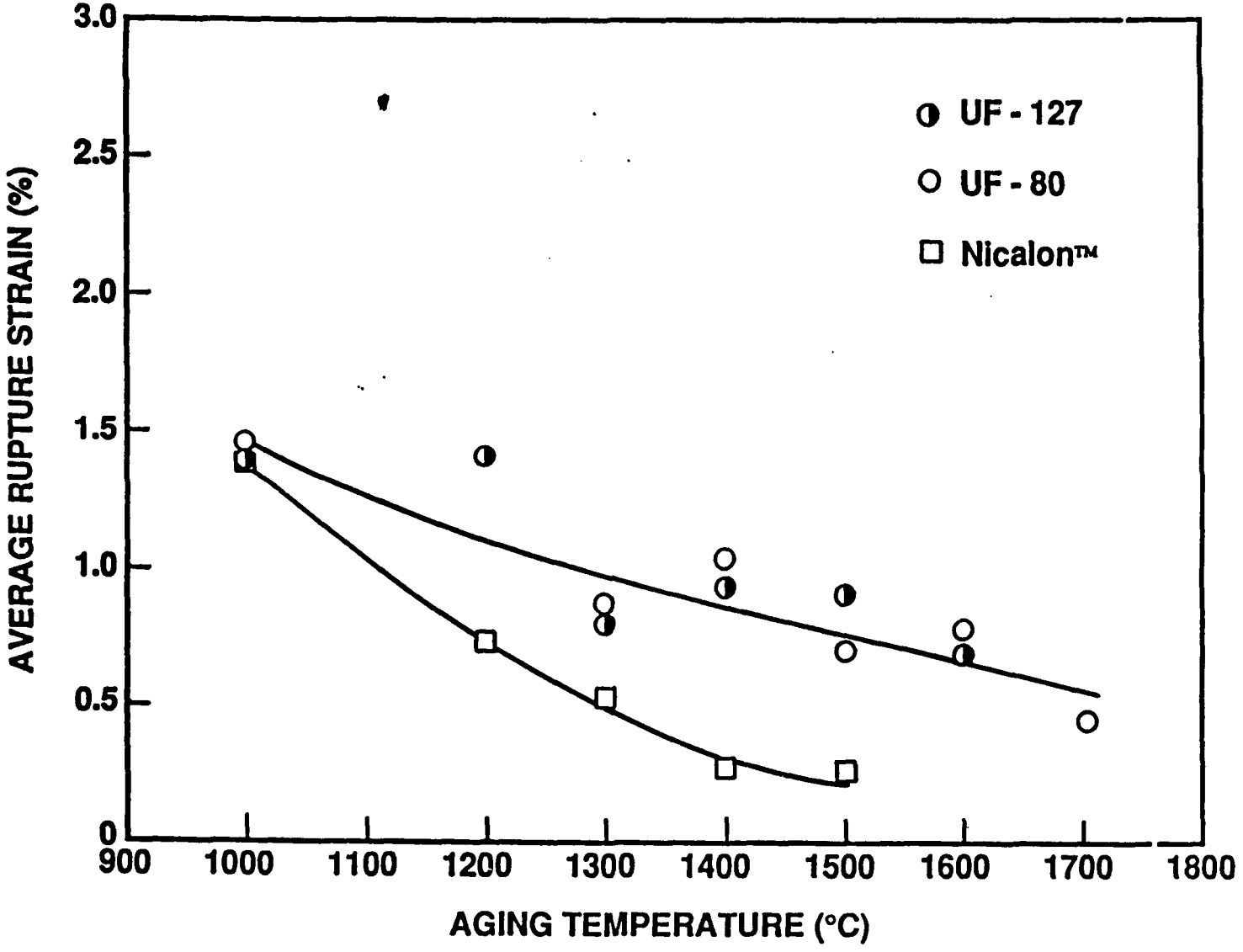
AVERAGE RUPTURE STRAIN (%)
3.0
2.5
2.0
1.5
1.0
0.5
0
900
1000
1100
1200
1300
1400
1500
1600
1700
1800
AGING TEMPERATURE (°C)
UF - 127
UF - 80
Nicalon™

Figure

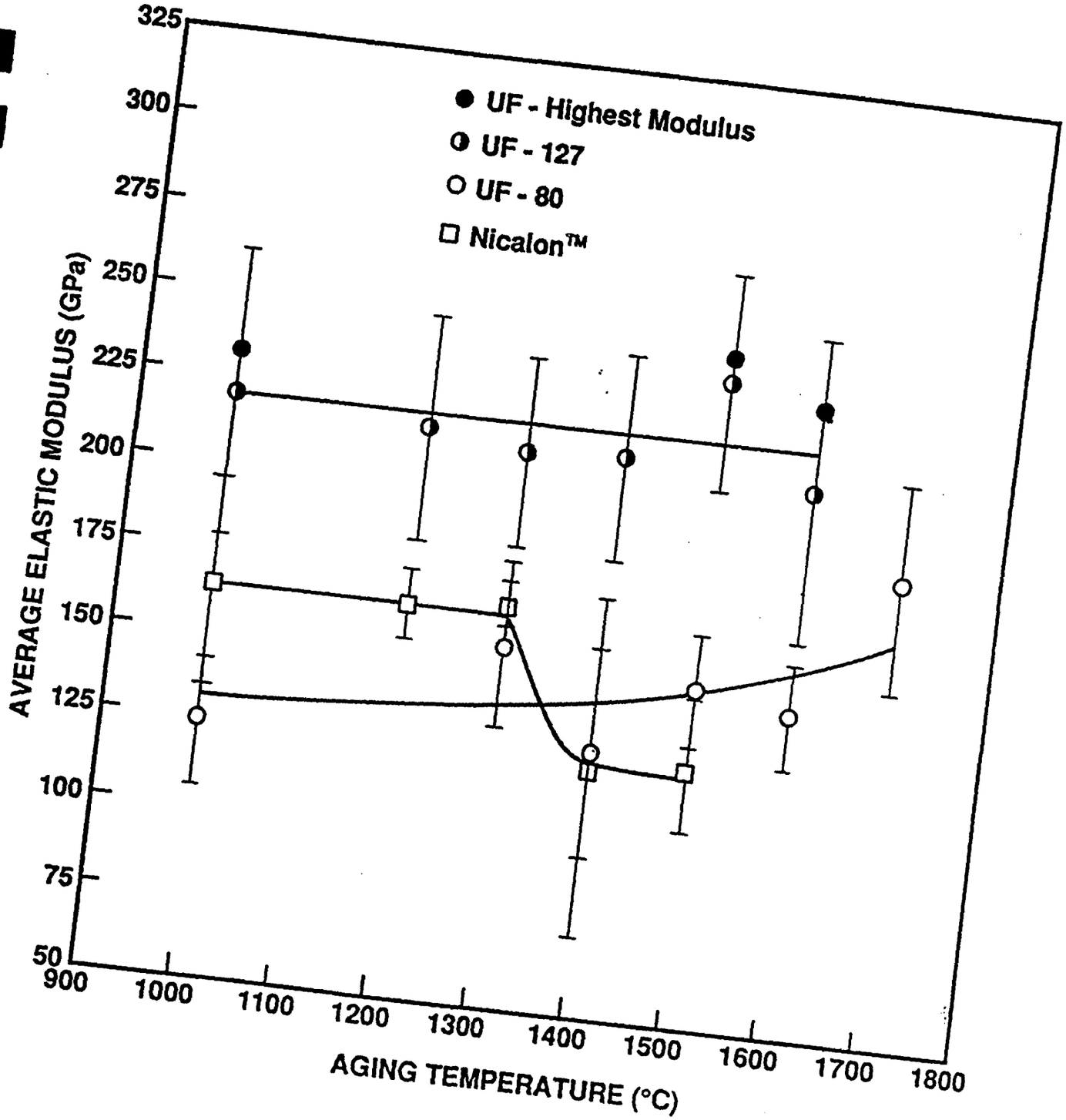
UF - Highest Modulus
UF - 127
UF - 80
Nicalon™
AVERAGE ELASTIC MODULUS (GPa)
325
300
275
250
225
200
175
150
125
100
75
50
900
1000
1100
1200
1300
1400
1500
1600
1700
1800
AGING TEMPERATURE (°C)

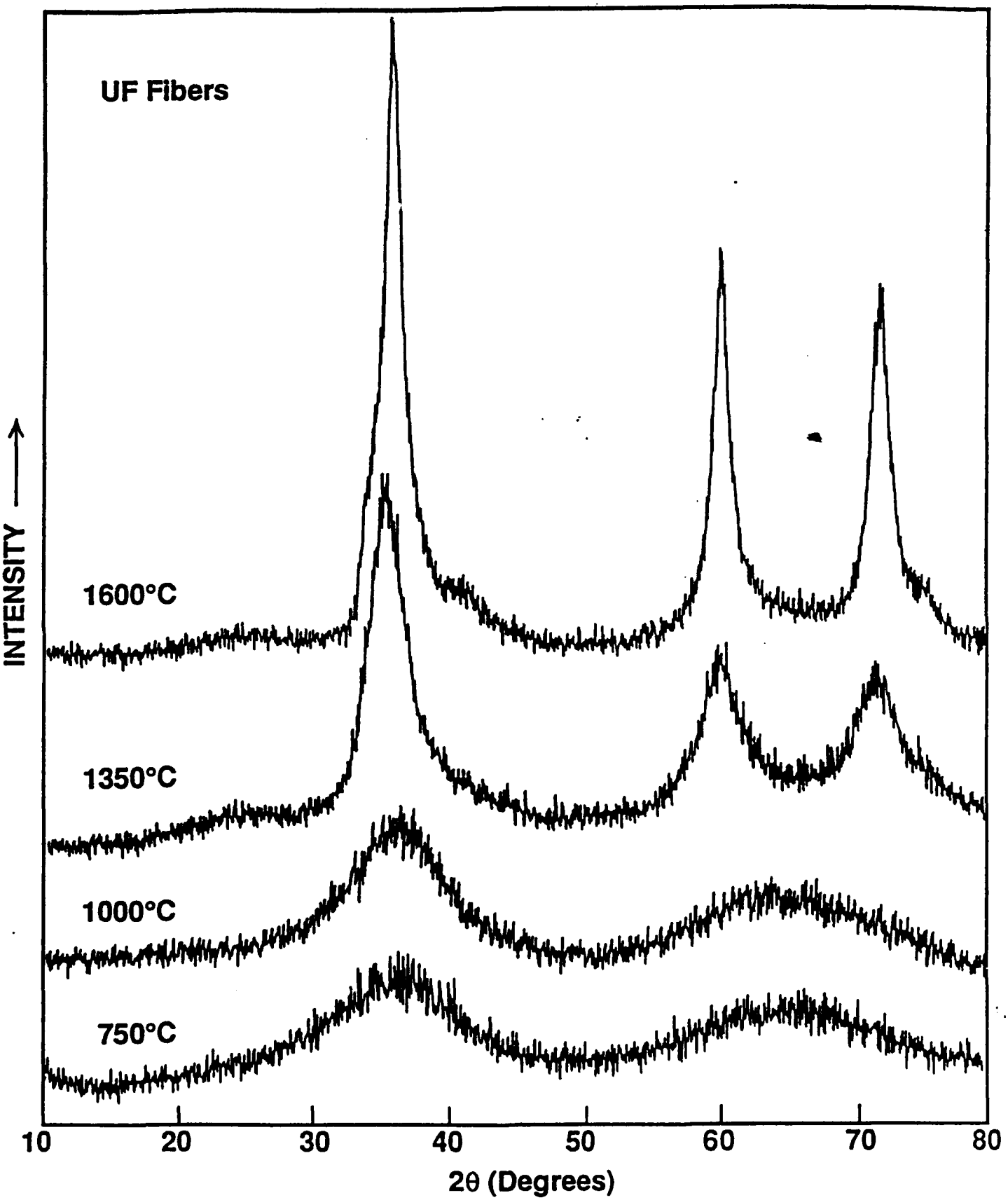
UF Fibers
1600°C
1350°C
1000°C
750°C
INTENSITY
10
20
30
40
50
60
70
80
2θ (Degrees)

US005171722A

United States Patent [19]

Toreki et al.

[11] Patent Number: 5,171,722

[45] Date of Patent: Dec. 15, 1992

[54] *SIC FIBERS HAVING LOW OXYGEN CONTENT AND METHODS OF PREPARATION*

[75] Inventors: William Toreki; Christopher D. Batich, both of Gainesville, Fla.

[73] Assignee: University of Florida, Gainesville, Fla.

[21] Appl. No.: 774,017

[22] Filed: Oct. 9, 1991

[51] Int. Cl.[5] C04B 35/52; C04B 35/56

[52] U.S. Cl. 501/88; 501/90; 501/95; 423/345

[58] Field of Search 501/90, 88, 95, 99; 423/345, 346, 347

[56] References Cited

U.S. PATENT DOCUMENTS

4,052,430	10/1977	Yajima et al.	260/448.2 D
4,100,233	7/1978	Yajima et al.	423/345
4,220,600	9/1980	Yajima et al.	556/434
4,283,376	8/1981	Yajima et al.	264/22
4,377,677	3/1983	Iwai et al.	528/35
4,414,403	11/1983	Schilling et al.	501/88
4,497,787	2/1985	Schilling et al.	501/88
4,546,163	10/1985	Haluska	423/345
4,595,472	6/1986	Haluska	501/88
4,608,242	8/1986	Schilling et al.	501/88
4,639,501	1/1987	Seyferth et al.	423/345
4,689,252	8/1987	Lebrun et al.	501/88
4,719,273	1/1988	Seyferth et al.	528/15
4,737,552	4/1988	Baney	501/90
4,889,899	12/1989	Bujalski et al.	525/479
4,889,904	12/1989	Burns	423/345
4,916,093	4/1990	Okamura et al.	264/DIG. 19

FOREIGN PATENT DOCUMENTS

2236078	3/1974	Fed. Rep of Germany .
3707225	9/1988	Fed. Rep. of Germany .

OTHER PUBLICATIONS

Yajima et al., *J. Mat. Sci.*, vol. 13, p. 2569 (1978).
Yajima, *Bull. Amer. Ceram. Soc.*, vol. 62, p. 893 (1983).
Hasegawa et al., *J. Mat. Sci.*, vol. 18, p. 3633 (1983).
Yajima et al., *Nature*, vol. 261, p. 683 (1976).
Hasegawa, *J. Mat. Sci.*, vol. 21, p. 4352 (1986).
Bunsell et al., *Composites Sci. and Tech.*, vol. 27, p. 157 (1986).
Okamura, *Composites*, vol. 18, No. 2 (1987).

Primary Examiner—William R. Dixon, Jr.
Assistant Examiner—Paul Marcantoni
Attorney, Agent, or Firm—Kerkam, Stowell, Kondracki & Clarke

[57] ABSTRACT

A method of preparing preceramic SiC fibers having a very low oxygen content by forming fibers from a solution of a polycarbosilane and a vinylic SiC precursor in a mutual volatile solvent, heating fibers in an oxygen-free inert atmosphere to effect a cross-linking reaction therebetween. Also disclosed is a method of preparing SiC fibers having superior high temperature properties and a very low oxygen content comprising heating the above-described cross-linked preceramic fibers in an inert atmosphere substantially free of oxygen for a time and at a temperature sufficient to pyrolyze the cross-linked fibers to SiC fibers. The disclosure also describes the novel fibers produced by the above-described methods.

14 Claims, 7 Drawing Sheets

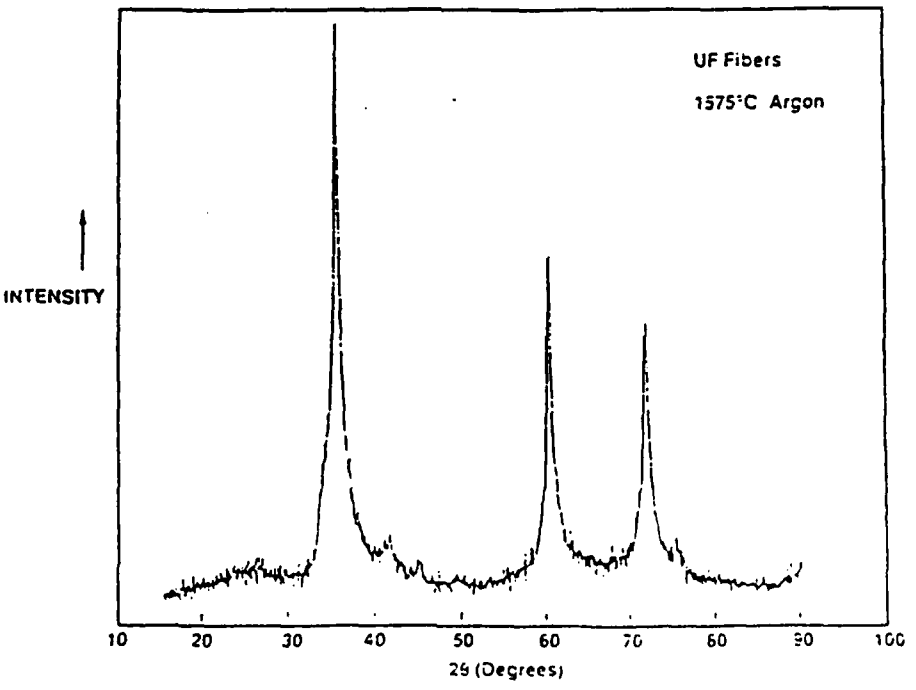

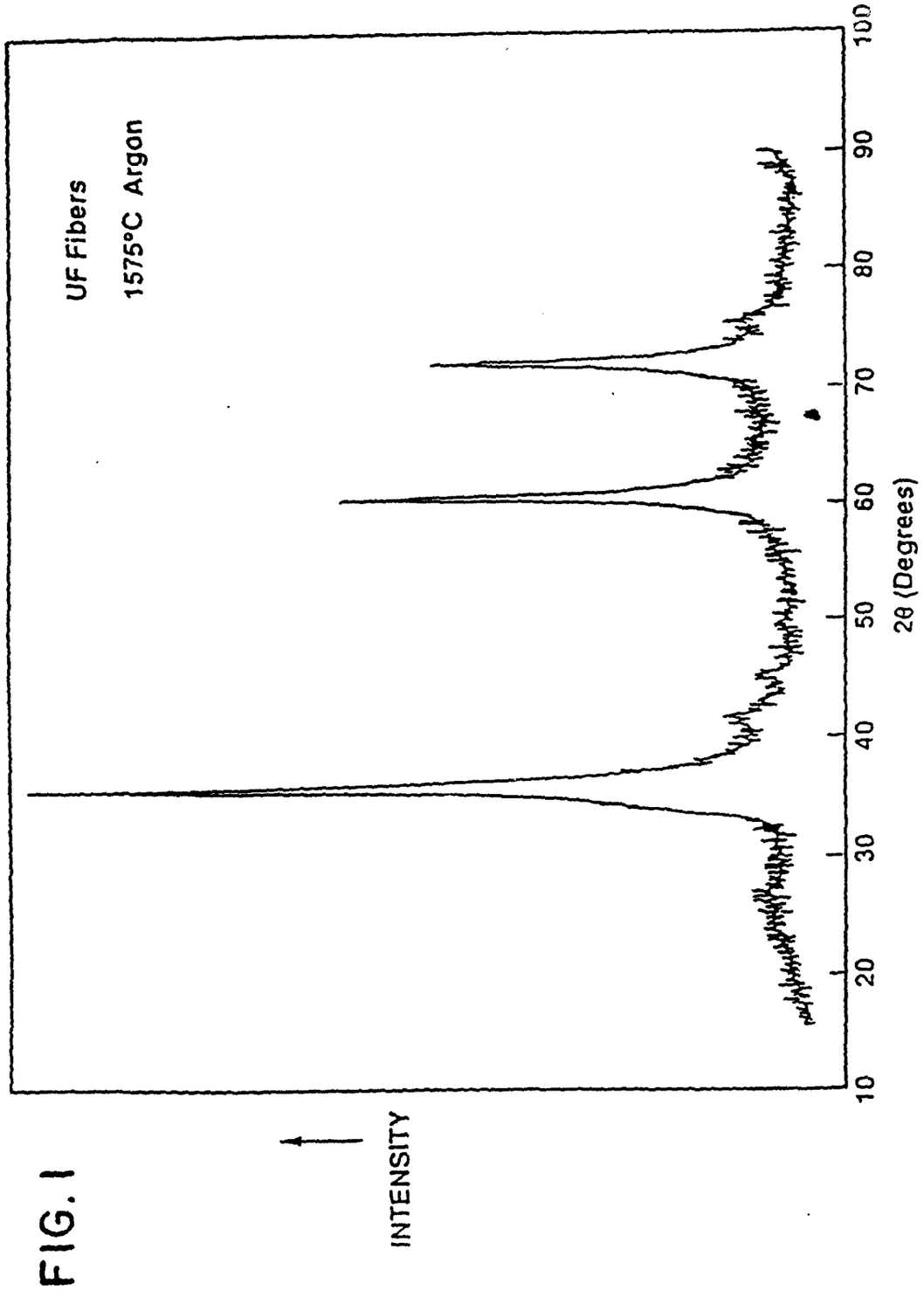
UF Fibers
1575°C Argon
INTENSITY
10
20
30
40
50
60
70
80
90
100
2θ (Degrees)

FIG. 1

FIG. 2

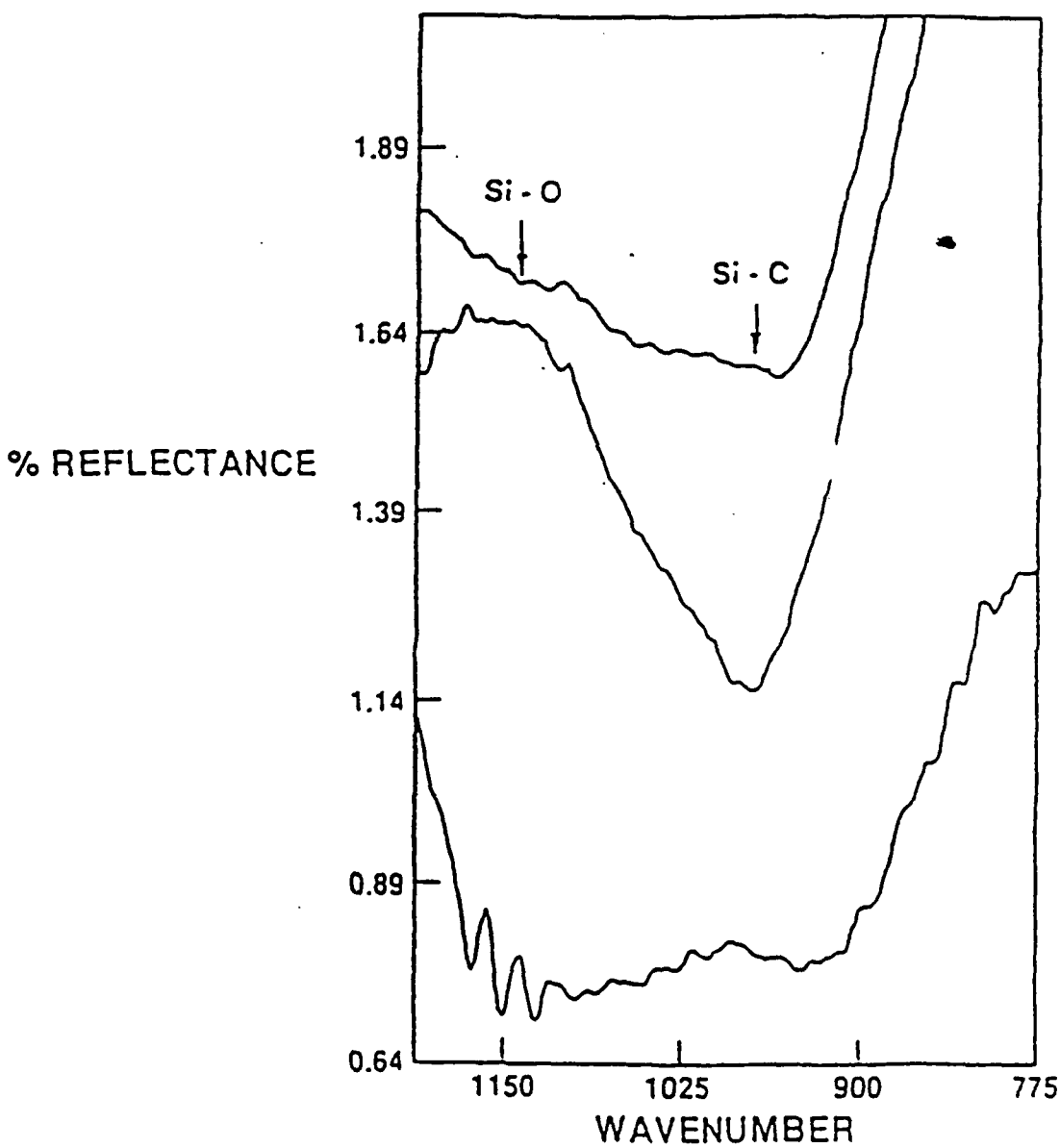
1.89
1.64
1.39
1.14
0.89
0.64
% REFLECTANCE
Si - O
Si - C
1150
1025
900
775
WAVENUMBER

FIG. 3

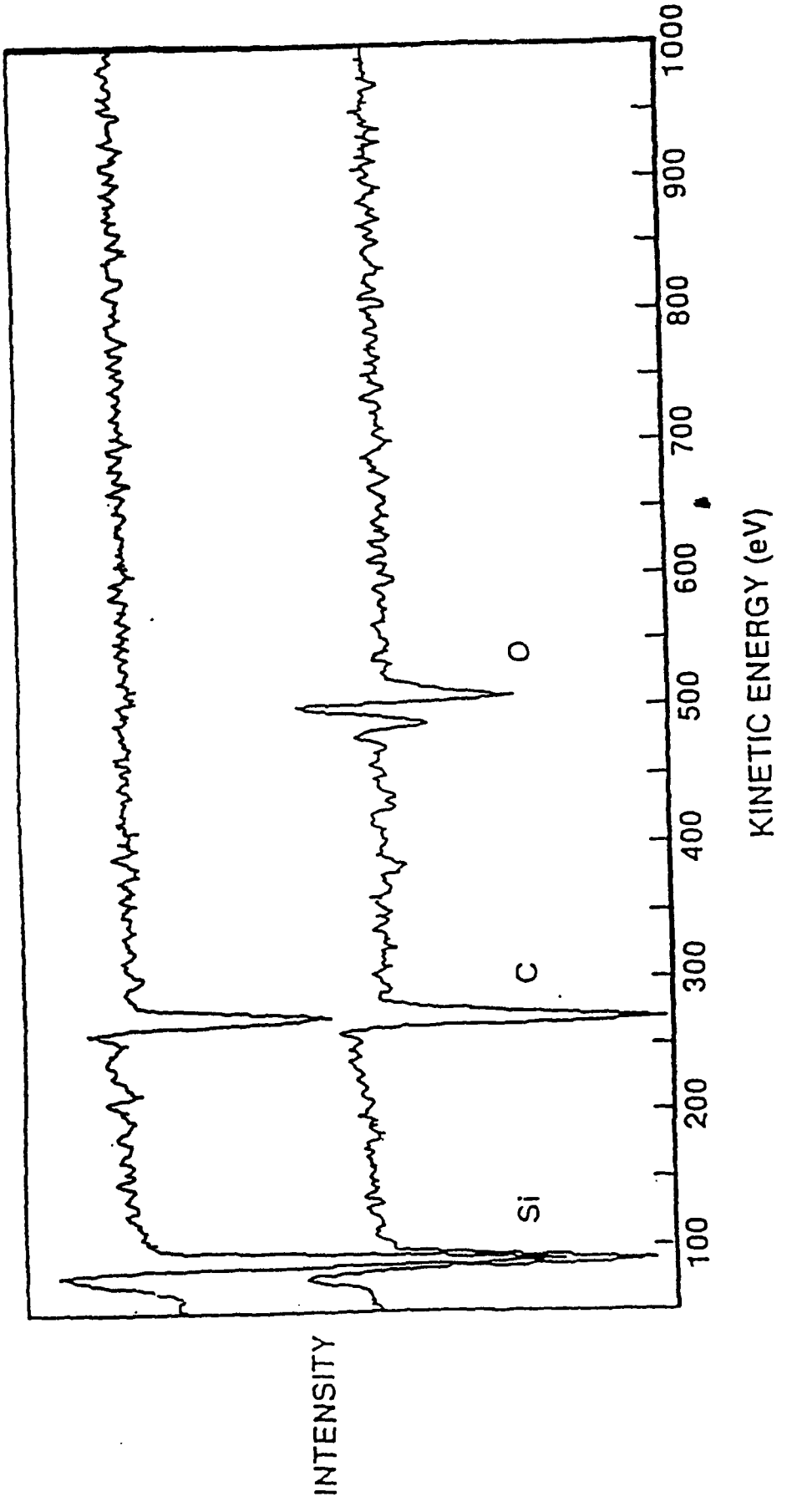
INTENSITY
Si
C
O
100
200
300
400
500
600
700
800
900
1000
KINETIC ENERGY (eV)

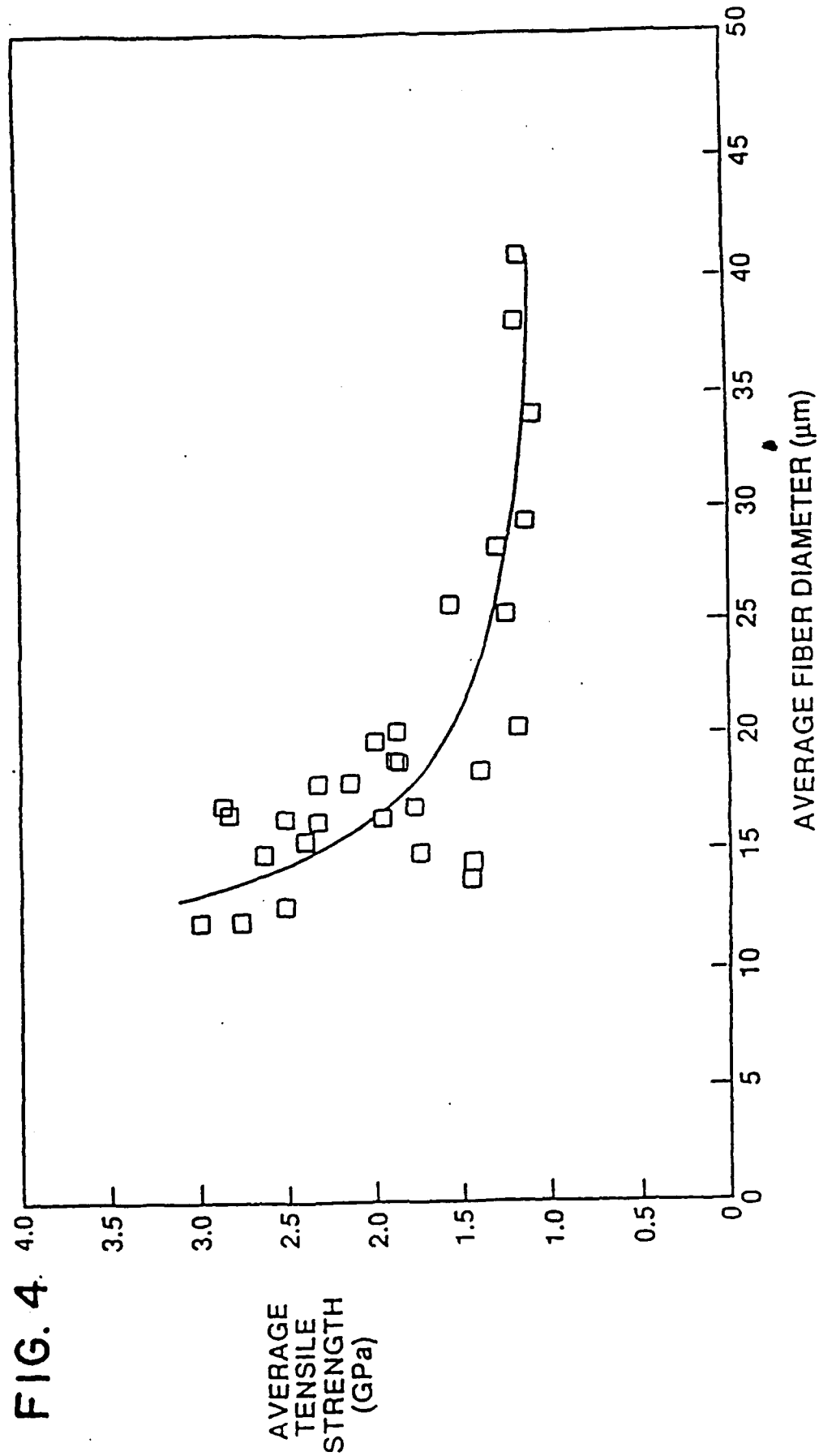
AVERAGE TENSILE STRENGTH (GPa)
4.0
3.5
3.0
2.5
2.0
1.5
1.0
0.5
0
AVERAGE FIBER DIAMETER (μm)
0
5
10
15
20
25
30
35
40
45
50

FIG. 4.

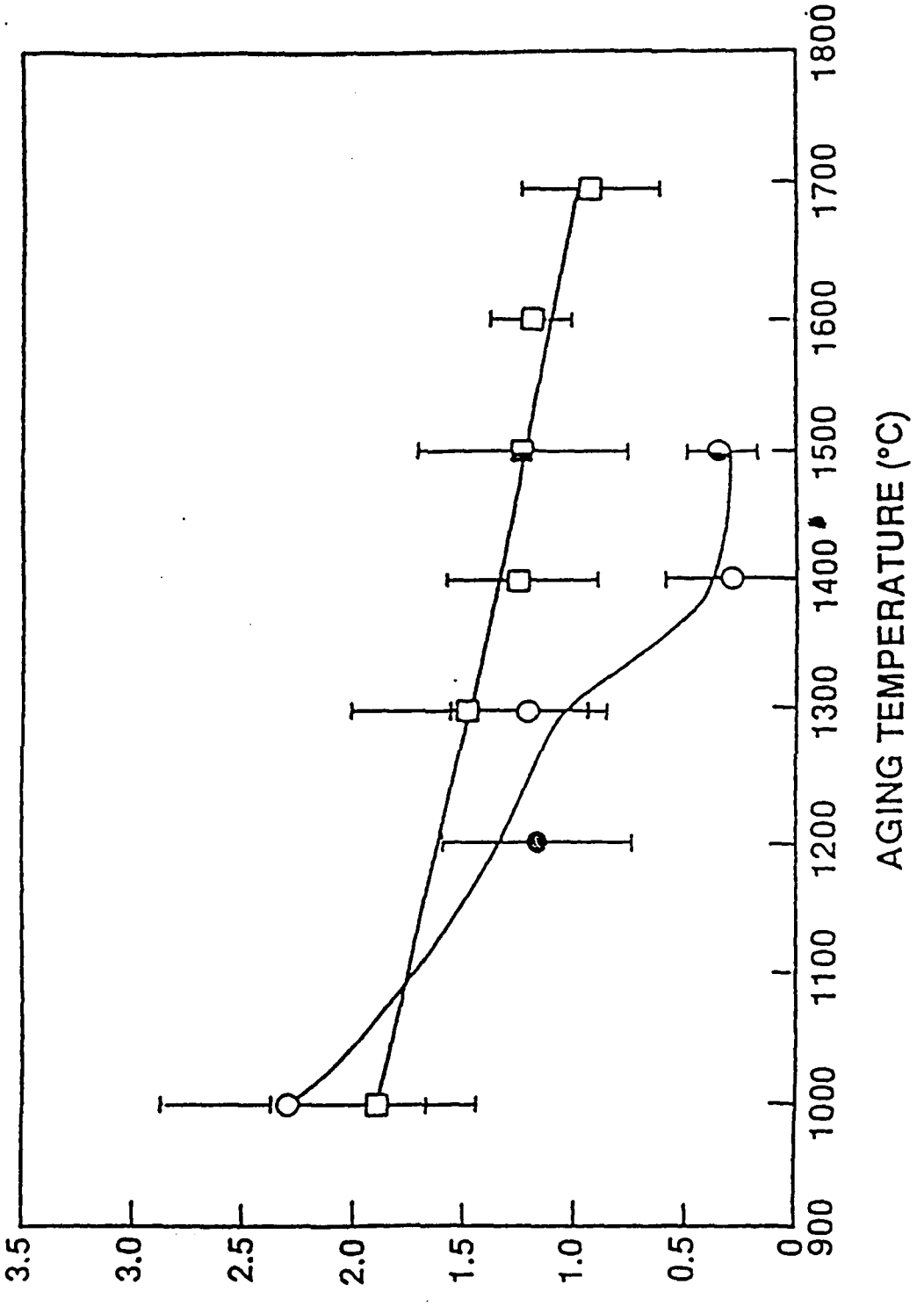
AVERAGE TENSILE STRENGTH (GPa)
3.5
3.0
2.5
2.0
1.5
1.0
0.5
0
900
1000
1100
1200
1300
1400
1500
1600
1700
1800
AGING TEMPERATURE (°C)

FIG. 5

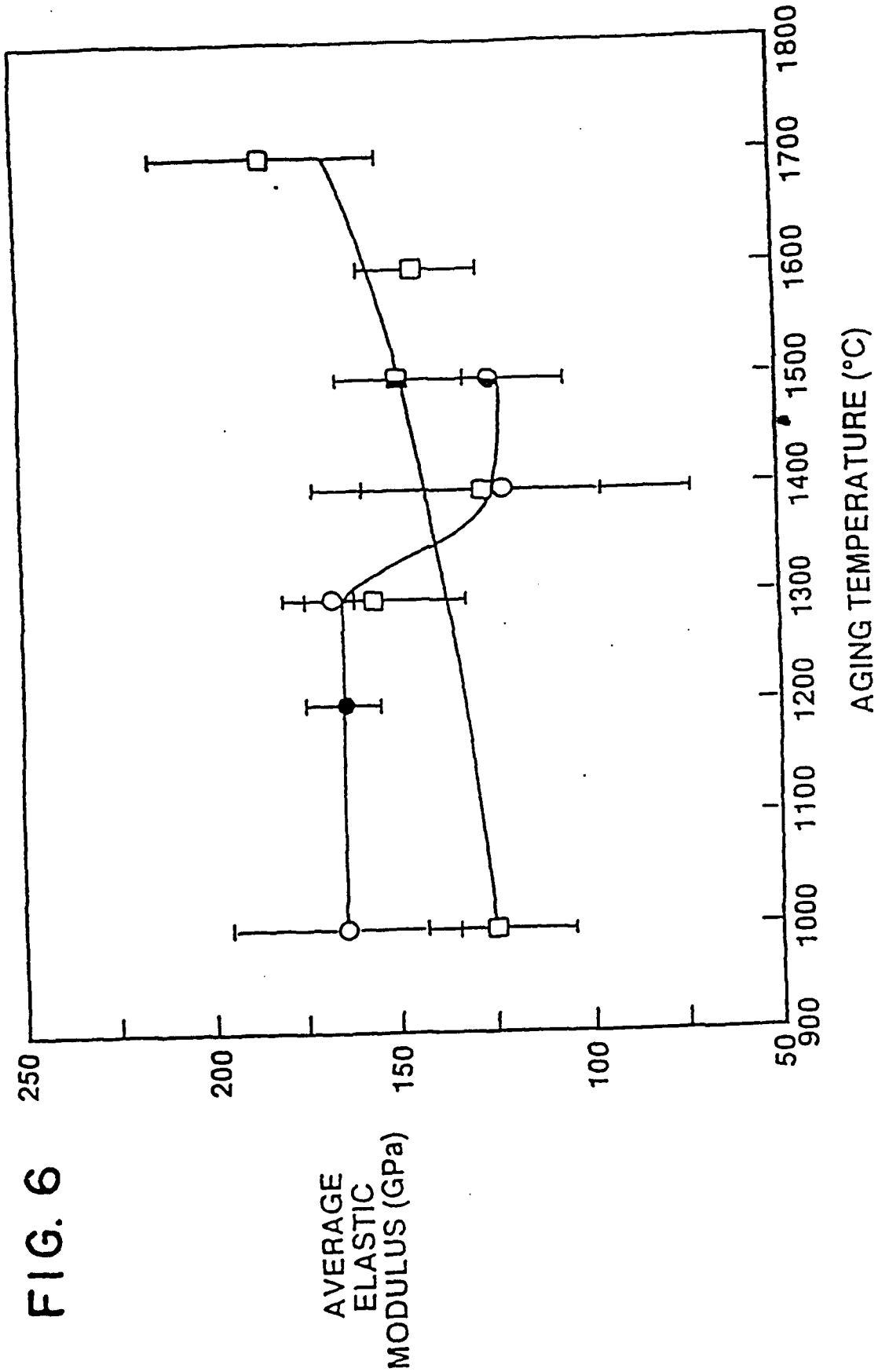
AVERAGE ELASTIC MODULUS (GPa)
250
200
150
100
50
AGING TEMPERATURE (°C)
900
1000
1100
1200
1300
1400
1500
1600
1700
1800

FIG. 6

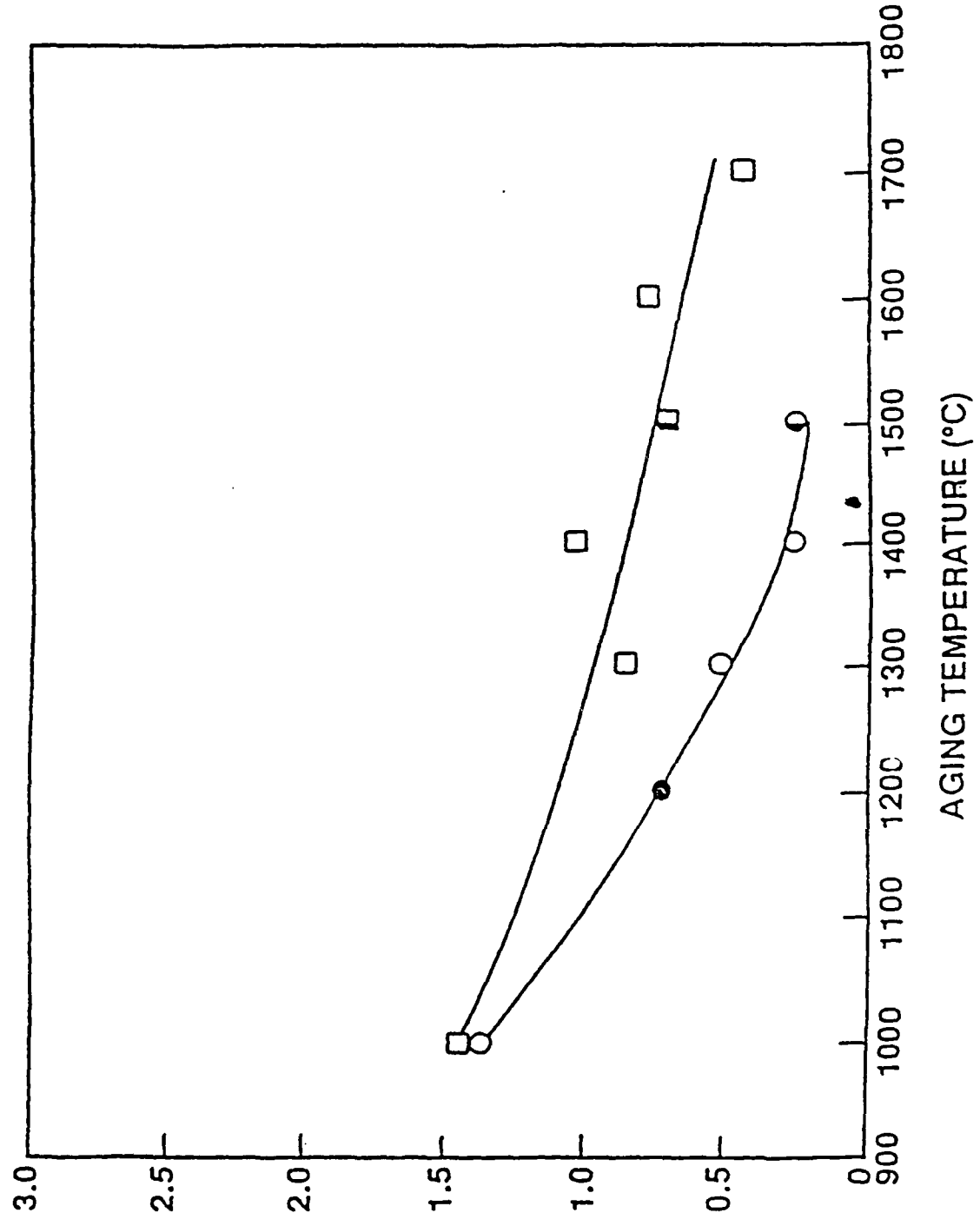
AVERAGE RUPTURE STRAIN (%)
3.0
2.5
2.0
1.5
1.0
0.5
0
900
1000
1100
1200
1300
1400
1500
1600
1700
1800
AGING TEMPERATURE (°C)

FIG. 7

SIC FIBERS HAVING LOW OXYGEN CONTENT AND METHODS OF PREPARATION

Research leading to completion of the invention was supported, in part, by Grant No. MDA 972-88-J-1006 issued by the Defense Advanced Research Projects Agency of the Department of Defense. The U.S. Government has certain rights to the invention described herein.

BACKGROUND OF THE INVENTION

1. Field of the Invention

The present invention relates to preceramic polymeric fibers, ceramic fibers prepared therefrom and methods for their preparation.

2. The Prior Art

Generally, in preparing a shaped ceramic article such as a fiber from a preceramic polymer by pyrolysis at elevated temperatures, it is necessary, prior to pyrolysis, to render the shaped article infusible. Otherwise, the shaped article will melt upon pyrolysis and thus the desired shape will be destroyed. The most common method of rendering the shaped article infusible has been an oxidation treatment. This method has the disadvantage of incorporating large amounts of oxygen in the resulting ceramic article. For example, standard grade Nicalon® ceramic fibers, prepared from polycarbosilanes by Nippon Carbon Company Ltd., Tokyo, Japan, normally contain about 10–15 weight percent oxygen. High oxygen content results in decreased thermal stability of the ceramic materials at elevated temperatures.

Ceramic materials prepared from polycarbosilanes are known in the art. Verbeek et al in German Application Publication No. 2,236,078, which is hereby incorporated by reference, prepared ceramic materials by firing a polycarbosilane prepared by the pyrolysis of monosilanes at elevated temperatures in an inert atmosphere. Linear high molecular weight polymers such as polyethylene oxide, polyisobutylene, polymethylmethacrylate, polyisoprene and polystyrene were reported to improve the fiber spinning characteristics of the polycarbosilanes. The polycarbosilane fibers were rendered infusible prior to pyrolysis by either thermal oxidation, sulfidation or hydrolysis treatment. The ceramic fibers were reported to contain between 0 and 30 weight percent of oxygen, but no details were given.

Yajima et al in U.S. Pat. Nos. 4,052,430 Oct. 4, 1977) and 4,100,233 (Jul. 11, 1978), which are both hereby incorporated by reference, prepared ceramic materials by the pyrolysis of polycarbosilanes in an inert atmosphere or in a vacuum at an elevated temperature. The polycarbosilanes were prepared by thermally decomposing and polycondensing polysilanes. Polycarbosilane fibers were treated for 2–48 hours at 350°–800° C. under vacuum prior to pyrolysis to remove low molecular weight material. In some cases, the fibers were first exposed to an oxidizing atmosphere at 50°–400° C. to form an oxide layer on the fibers and then treated under vacuum at 350°–800° C. The oxygen content of the resulting ceramic fibers was not reported.

Yajima et al in U.S. Pat. Nos. 4,220,600 (Sep. 2, 1980) and 4,283,376 (Aug. 11, 1981), which are both hereby incorporated by reference, prepared ceramic materials by the pyrolysis of polycarbosilanes partly containing siloxane bonds at an elevated temperature under an inert atmosphere or a vacuum. These polycarbosilanes were prepared by heating polysilanes in the presence of about 0.01 to 15 weight percent of a polyborosiloxane in an inert atmosphere. Polycarbosilane fibers were rendered infusible prior to pyrolysis by either treatment with an oxidizing atmosphere at about 50°–400° C. to form an oxide layer on the fiber surface or by irradiation with gamma-rays or an electron beam under an oxidizing or non-oxidizing atmosphere. The oxygen content of the resulting ceramic fibers were in the range of 0.01 to 10 weight percent by chemical analysis. Oxygen in the form of silica could be further removed from the ceramic fiber by treatment in a hydrofluoric acid solution.

Iwai et al in U.S. Pat. No. 4,377,677 (Mar. 22, 1983), which is hereby incorporated by reference, also produced ceramic materials by the pyrolysis of polycarbosilanes at elevated temperatures under an inert atmosphere or vacuum. The polycarbosilanes of Iwai et al were prepared by heating a polysilane at 50°–600° C. in an inert gas, distilling out a low molecular weight polycarbosilane fraction and then polymerizing the distilled fraction at 250°–500° C. in an inert atmosphere. Polycarbosilane fibers were rendered infusible prior to pyrolysis by heating at relatively low temperatures in air. The oxygen content of the resulting ceramic fibers was not reported.

Schilling et al in U.S. Pat. No. 4,414,403 (Nov. 8, 1983), which is hereby incorporated by reference, produced ceramic material by the pyrolysis of branched polycarbosilanes at elevated temperatures under an inert atmosphere or vacuum. The branched polycarbosilanes were prepared by reacting monosilanes with an active metal in an inert solvent at elevated temperatures where at least some of the monosilanes contained vinyl groups or halomethyl groups capable of forming branching during the polymerization. Methods of rendering the material infusible were not discussed.

Yajima et al. *J. Mat. Sci.*, Vol. 13, p. 2569 (1978); Yajima, *Bull. Amer. Ceram. Soc.*, Vol. 62, p. 893 (1983), and Hasegawa et al. *J. Mat. Sci.*, Vol. 18, p. 3633 (1983) also discuss polycarbosilanes which are useful as preceramic polymers for preparing silicon carbide ceramics. In the *Bull. Amer. Ceram. Soc.* article, Yajima prepared ceramic fibers from polycarbosilanes which had been rendered infusible prior to pyrolysis by heating in air at 190° C. The resulting fibers contained 15.5 weight percent oxygen, most of which was thought to be incorporated into the fiber during the curing step.

Baney et al in U.S. Pat. No. 4,737,552 Apr. 12, 1988), which is hereby incorporated by reference, relates to a method of rendering a preceramic polycarbosilane composition infusible prior to pyrolysis by treating the preceramic polycarbosilane composition at a temperature of 150°–400° C. under an inert atmosphere or vacuum for a time sufficient to render the preceramic polycarbosilane composition infusible wherein the preceramic polycarbosilane composition contains (1) a polycarbosilane, (2) a hydrosilylation catalyst, and (3) an unsaturated compound selected from the group consisting of reactive alkynes, polyolefins, vinylsiloxane and unsaturated siloxanes. Baney et al also disclose a method of rendering preceramic polycarbosilane polymers infusible prior to pyrolysis by treating the preceramic polycarbosilane composition with a gas selected from the group consisting of reactive diolefins, reactive alkynes and vinylsilanes at a temperature of 150°–400° C. for a time sufficient to render the preceramic polycarbosilane composition infusible wherein the prece-

ramic polycarbosilane composition contains (1) a polycarbosilane and (2) a hydrosilylation catalyst.

Seyferth et al in U.S. Pat. No. 4,719,273 Jan. 12, 1988), the entire contents of which are incorporated herein by reference, describe a process of reacting a polycarbosilane with an organo-silicon compound having at least two alkenyl groups and then forming fibers from the reaction product.

Bujalski et al in U.S. Pat. No. 4,889,899 Dec. 26, 1989), the entire contents of which are incorporated herein by reference, describe a method of preparing fibers employing a vinylic polysilane.

The use of polycarbosilane (PC) as a precursor to SiC fibers was first reported by Yajima et al in *Nature*, Vol. 261, p. 683 (1976). This method involved the synthesis of PC from a polydimethylsilane precursor. The PC was then spun into fibers and reacted with oxygen in order to cross-link the fibers and keep them from melting upon pyrolysis to ceramic. The oxygen treatment led to the presence of up to 20% SiO_2 in the final ceramic. This process is currently used by Nippon Carbon Company to produce Nicalon® fibers. The polycarbosilane used in this process has a molecular weight of $\simeq$1,500 and is marketed by Dow Corning Corporation as a ceramic precursor. An oxidative treatment is required and an 80% yield of ceramic (containing 20% SiO_2) is obtained. Pyrolysis of unoxidized material results in a lower ($\simeq$60%) ceramic yield. The presence of large amounts of SiO_2 in the ceramic is known to have adverse effects on the mechanical properties at high temperatures. [See Hasegawa et al, *J. Mat. Sci.*, Vol. 21, p. 4352 (1986)]. One review of the properties of Nicalon® fibers states that "[i]t seems clear that a fiber having a very low oxygen content would be desirable and this could only be achieved by changing the process of conversion to the precursor into the finished fiber." [Bunsell et al, *Composites Science and Technology*, Vol. 27, p. 157 (1986).] This has been accomplished to some degree by an electron beam cross-linking process; however, this is an expensive and complicated procedure [Okamura, *Composites*, Vol. 18, No. 2 (1987)]. Even though these fibers have serious drawbacks, they are considered to be state of the art and are currently enjoying widespread use in the area of composite materials.

It is an object of the present invention to provide novel SiC fibers having an extremely low oxygen content and superior high temperature mechanical properties to those produced according to present day methods.

It is another object of the invention to provide novel methods for the preparation of the above-described SiC fibers as well as intermediates therefor.

BRIEF DESCRIPTION OF THE DRAWINGS

FIG. 1 is an X-ray diffraction pattern of fibers of the invention after heat treatment to 1,575° C. in argon.

FIG. 2 is an FTIR comparison of the various fibers described herein.

FIG. 3 is a Scanning Auger Microprobe spectra of the various fibers described herein.

FIG. 4 is a graphical depiction of the tensile strength of various of the fibers described herein as a function of the fiber diameter.

FIG. 5 depicts the variation of the tensile strength of various fibers described herein as a function of the heat treatment temperature.

FIG. 6 depicts the variation of the elastic modulus of various fibers described herein as a function of the heat treatment temperature.

FIG. 7 depicts the variation of the rupture strain of various fibers described herein as a function of the heat treatment temperature.

SUMMARY OF THE INVENTION

The above and other objects are realized by the present invention which provides a method of preparing preceramic SiC fibers having a very low oxygen content comprising providing a solution of a polycarbosilane and a vinylic SiC precursor in a mutual volatile solvent therefor, forming fibers from the solution, heating the fibers in an oxygen-free, inert atmosphere for a time and at a temperature sufficient to effect a cross-linking reaction between the polycarbosilane and the vinylic SiC precursor, the temperature being below that which results in pyrolysis of the cross-linked fibers, the vinylic SiC precursor:

a) being capable of yielding stoichiometric crystalline SiC upon pyrolysis;

b) having an oxygen content below about 1% by weight;

c) being compatible with the polycarbosilane in solution therewith such that no phase separation occurs;

d) being cross-linkable with the polycarbosilane as well as homo-cross-linkable; and

e) contributing favorably to the processability and spinnability of the polymer mixture by affecting the viscoelastic behavior of the polymer solution and strength and flexibility of the spun fibers, the polycarbosilane possessing a combination of molecular weight and degree of branching sufficient to impart thereto the characteristic property that it does not melt at all, or just softens slightly when it is heated in an inert atmosphere to a temperature approaching that at which polycarbosilane begins to convert into a ceramic material (ca. 450° C.).

A further embodiment of the invention comprises a method of preparing SiC fibers having superior high temperature properties and a very low oxygen content comprising heating the cross-linked preceramic fibers described above in an inert atmosphere substantially free of oxygen for a time and at a temperature sufficient to pyrolyze the cross-linked fibers to SiC fibers.

Additional embodiments of the invention comprise the preceramic SiC fibers and the SiC fibers produced by the above-described methods.

DETAILED DESCRIPTION OF THE INVENTION

The present invention is predicated on the discovery that the formation of fibers from a mixture of a polycarbosilane (PC) and a vinylic SiC precursor having certain properties dissolved in a solvent and heating the fibers in an oxygen-free atmosphere results in the production of preceramic fibers which can be pyrolyzed in the absence of oxygen to yield SiC fibers having very little oxygen and mechanical properties at high temperatures, i.e., 1,400° C., which are vastly superior to SiC fibers currently available.

Although the above process is described as a two-stage mechanism, i.e., cross-linking followed by pyrolysis, those skilled in the art will appreciate that the method may be conducted as a one-step or a two-step method. Thus, the first heating step can be stopped after cross-linking has occurred and the cross-linked struc-

ture cooled and later pyrolyzed to produce the final product. Alternatively, and preferably, cross-linking and pyrolysis can be effected in one step by conducting a single heating step and sequentially cross-linking and pyrolyzing the article without interruption of the heating cycle.

The crux of the invention resides in the selection of the vinylic SiC precursor, i.e., a compound or polymer having vinylic unsaturation and capable of being pyrolyzed to produce SiC.

It is preferred to employ a polyvinylsilazane such as those described by Porte et al in U.S. Pat. No. 4,722,988 Feb. 2, 1988), the entire contents of which are incorporated herein by reference, or a polyvinylsilane such as those described by Bujalski et al [supra], the entire contents of which are incorporated herein by reference.

It will be understood by those skilled in the art, however, that any vinylic SiC precursor which meets the criteria listed hereinabove may be utilized in the practice of the invention.

The polycarbosilane employed in the practice of the invention is most preferably one which (1) is completely soluble in the solvent used to prepare the fibers and (2) undergoes little or no melting when heated to a temperature approaching that at which the polymer starts to convert to a ceramic (approx. 450° C.).

A PC which softens only slightly when heated in an inert atmosphere is preferred to one which is completely infusible because of the greater ease of workability of concentrated solutions thereof and the superior mechanical properties of the SiC fibers prepared therefrom. It is also preferred to one which melts completely when heated because of better retention of the shape of the fibers during the pyrolysis. A PC which exhibits little or no melting when heated typically is one which has a significantly higher MW than one which melts, although the melt behavior is not determined by the MW per se, but rather by the degree of branching of the molecule.

All of the spinning operations according to the invention are carried out at room temperature. The cross-linking occurs at approximately 125° C. The melting point of even a low MW PC is above 200° C. A slightly higher working temperature (60°-80° C.) could have engineering benefits in some cases, but this has nothing to do with the presence or absence of a melting point for the PC.

One of the keys to the success of the method of the invention is that the fibers maintain their shape during pyrolysis. High MW PC alone (without silazane) will do this, but the SiC fibers are brittle and the spinning is difficult; this is improved by using the silazane. A PC which "softens slightly" is converted by the silazane and dicumylperoxide into one which does not melt at all. Low MW PC (that which melts completely) is converted by the silazane and dicumylperoxide into one which "softens slightly" during pyrolysis and thus produces deformed fibers.

The vinylic SiC precursor imparts a plasticizing effect on the PC solution, facilitating the preparation and handling thereof, as well as the preparation of fibers therefrom. The free vinyl groups on the SiC precursor can react with the Si-H bonds on the PC, preferably in the presence of a hydrosilylation catalyst, and most preferably a free radical generator such as a peroxide, e.g., dicumylperoxide, di-t-butylperoxide, cumyl hydroperoxide, cumyl-t-butyl peroxide, 1,1-di-(t-butylperoxy)-3,5,5-trimethylcyclohexane, 1,1-di-(t-butylperoxy)-cyclohexane, t-butylperoxybenzoate, benzoylperoxide and others, particularly those which are known to be effective hydrogen abstracters or those which generate very reactive radicals such as CH_3. This results in a more highly cross-linked polymer which better maintains its shape during pyrolysis to form the SiC ceramic fibers of higher strengths. The fact that the ceramic resulting from pyrolysis of the vinylic precursor remains amorphous in nature up to a very high temperature also contributes favorably to the high temperature stability of the SiC fibers.

Suitable solvents will depend on the nature of the vinylic SiC precursor and the PC. It is essential that the solvent be a good solvent for both materials and that they are compatible with each other in the solvent, i.e., no phase separation in solution occurs. Additionally, the solvent should be non-reactive with respect to the solutes, and be volatile enough to be completely removed from the fibers at a temperature below that used for cross-linking, preferably as they are spun, thus preventing the uncross-linked fibers from sticking together. This evaporation can be facilitated by conducting the spinning operation in a heated environment or by keeping the solution at an elevated temperature prior to spinning, if necessary. The temperatures should, however, be maintained below that at which the cross-linking reaction starts to occur and below that temperature at which the polymers start to oxidize in the presence of air (around 100° C.).

Furthermore, solvents which contain oxygen are best avoided since small traces of solvent may remain trapped in the fibers and thus lead to higher oxygen contents in the pyrolyzed material. The best solvents are either aliphatic or aromatic hydrocarbons or halogenated hydrocarbons. Suitable solvents include: toluene, benzene, xylene, ethylbenzene, chlorobenzene, hexane, pentane, heptane, octane, cyclohexane, chloroform, methylene chloride, carbon disulfide and others.

Suitable concentrations of PC and vinylic SiC precursor in the solvent should be such as to enable the efficient formation of fibers. Generally, a solution containing from about 40% to about 90% total polymer by weight is appropriate for forming fibers according to conventional methods, e.g., dry spinning, wet spinning, extrusion and/or drawing from solution.

Preferably, the weight ratio of PC to vinylic SiC precursor should be in the range of from about 20:1 to about 1:2.

Generally, the formed fibers are heated to a temperature in the range of from about 25° to about 200° C. for a period of time of from about 0.5 hour to about 24 hours in order to fully cross-link the preceramic fiber. Generally, the cross-linked fibers are pyrolyzed by heating them under an inert atmosphere such as argon, nitrogen or a vacuum to a maximum temperature in the range of from about 600° C. to about 1,200° C. for a time of about 1 hour to about 6 hours in order to fully convert the polymer into a ceramic. Those skilled in the art will appreciate that the cross-linking and pyrolysis can be accomplished in a single heating step.

Alternatively, the cross-linked fibers can be pyrolyzed in a reactive atmosphere in order to impart a different chemical composition to the ceramic fibers. Pyrolysis in an ammonia atmosphere, for example, serves to reduce the relative amount of carbon in the samples while at the same time incorporating a substantial amount of nitrogen. In this manner, fibers containing varying amounts of silicon carbide and silicon ni-

tride can be formed. Pyrolysis of preceramic polymers in an ammonia atmosphere has been described by Okamura et al in U.S. Pat. No. 4,916,093 (Apr. 10, 1990).

The invention is illustrated by the following non-limiting example.

EXAMPLE

The polycarbosilane used in the following example is described in U.S. Pat. Nos. 4,052,430 and/or 4,220,600, the entire contents of which are incorporated herein by reference. The material is a white powder at room temperature and is postulated to have a nominal structure as follows:

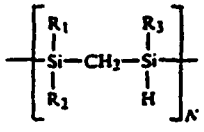

wherein R_1, R_2 and R_3=lower alkyl (preferably methyl) and/or hydrogen.

The polycarbosilane was synthesized by pressure pyrolysis of polydimethylsilane in a stainless steel autoclave under a nitrogen atmosphere. By varying the initial pressure of N_2 in the autoclave and the pyrolysis time and temperature, polycarbosilane with differing molecular weights, extents of branching, solubilities and melting behaviors can be obtained (see Table 1). The polycarbosilane was purified by dissolving the product in chloroform, filtering the solution and then precipitating the solid in a large excess of acetone followed by drying in a vacuum. The polymers were generally soluble in toluene, hexane, THF and chloroform. Molecular weights were determined by size-exclusion-chromatography in THF relative to polystyrene standards.

TABLE 1

RELATIONSHIP OF PC PROPERTIES TO SYNTHESIS CONDITIONS

Time[a]	Temp[b]	Press[c]	MW[d]	Melting[e]	Ceramic Yield[f]
1	450	1	1,000	complete	0
24	460	1	3,700	foams	65
20	480	1	5,000	none	82
24	510	1	insoluble	none	79
22	435	7	9,500	foams slightly	78

[a]pyrolysis time in hours
[b]pyrolysis temperature in °C.
[c]initial nitrogen pressure in autoclave
[d]molecular weight as determined by SEC
[e]behavior upon heating from 25° C. to approx. 500° C.
[f]percent of original solid remaining upon pyrolysis to 1,000° C. in nitrogen.

The polyvinylsilazane used in this experiment was prepared by refluxing a mixture of 1,3,5,7-tetravinyl-1,3,5,7-tetramethylcyclotetrasilazane (30 g), toluene (14 g) and dicumylperoxide (150 mg) for 18 hours under nitrogen and then removing the solvent and volatile portions at 100° C. on a rotary evaporator. The resulting polymer is a viscous liquid at room temperature and has a weight-average molecular weight of approximately 150,000. Note that if a substantially higher concentration of peroxide or a substantially lower concentration of toluene is used, then an insoluble gel will result. If 1% of dicumylperoxide is dissolved in the polyvinylsilazane and it is then heated above 115° C., a hard insoluble solid will be obtained. Pyrolysis of this solid to 1,000° C. in nitrogen results in a 67% yield of black ceramic material. The nature of this ceramic is discussed in two scientific papers Toreki et al, *Ceram. Eng. Sci. Proc.*, 11(9-10), p. 1371 (1990) and Toreki et al, *Materials Letters*, 11(1,2), p. 19 (1991), the entire contents of each being incorporated herein by reference.

A solution containing 3 g of polycarbosilane (MW 9,500—see Table 1), 0.4 g of polyvinylsilazane and 70 mg of dicumylperoxide in 12 ml of toluene was filtered through a 2-4 μm glass frit, and then a 0.20 μm PTFE filter, and then concentrated on a rotary evaporator until the solution contained approximately 30% solvent by weight.

The solution was transferred to a stainless steel fixture equipped with a spinnerette head containing three 74 μm diameter holes. The fixture was attached to a high pressure nitrogen cylinder. A pressure of approximately 350 psi was applied to the fixture. This caused the polymer solution to be forced through the three holes and exit the fixture in the form of fibers which were taken up on a 4-inch diameter rotating (120 rpm) aluminum drum placed 12 inches below the fixture. The spinning operation was conducted in the normal laboratory atmosphere at room temperature. Solvent evaporation from the fibers between the time they left the fixture and reached the drum was sufficient to dry the fibers to the point that they maintained their shape and did not stick together on the drum. When the spinning operation was complete, a single cut was made across the axis of the fibers and the fibers were removed from the drum. This resulted in a bundle of several thousand parallel fibers approximately 20-35 microns in diameter. The entire bundle was placed on a 12-inch long quartz combustion boat which was then placed inside a tube furnace. Under a slow nitrogen flow, the fibers were heated such that the temperature rose from room temperature to 150° C. during the course of 4 hours and then from 150° C. to 1,000° C. over the course of 4 additional hours. The furnace was then slowly cooled overnight. The pyrolyzed fibers were straight, shiny and black in appearance. The longitudinal shrinkage was approximately 30% and the weight loss was approximately 20%.

Analysis of the fibers by Scanning Electron Microscopy revealed that the fiber surfaces were smooth and that the diameters were in the range of 15-20 nm. The fibers generally had round or oval cross-sections. The fibers heated to 1,000° C. were amorphous in nature as determined by X-ray diffraction (XRD) and transmission electron microscopy (TEM). Heating to temperatures above 1,200° C., however, results in the formation of crystalline B-SiC. This is shown by the XRD spectrum of fibers treated at 1,575° C. in FIG. 1. Infrared spectroscopy, Scanning Auger Microprobe and neutron activation analysis indicate that the fibers have a very low oxygen content.

A comparison of the FTIR spectra of the SiC fiber of the above example (with and without an oxidation treatment consisting of heating the uncross-linked fiber in air at 150° C. for 5 hours) [hereinafter referred to as the UF fiber] with that of the commercially available Nicalon ® fiber is set forth in FIG. 2. The results indicate significantly less Si-O signal in the UF fiber than in the Nicalon ® fiber.

The Scanning Auger Microprobe spectra of Nicalon ® and the UF fibers are compared in FIG. 3 where, again, the UF fiber demonstrates a dramatically lower oxygen content. In fact, an oxygen signal is not detected at all. The limit of detection of oxygen by this method is

approximately 2% by weight. Note that the nitrogen content is also very low, but this is considered neither an advantage or a disadvantage.

Neutron activation analysis had established that the UF fibers of the above example have an oxygen content of 1.6% by weight. Analysis of Nicalon ® fibers by the same method indicates their oxygen content to be 15%.

Mechanical testing of the UF fibers have established that fibers with average tensile strengths greater than 2.5 GPa (360,000 psi) can be obtained for the 1,000° C. pyrolyzed fibers. Similarly, average elastic moduli of greater than 185 GPa (2.6×10^7 psi) and average rupture strains of greater than 1.5% can be obtained. The tensile strengths of the UF fibers are seen to increase with decreasing fiber diameter, as shown graphically in FIG. 4.

In order to evaluate the retention of mechanical properties after exposure to high temperatures, both UF and Nicalon ® fibers were heated to various temperatures under inert atmospheres. After cooling to room temperature, the mechanical properties were re-evaluated. Comparisons of UF and Nicalon ® with respect to tensile strength, elastic modulus and rupture strain are shown graphically in FIGS. 5, 6 and 7. It can be seen that the lower oxygen content resulted in significantly better retention of properties after high temperature exposure for the UF fibers as compared to Nicalon ®.

The loss of strength of Nicalon ® fibers is known to be a direct result of the loss of oxygen-containing species as the fiber is heated above 1,200° C. Thermogravimetric analysis [M. Jaskowiak et al, *J. Am Cer. Soc.*, 72(2), p. 192 (1989)] indicates weight losses of in excess of 25% when Nicalon ® is heated to 1,500° C. in argon. TGA analysis of UF fibers show that upon heating to 1,575° C. in argon, the weight loss is only 2%.

The following factors affect the properties of the final ceramic fibers:

1. Polycarbosilane (PC) molecular weight and melting point
2. Polyvinylsilazane (PSZ) molecular weight
3. Ratio of PC to PSZ
4. Solvent content and composition
5. Catalyst content
6. Spinnerette diameter
7. Spinning pressure and temperature
8. Draw-down ratio (winding, speed and distance)
9. Pyrolysis time, temperature and atmosphere.

The nature of the cross-linking reaction is a hydrosilylation reaction between Si—H groups of the PC and vinyl groups of the PSZ. Any oxygen in these fibers is purely from incidental exposure; it is not a necessary part of the cross-linking process and can be avoided entirely through proper handling.

An additional benefit to this process is that the fibers are solution (dry) spun, rather than spun from the melt (as is the case with Nicalon ®). This, along with the complete elimination of an entire processing step, provides economic benefits during the manufacturing process.

The processing variables described above (#1, 2, 3, 4 and 7) can be varied in order to achieve a wide range of rheological properties for the precursor blend. This allows the system to be tailored in order to obtain optimum ease of spinnability for the available equipment, and is thus more versatile than the current (Nicalon ®) process.

We claim:

1. A method of preparing preceramic SiC fibers having a very low oxygen content comprising providing a solution of a polycarbosilane and a vinylic SiC precursor selected from the group consisting of a polyvinylsilazane, a polyvinylsilane and mixtures thereof in a mutual volatile solvent therefor, forming fibers from said solution, heating said fibers in an oxygen-free inert atmosphere for a time and at a temperature sufficient to effect a cross-linking reaction between said polycarbosilane and said vinylic SiC precursor, said temperature being below that which results in a pyrolysis of said cross-linked fiber, said vinylic SiC precursor:
   a) being capable of yielding stoichiometric crystalline SiC upon pyrolysis;
   b) having an oxygen content below about 1% by weight;
   c) being compatible with said polycarbosilane in solution therewith such that no phase separation occurs;
   d) being cross-linkable with said polycarbosilane as well as homo-cross-linkable; and
   e) contributing favorably to the processability and spinnability of the polymer mixture by affecting the viscoelastic behavior of the polymer solution and strength and flexibility of the spun fibers, the polycarbosilane possessing a combination of molecular weight and degree of branching sufficient to impart thereto the characteristic property that it does not melt at all, or just softens slightly when it is heated in an inert atmosphere to a temperature approaching that at which polycarbosilane begins to convert into a ceramic material.

2. The method of claim 1 wherein said crosslinking reaction is effected in the presence of a hydrosilylation catalyst.

3. The method of claim 2 wherein said hydrosilylation catalyst is a free-radical generating catalyst.

4. The method of claim 3 wherein said catalyst is a peroxide.

5. The method of claim 4 wherein said catalyst is dicumylperoxide.

6. The method of claim 1 wherein said solvent is an aliphatic or aromatic hydrocarbon or halogenated hydrocarbon.

7. The method of claim 7 wherein said solvent is toluene.

8. The method of claim 1 wherein said solution of polycarbosilane and said vinylic SiC precursor contains from about 40% to about 90% total polymer by weight.

9. The method of claim 1 wherein said fibers are formed from said solution by dry spinning, wet spinning, extrusion and/or drawing from solution.

10. The method of claim 1 wherein said fibers are heated at a temperature of from about 25° C. to about 200° C. to effect said cross-linking reaction.

11. The method of claim 1 wherein the weight ratio of polycarbosilane to vinylic SiC precursor is in the range of from about 20:1 to about 1:2.

12. A method of preparing SiC fibers having superior high temperature properties and a very low oxygen content comprising heating said cross-linked preceramic fibers of claim 1 in an inert atmosphere substantially free of oxygen for a time and at a temperature sufficient to pyrolyze said cross-linked fibers to SiC fibers.

13. The method of claim 12 wherein said heating to effect said cross-linking reaction and said heating to pyrolyze said cross-linked fibers are conducted in one step.

14. The method of claim 12 wherein said atmosphere utilized for pyrolysis is a reactive atmosphere containing ammonia whereby said product fibers contain nitrogen.

* * * * *

BOOK I

Section 2

Processing

of

Mullite Composite Fibers

Principal Investigators: A. B. Brennan
J.H. Simmons

Processing of Mullite Composite Fibers

Principal Investigators: **A.B. Brennan**
J.H. Simmons

Objectives

(1) To develop a sol-gel process for the continuous extrusion of high performance mullite fibers with improved thermomechanical properties compared to commercially available mullite fibers.

(2) To optimize mullite formation for improved retention of high temperature strength through the control of microstructure and composition.

Research Summary

University of Florida researchers have developed a sol-gel process for the production of high strength, fine grain mullite fibers. The green fibers which are now produced in a continuous process have significantly higher green strength for improved handling characteristics. The process developed by the University of Florida group represents the combination of previously described non-continuous colloidal silica process with a continuous process. Independently the processes were successful in producing mullite fibers in a non continuous manner. The quality of the UF mullite fibers is apparent in their stability in 50% hydrofluoric acid compared with Nextel 440 and 480 fibers which readily dissolve in the same solution. The specific properties of the UF mullite fibers are:

(1) UF mullite fibers are produced in a continuous process as described in Figure 1. A tri-sec-butoxy aluminum sol is produced using sec-butanol and triethylamine. A second sol is produced by combining tetraethoxysilane, ethanol and stoichiometric amount of water. The two sols are combined, concentrated, and spun in a continuous manner. The resultant fibers are further condensed in high humidity and then sintered at 1400°C. This process represents significant improvements in green strength of the fibers, and the grain size of the sintered mullite fibers. The previous process reported for this project used sec-butanol as the solvent for both the tri-sec-butoxy aluminum solution and the tetraethoxysilane solution. However, we have determined that hydrolysis is inhibited by this process and thus the process outlined in Figure 1 was developed. The fibers produced using the old process did not sinter effectively such that there was macrophase segregation and a significant glassy structure. These deficiencies have been corrected by the improved process.

(2) The surface microstructure of the UF mullite was compared with that of Nextel 440

and 480 fibers by SEM. The quality of the UF mullite fibers compares favorably with that of the Nextel fibers as revealed by the SEM micrographs in Figure.

(3) The chemical stability of the UF fibers outperforms that of the Nextel fibers when both are immersed in 50% concentrated HF for 30 seconds. The Nextel fiber has significant mass reduction as illustrated in the bottom micrograph was observed for both the Nextel 440 and Nextel 480 fibers that were exposed to HF. There is no evidence of etching of the UF fiber exposed to the HF. Indeed, the stability of the UF fiber is clearly evident by a comparison the microstructure using SEM (15,000X). The upper micrograph in Figure 4 is of an unetched UF mullite fiber and the lower is a micrograph of a UF mullite fiver etched in HF. There are some minor differences in grain size between the two structures which could be due to batch to batch variation or the HF. However, more complete etching studies will be required to determine the effect of HF on the microstructure of the UF mullite fibers and its significance in terms of their overall performance.

(4) The thermal characteristics of the UF mullite fibers was characterized by a single experiment whereby thermal transitions are measured simultaneously with weight changes up to temperatures of 1300°C (Figure 5). The DTA signal is plotted separately from the TG signal for illustrating the improvements achieved through our modified proces The two thermograms plotted in Figure 5 are for the previously developed continuous process and the modified process. The current process involves a substitution of ethanol for sec-butanol in the TEOS solution. The need for this substitution was determined by kinetics studies by FTIR wherein the rate of hydrolysis of the TEOS was maximized. The solid line plot of the DTA profile illustrates a low temperature endotherm due to vaporization of ethanol, sec-butanol and water (60°C to 110°C). The higher temperature exotherms are due to thermal oxidative decomposition of carbonaceous material in the fibers (250°C to 650°C). The small exotherm at 980°C is due to the formation of mullite. The exotherm at 980°C is significant in that it represents the formation of mullite in the absence of segregation of Al_2O_3 and SiO_2 phases. The absence of the 980°C exotherm in the dashed line plot (Figure 5) is for the fibers processed under conditions that inhibited hydrolysis of the TEOS. The resultant fibers formed mullite only at temperatures of greater than 1300°C.

The thermograms in Figure 5 illustrates the improved thermal stability of the mullite fibers formed by the improved continuous process. There is no weight loss apparent (solid line) beyond the elimination of sol-gel reaction by-products at 650°C. The thermogram for the old process (dashed line) reveals weight losses up to temperatures approaching mullite formation (980°C). This exemplified the improved thermal stability of the UF mullite fibers achieved by changes in the process.

(5) The UF green fibers and sintered mullite fibers can be bent back 180° with an approximate radius of curvature of 0.25". Preliminary room temperature tensile

testing of the UF mullite fibers sintered at 1400°C indicate strengths of approximately 0.5 GPa. These values are quite low and studies are currently in progress to characterize the defect structure. Comparison testing of the Nextel fibers reveal room temperature strengths of approximately 1.0 to 1.5 GPa.

The next phase of this project is to reduce the processing time through experimental designs that will optimize, hydrolysis, concentration, viscosity and spinning rates. The defect structure of the fibers is believed to be a function of the firing procedure. However, it may also be related to the condensation of the green fibers. It is anticipated that this will be resolved within the next quarter. The introduction of zirconia into these fibers will be achieved within the next six month. It is expected that a continuous process for the fabrication of high purity mullite fibers and zirconia doped mullite fibers will be ready for pilot plant studies within the next six to eight months.

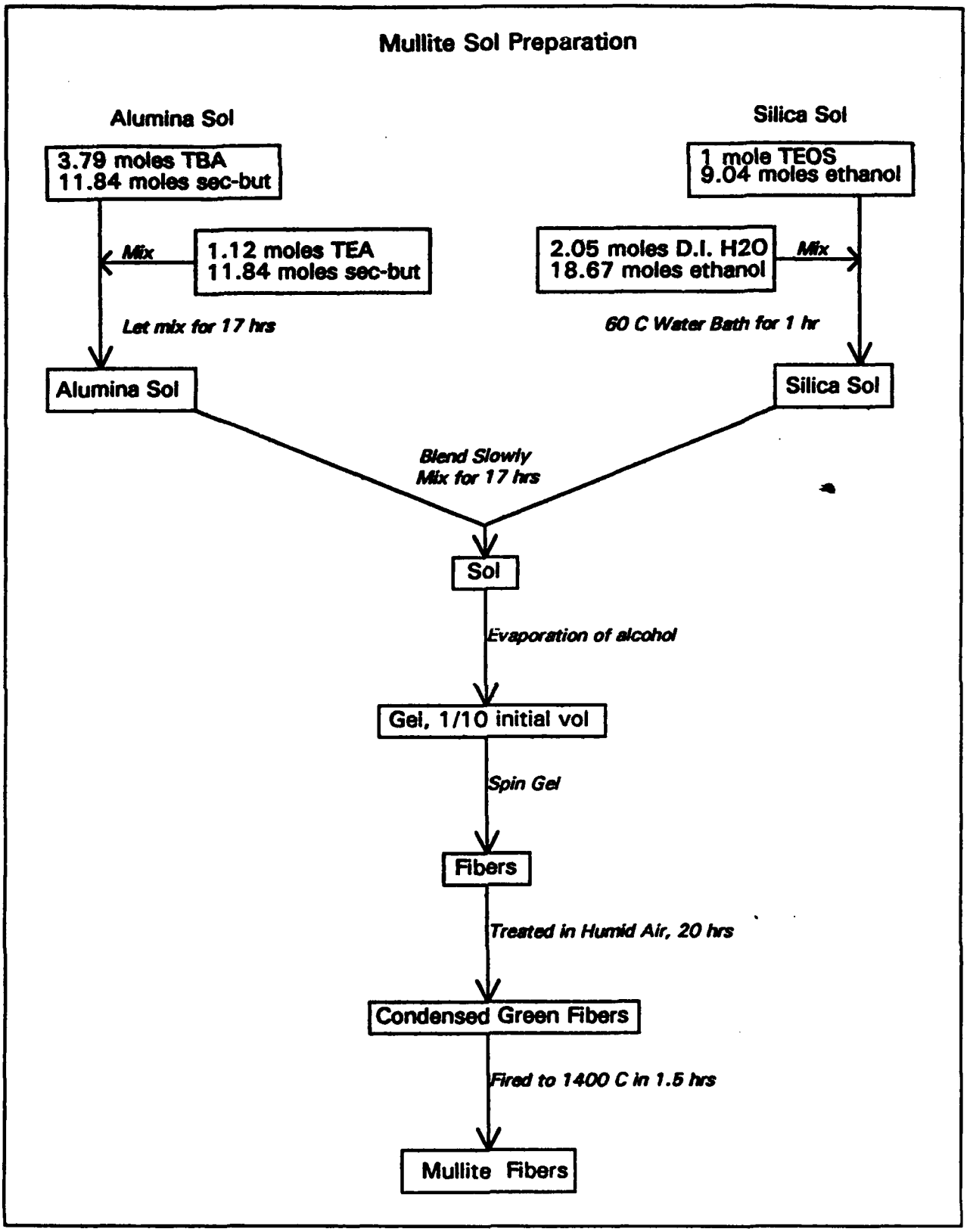

Figure 1 - UF Mullite Fiber Processing Scheme

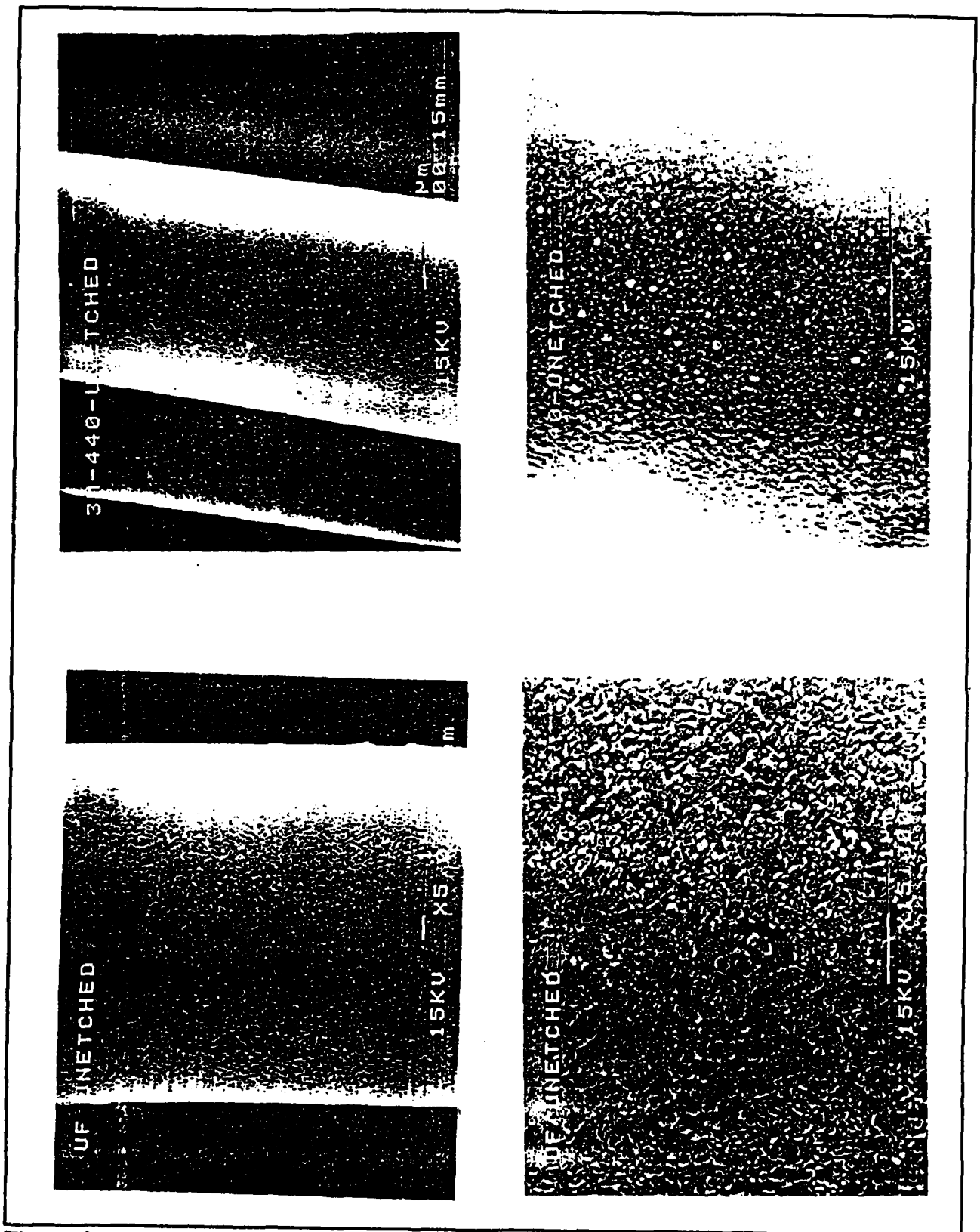

Figure 2 - UF Mullite Fiber Microstructure Compared to 3M's Nextel Fiber

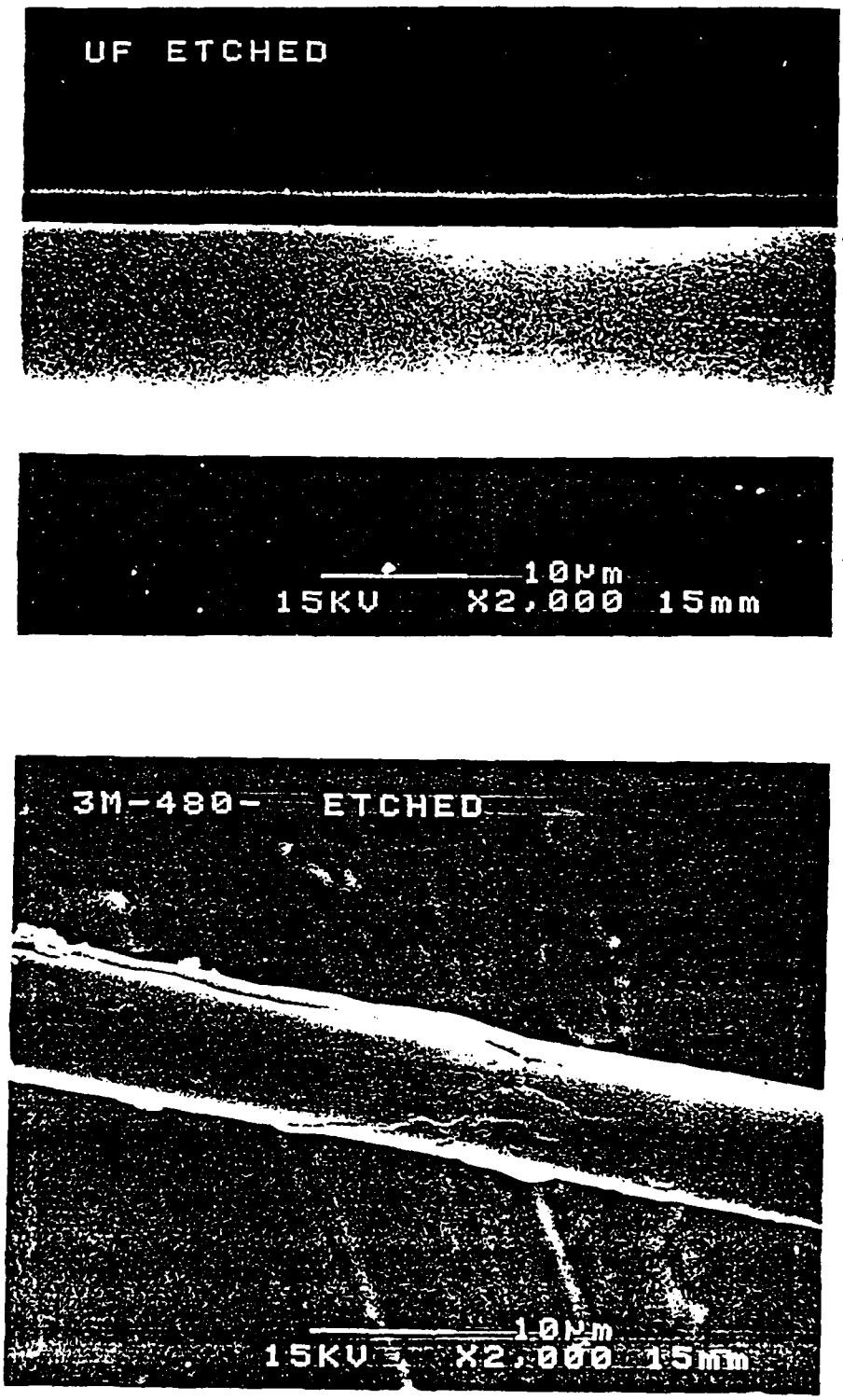

Figure 3 - Comparison of UF Mullite Fiber and 3M Nextel Fiber Stability in HF

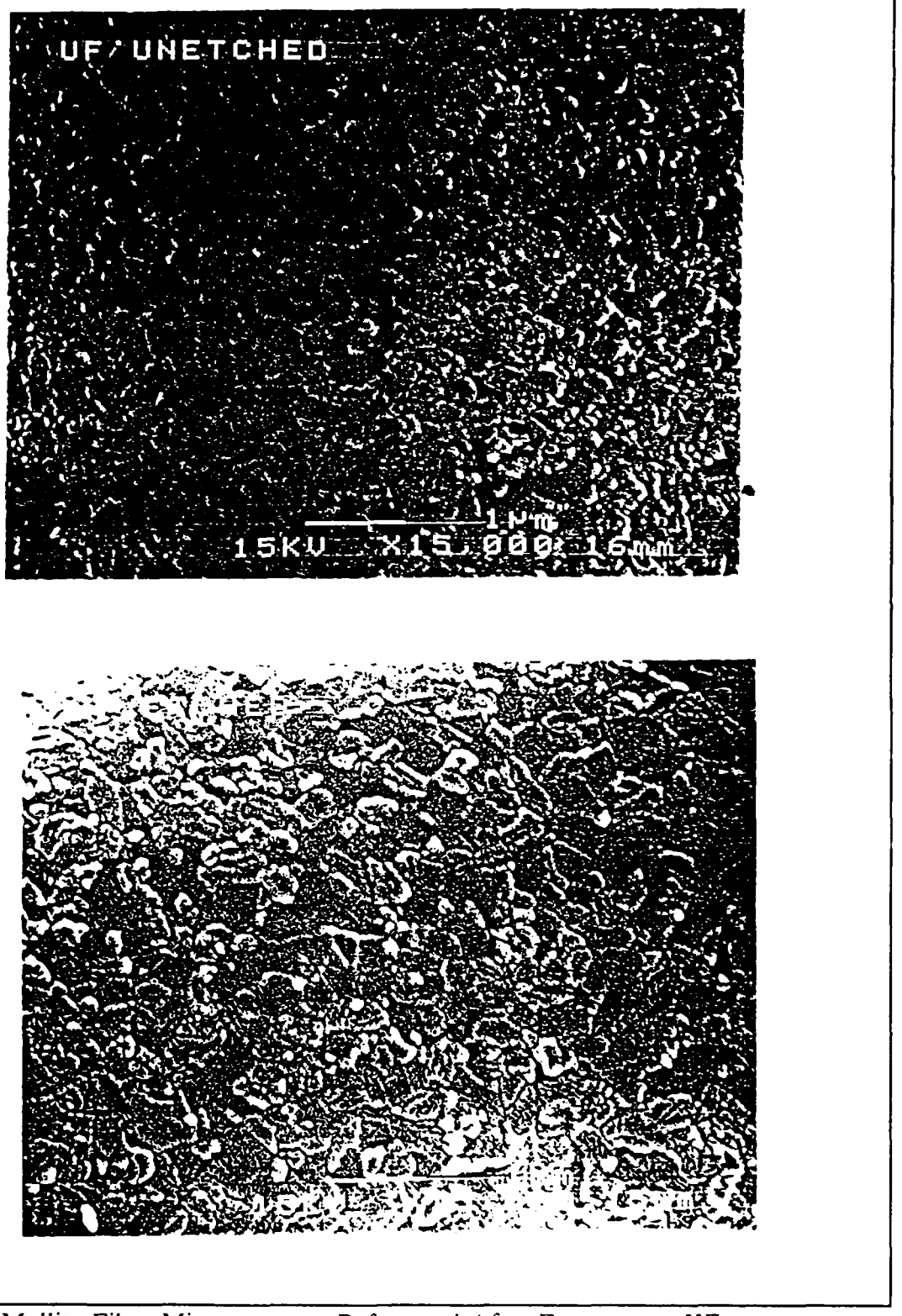

Figure 4 - UF Mullite Fiber Microstructure Before and After Exposure to HF.

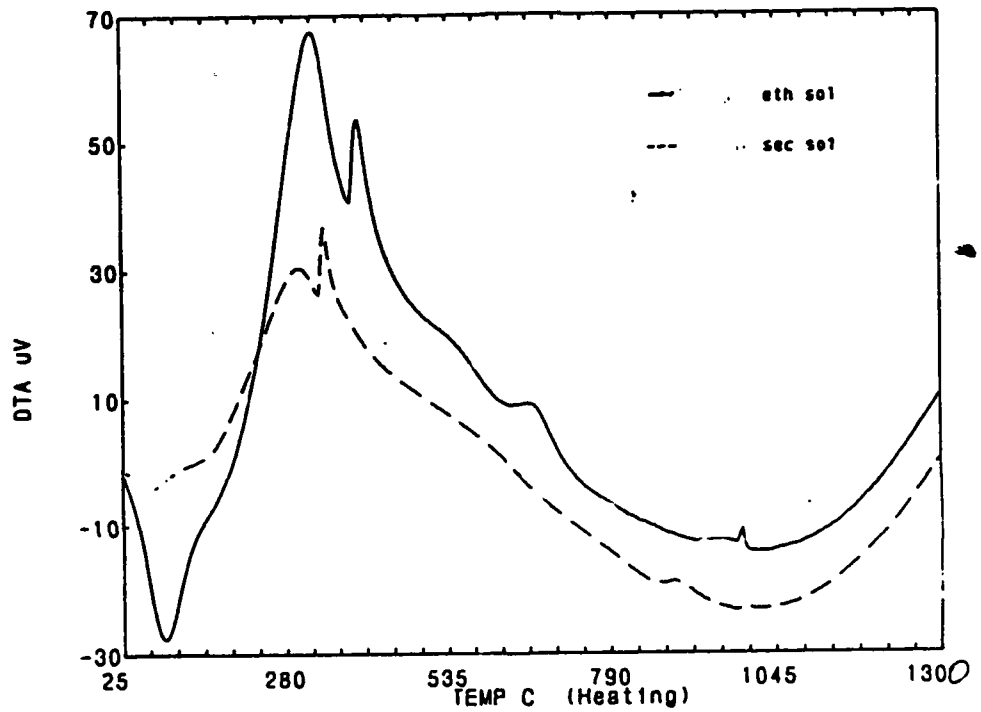

Figure 5 - DTA Profile of Sintering Process for Production of UF Mullite Fiber: Ethanol (solid) vs sec-Butanol (dashed)

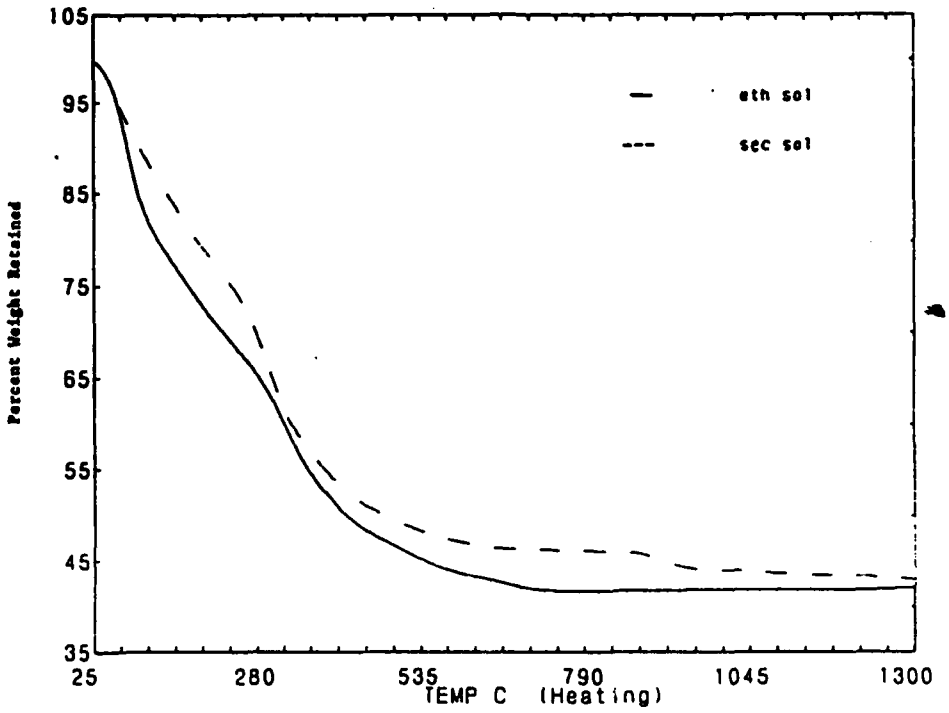

Figure 6 - TG Profile of Sintering Process for Production of F Mullite Fiber Ethanol (solid) versus sec-Butanol (dashed)

BOOK I

Section 3

Chemical Vapor Deposition (CVD)

and

Chemical Vapor Infiltration (CVI)

Principal Investigator: T. Anderson

Chemical Vapor Deposition (CVD) and Chemical Vapor Infiltration (CVI)

Principal Investigator: **T. Anderson**

Objectives

The study of the process of Chemical Vapor Deposition (CVD) in this project has pursued two major objectives.

(1) The investigation of Chemical Infiltration (CVI) in the densification of fibrous Nicalon preforms with a TiC matrix.

(2) The modification of the properties of the resulting composite via variation of the interfacial interaction between the fibers and matrix. To achieve this goal, Atomic Layer Deposition (ALD) has been proposed to precoat or "treat" the fibers with thin coatings of BN.

Research Summary

In route to the first goal, the project's first step was to obtain a quantitative understanding and to characterize the growth process of TiC on flat substrates [1,2,3]. The focus of these studies involved the determination of growth conditions leading to reaction-limited deposition, and the subsequent measurement of the process kinetics under these conditions. These results would later be used in selecting suitable operating parameters for CVI.

Although, some CVI experiments have been performed, it became clear at the beginning of this year that the requirements of the proposed goals had outgrown the existing equipment capabilities [2]. As a result, a new 4-gas, 3-bubbler CVD system was designed and constructed. This system is capable of depositing a number of carbide, nitride, boride and silicide chemistries which have already been demonstrated. The system features computer operated mass flow controllers, pressure control and a rapid reactant switching run-vent manifold. These features will allow the investigation of mixed chemistries, compositionally graded coating, multilayer structures, chloride etching effects and extended time ALE.

In our initial CVI work, we have used the forced-flow, temperature-gradient (FCVI) scheme developed by ORNL. However, as part of our CVI objectives, we have proposed a novel CVI scheme which supplements the ORNL technique with the addition of HC1 to the gaseous feed. The addition of HC1 is meant to provide a control parameter for the densification process. In the traditional FCVI scheme, infiltration occurs faster on one side of the fibrous preform due to the temperature gradient. Unfortunately, reaction still occurs

in intermediate (colder) zones because the temperature is high enough for the deposition to be allowed thermodynamically. Under ideal infiltration conditions, densification should begin at the hotter side of the preform and be restricted to a narrow thickness of the preform (reaction plane). After densification in this zone, the process should proceed by slow displacement of the reaction plane throughout the preform. In theory, the addition of HC1 should produce this effect. T prove this, the new scheme was modeled by using a complex multi-species, multi-reaction equilibrium algorithm. The results of these calculations (Figures 1 and 2) demonstrate the existence of an etch-deposition boundary for the equilibrium yield of TiC. In practice, this indicates that there is a critical concentration of HC1 under which no TiC will be formed for a given temperature gradient. By gradually lowering the HC1 concentration, colder areas of the preform gradually fall on the deposition side of the boundary, thus affording more controlled densification. The next step involved the experimental demonstration of the new scheme using the conditions resulting from the model. However, the current configuration of heating element and sample holder resulted in relatively low temperature gradients, and thus, little densification and long infiltration times, even for the traditional FCVI scheme. This set-up is under current redesign. The short term goal is, ten, to experimentally demonstrate the technique and compare it to ORNL's FCVI process. In addition, since the fast switching manifold of the new system is now available, we have resumed work on the ALD area. Currently, we are trying to deposit several chemistries on flat sapphire substrates. These results will also be available for the annual review.

Publications

(1) R. Aparicio, J.L. Ponthenier, F. Hong and T. Anderson, "Chemical Vapor Deposition on TiC_x on Al_2O_3 Substrates," Ceram. Eng. Sci. Proc., **10** [9-10] pp. 1462-1471 (1989).

(2) M.S. Dariel, R. Aparicio, T.J. Anderson and M.D. Sacks, "CVD if TiC_x on Refractory Materials," Proc. 11th International Conference on Chemical Vapor Deposition, Seattle, WA, 1990.

(3) R. Aparicio, T.J. Anderson and M.D. Sacks, "Chemical Vapor Deposition of TiC_x on Single Crystal Structures," pp. 145-152, Ceramic Transactions, Vol. 19, Advanced Composite Materials. Edited by Michael Sacks. The American Ceramic Society, Westerville, Ohio, 1991.

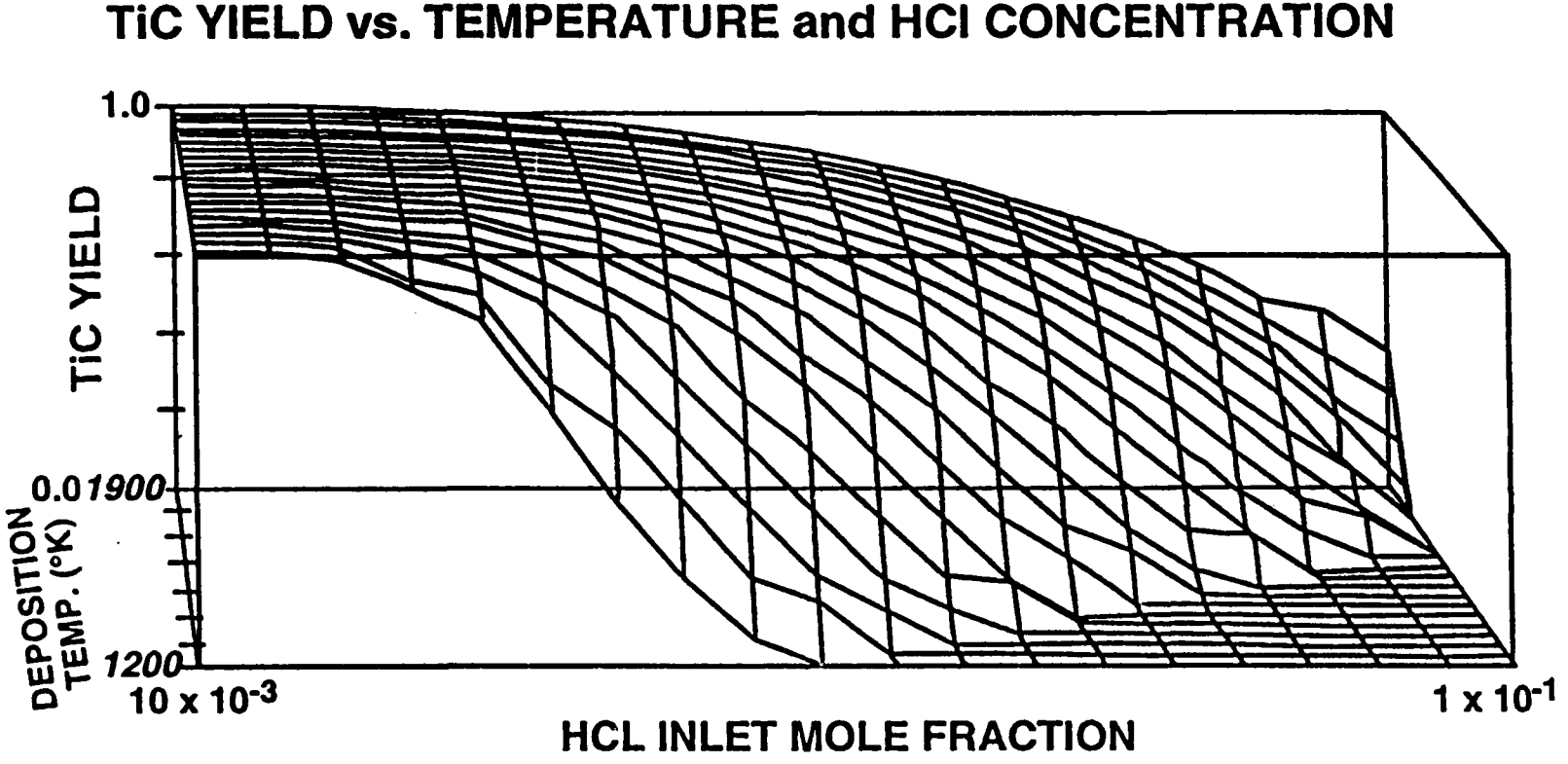

Fig 1. Equilibrium yield of TiC as a function of deposition temperature and HCl inlet concentration. The etch or no-deposition zone lies where the temperature is low and the HCl concentration is high.

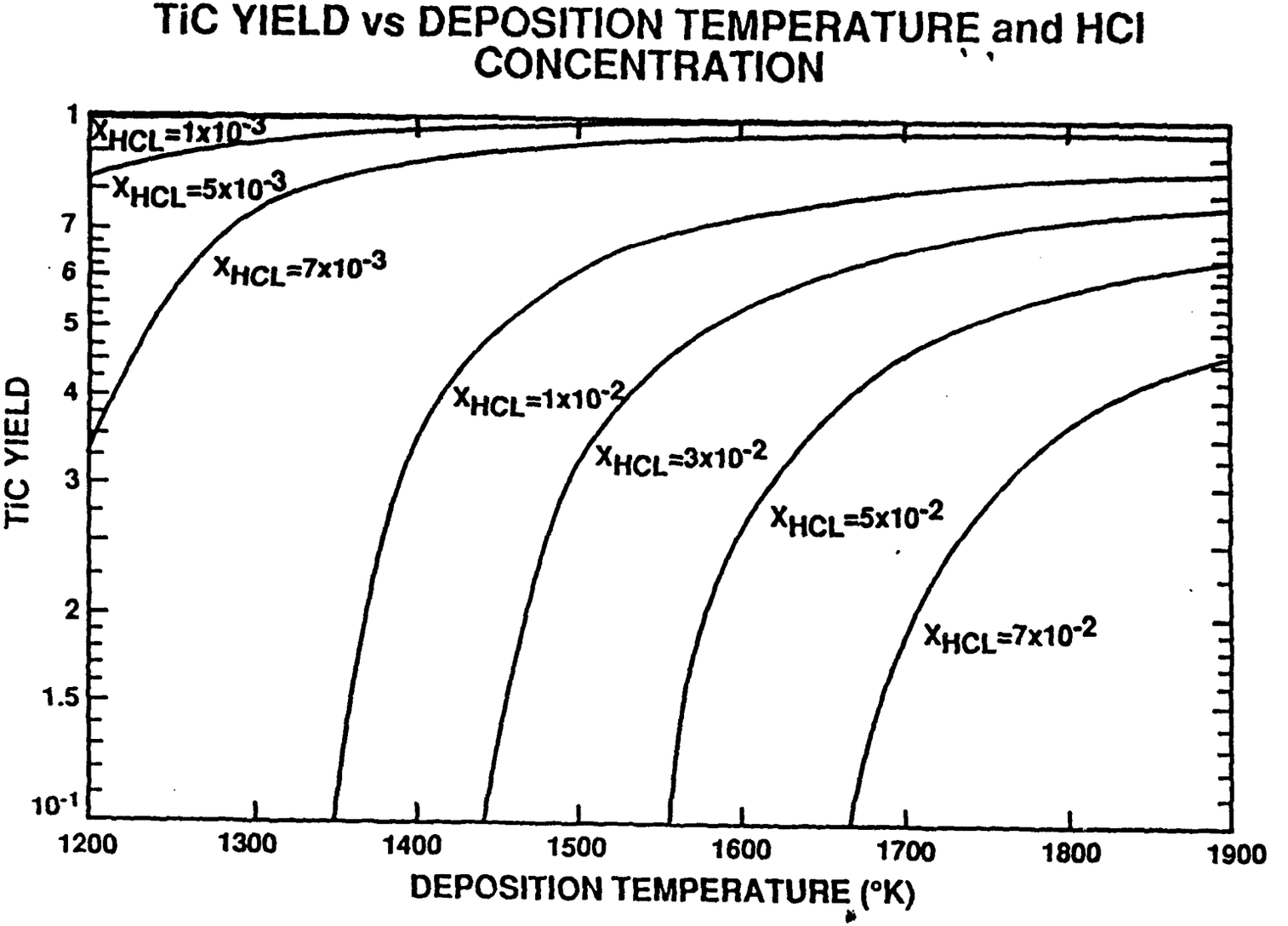

Fig 2. Equilibrium yield of TiC as function of deposition temperature for various HCL inlet concentrations.

Chemical Vapor Deposition of TiC_x on Al_2O_3 Substrates

R. APARICIO, J. L. PONTHENIER, F. HONG, AND T. ANDERSON

Chemical Engineering Department
University of Florida
Gainesville, FL

M. D. SACKS AND G. JOHNSON

Materials Science and Engineering Department
University of Florida
Gainesville, FL

Deposition of TiC_x films on Al_2O_3 substrates by chemical vapor deposition using $TiCl_4$ and CH_4 sources in H_2 was studied as a function of growth temperature and inlet feed composition. Arrhenius-type behavior was observed with an apparent activation energy of 129.9 kJ/mole. The stoichiometry of the film was measured as a function of inlet composition. The carbon content increased slightly with increasing CH_4 partial pressure, in agreement with equilibrium predictions. The TiC_x grain size increased with deposition rate, and grains were highly oriented.

Introduction

Titanium carbide is an attractive material for many applications because of its high melting temperature (3340 K), high hardness, and excellent strength. As an example, titanium carbide coatings deposited by chemical vapor deposition (CVD) have been widely used to improve the wear resistance of cemented carbide tools. Yang et al.[1] have recently proposed coating Al_2O_3 powders with TiC_x to increase the wetting of alumina by metals in metal-matrix ceramic composites.

Thermal CVD of TiC_x is most commonly performed with a chloride chemistry using $TiCl_4$ and saturated hydrocarbon precursors. Methane is easily transported, available in high purity, and the rate of thermal decomposition is expected to be relatively rapid. This expectation was confirmed by the study of Teyssandier[2] who compared the rate of depositing TiC_x on Mo substrates using either CH_4 or C_3H_8 as the carbon source. The deposition rate using CH_4 was found to be approximately three times that using C_3H_8. Deposition of TiC_x from CH_4-$TiCl_4$-H_2 mixtures on Al_2O_3 has received very little experimental study to date.

Stjernberg et al.[3] measured the influence of inlet $TiCl_4$ and HCl partial pressures on the growth rate of TiC_x at 1000°C. The average growth rate of TiC_x was quite different on Al_2O_3 substrates than on a cemented carbide substrate. More recently, Yang, et al.[1] examined the use of plasma-enhanced CVD to deposit TiC_x on fine Al_2O_3 particles and flat Al_2O_3 substrates.

The overall deposition reaction for formation of TiC_x from $TiCl_4$ and CH_4 is

$$TiCl_4(g) + xCH_4(g) + 2(1-x)H_2(g) = TiC_x + 4HCl(g) \quad (1)$$

Lindstrom and Amberg[4] reported that the deposition rate of TiC_x was independent of the total flow rate, suggesting the deposition reaction is controlled by surface reaction. Titanium tetrachloride decomposition is believed to occur by heterogeneous and parallel disproportionation to form Ti sub-chlorides and HCl. The extensive studies of Stjernberg et al.[3] on deposition of TiC_x by this chemistry suggested that a Langmiur-Henshelwood mechanism is operative and identified adsorption of CH_4 as the rate controlling step. It was also suggested that adsorption of HCl, produced by decomposition of $TiCl_4$ or intentionally added, was competitive with CH_4 adsorption. The purpose of this study was to examine in greater detail the deposition of TiC_x from $TiCl_4$-CH_4-H_2 mixtures on Al_2O_3 substrates. The effect of deposition temperature on growth rate, inlet Ti/C molar ratio on the solid composition, and growth conditions on microstructure were studied.

Experimental Apparatus

A schematic of the experimental CVD system is shown in Fig. 1. The reactor was a vertical pedestal type, heated by a 7.5 kw rf generator. The pedestal susceptor was made of graphite and supported by a closed-one-end alumina tube placed in a centered hole in the susceptor. A Pt/Pt-10% Rh control and measurement thermocouple was placed inside this support tube. The reactor was enclosed by a 76 mm quartz tube, o-ring sealed at both ends by water-cooled flanges.

Reactant and carrier gases were delivered to the reactor by a gas manifold system. Cylinder H_2, CH_4, and Ar were provided along with liquid $TiCl_4$. The $TiCl_4$ was contained in a Pyrex bubbler immersed in a constant temperature bath. Research grade H_2 was bubbled through the $TiCl_4$ source to transport $TiCl_4$. Ar was used as an inert gas to purge the system before opening the reactor to ambient.

The exit gases were first passed through a cold trap to condense $TiCl_x$ species. The remaining exhaust gases were bubbled through an Hg check valve and finally vented to atmosphere. A chemical series mechanical pump could also be connected to the exhaust line to evacuate the system before each run. Stainless steel construction was used in the exhaust system to minimize reaction with deposition reaction products.

Results and Discussion

Over 150 films of TiC_x were deposited on Al_2O_3 substrates. A majority of the alumina substrates were hot pressed pellets, 0.9 cm in diameter and 0.3 cm thick. Several depositions were also performed using high smoothness Al_2O_3 squares, 1 cm^2 in area and 0.1 cm thick. The films were characterized by x-ray diffraction and XPS to verify the deposition of single phase TiC_x.

Several experiments were performed to determine the growth rate as a function of deposition temperature. The growth rate was determined by measuring the weight gain of the substrate after deposition, assuming uniform deposition on all sides. Figure 2 shows the weight gain of the substrate as a function of growth time at three different temperatures. The $CH_4/TiCl_4$ inlet mole ratio was unity and the reactant flow rate was 2% of the total flow rate (500 sccm). The observed rate is a linear function of growth time. The thickness extrapolates to a value of zero at the beginning of growth for each temperature, indicating no significant nucleation limitation. An average growth rate was calculated from the slope of these three lines and plotted vs reciprocal temperature in Fig. 3. Arrhenius-type behavior is clearly illustrated in Fig. 3, with an apparent activation energy of 129.9 kJ/mole TiC_x. A linear regression of the data resulted in the following expression for the growth rate, r

$$\ln (r) = 6.9 \times 10^4 \text{ mg/h} \exp [-1.56 \times 10^4/T(K)] \quad (2)$$

This represents the first report of an activation energy for deposition of TiC_x on alumina. Other substrates have been used in the deposition of TiC_x and the reported activation energies are compared in Table I. The apparent activation energy of this study is the lowest reported using CH_4 as the carbon source. The substrate should influence the nucleation structure of TiC_x and therefore the grain orientation. The samples were found to have a preferred orientation in the <200>. If the process is truly controlled by heterogeneous reaction, the surface orientation will affect the apparent activation energy and may be responsible for the various observed activation energies.

A series of experiments was also performed to determine the effect of reactant inlet composition on the stoichiometry of TiC_x. In initial studies the inlet partial pressure of $TiCl_4$ was maintained constant at a value of 10^{-3} atm and the CH_4 partial pressure was varied at a constant growth temperature of 1500 K and total flow rate of 1000 sccm.

The value of the C/Ti molar ratio was determined from the lattice parameter measured by x-ray diffraction. The results for several runs are shown in Fig. 4. The reproducibility for a given set of operating parameters is seen to be excellent. All films were found to be near the TiC-Ti 2-phase boundary. The carbon content gradually increased with increasing CH_4 partial pressure. This rather flat response to

Table I. Comparison of Activation Energies for Deposition of TiC_x on Various Substrates

Substrate	E (kJ/mole)	Hydrocarbon Source	P (atm)	Reference
WC-Co	351-393	C_3H_8	1	5,6
WC-Co	276	CH_4	1	7
WC-Co	184	CH_4	1	6
WC-Co	372	CH_4	1	4
Graphite	418	CH_4	0.132	8
Graphite	159	Ch_4	1	7
Graphite	84	none	1	9
Graphite	100	none	1	10
Porous Graphite	62	none	1	11
Pseudocrystal Graphite	71	none	1	11
Mo	192	CH_4	1	9
WC-Co	108	none	1	4
Steels	201	CH_4	1	12
Al_2O_3	129.9	CH_4	1	this study

methane partial pressure is consistent with the predictions of thermodynamic analysis,[11,13,14] though the predicted C/Ti molar ratio is slightly higher.

The microstructure of deposited TiC_x was also examined as a function of growth conditions. Shown in Fig. 5(*a–f*) are scanning electron micrographs of TiC_x films deposited on high smoothness Al_2O_3 substrates at various growth conditions. All micrographs are at the same magnification. Figure 5(*a*) shows the clean Al_2O_3 substrate has surface roughness on the order of a few microns. Figures 5(*b–f*) show the microstructure of TiC_x films deposited at a constant pressure of 1 atm and total flow rate of 500 sccm. The effect of deposition temperature is seen by comparing Fig. 5(*b*) (1500 K) and (*d*) (1600 K). The increase in growth rate produces a considerably larger grain size. Very little growth occurred under the growth conditions represented by Fig. 5(*b*). It appears that growth is initiated on the flat portions of the individual Al_2O_3 grains. The influence of $CH_4/TiCl_4$ molar ratio at constant temperature on the microstructure is shown in the series of micrographs (*c–f*). Since growth rate is first order in CH_4 partial pressure, a significant increase in the grain size is produced as the $CH_4/TiCl_4$ molar ratio is increased. It is also observed that the TiC_x grains are highly oriented. A microstructure similar to that shown in Figs. 5(*c*) and (*d*) was reported by Yang et al.[1]

Conclusions

Chemical vapor deposition has been used to grow TiC_x films on both rough and high smoothness Al_2O_3 substrates. The films were confirmed to be single phase TiC_x by both x-ray diffraction and XPS.

The deposition appears to be rate-limited by heterogeneous reaction with a measured apparent activation energy of 129.9 kJ/mole. The stoichiometry of TiC_x was measured as a function Ti/C molar ratio and the results were qualitatively consistent with equilibrium predictions. The deposited films consisted of oriented grains that increase in size as the growth rate increased (i.e., increasing deposition temperature and increasing $CH_4/TiCl_4$ molar ratio).

Acknowledgment

The authors gratefully acknowledge that this work was supported by the Defense Advanced Projects Agency (MDA972-88-J-1006). The authors thank Dr. John Halloran of Ceramics Process Systems for providing the high smoothness of Al_2O_3 substrates.

References

[1]M. Y. Yang, S. P. Kohler, and B. M. Kramer, *Adv. Ceram. Mat.*, 3, 341 (1988).
[2]F. Teyssandier, Ph.D. Thesis, University of Grenoble (1986).
[3]K. G. Stjernberg, *Thin Solid Films*, 40, 81 (1977).
[4]J. N. Lindstrom and S. Amberg, Proc. IV Int. Conf. CVD, 115 (1973).
[5]M. Lee and M. N. Richman, *J. Electrochem. Soc.*, 120, 993 (1978).
[6]J. S. Chun and C. W. Lee, Proc. IX Int. Conf. CVD, 573 (1981).
[7]J. S. Cho and J. S. Chu, Proc. VIII Int. Conf. CVD, 540 (1988).
[8]F. Langlais, R. Naslain, and J. Y. Rossignol, Proc. IX Int. Conf. CVD, 596 (1984).
[9]L. Agour, E. Fitzer, and J. Schlichting, Proc. V Int. Conf. CVD, 600 (1975).
[10]R. S. Ambertsumyan and B. N. Babich, *Akad. Nauk. SSSR. Neorg. Materialy*, 5, 301 (1969).
[11]C. Vincent, Ph.D. Thesis, University of Lyon (1987).
[12]T. Takalashi, K. Tomita, and K. Sugiyama, *J. Electrochem. Soc.*, 114, 1 (1974).
[13]C. Bernard, M. Ducarrior, and F. Teyssandier, *J. Less-Common Metals*, 78, 269 (1981).
[14]C. Bernard, M. Ducarrior, and F. Teyssandier, *J. Electrochem. Soc.*, 135, 225 (1988).

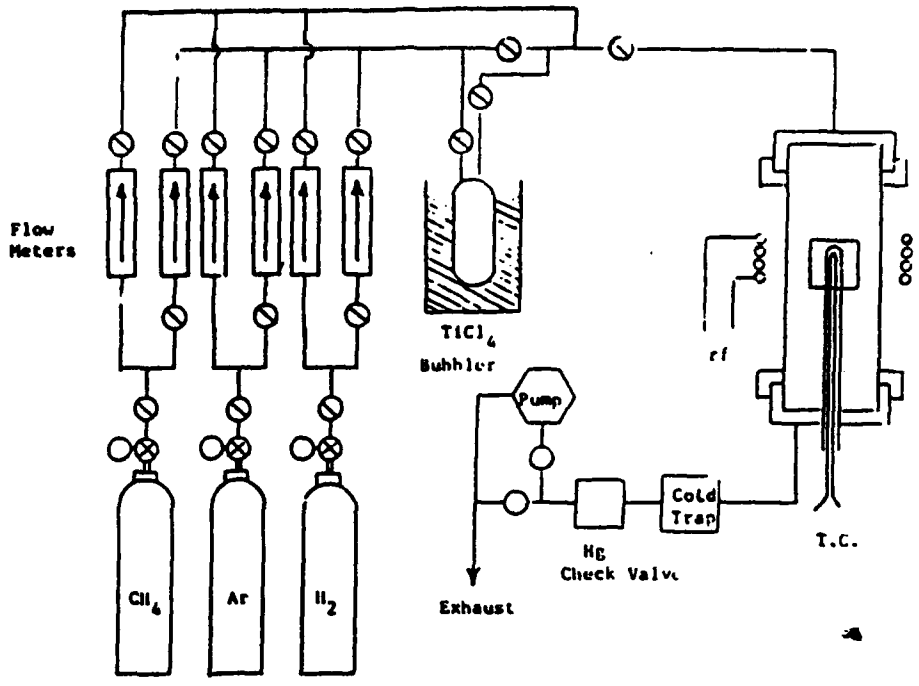

Fig. 1. Schematic of CVD system.

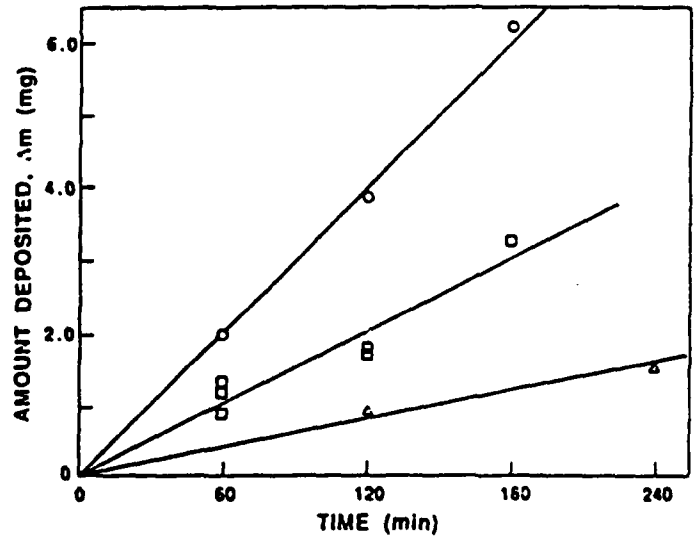

Fig. 2. Amount of TiC_x deposited on Al_2O_3 substrates as a function of deposition time for three deposition temperatures: O, 1500 K; ⧈, 1400 K; Δ, 1300 K. The deposition pressure was 1 atm and inlet flow rates were: $TiCl_4$, 5 sccm; CH_4, 5 sccm; and H_2, 490 sccm.

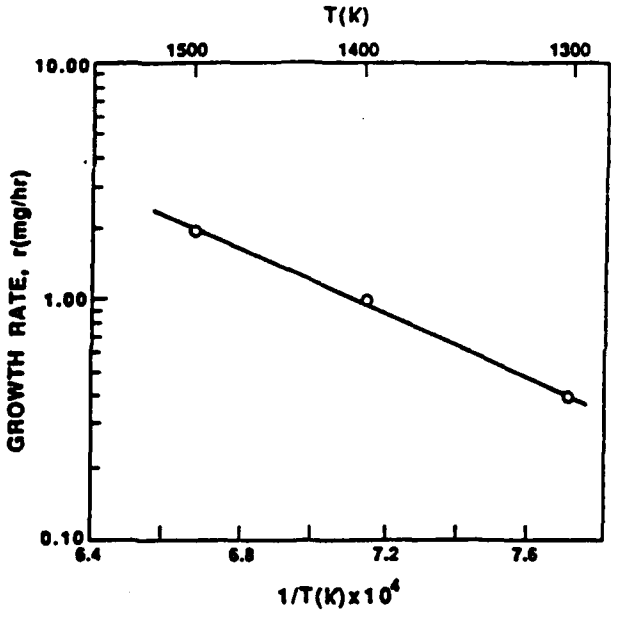

Fig. 3. Growth rate, mg/h, of TiC_x as a function of reciprocal deposition temperature.

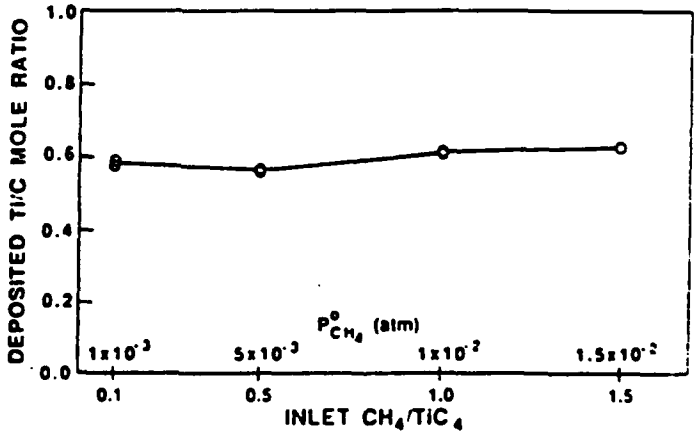

Fig. 4. Effect of inlet $CH_4/TiCl_4$ molar ratio on the stoichiometry of deposited TiC_x at 1500 K. The total flow rate was 1000 sccm and the $TiCl_4$ flow rate was constant at 10 sccm.

Fig. 5. Scanning electron micrographs of TiC_x deposited on Al_2O_3 substrates by CVD at 1 atm pressure and total flow rate of 500 sccm: (*a*) clean Al_2O_3 substrate; (*b*) deposition temperature, 1500 K, $CH_4/TiCl_4$ inlet molar ratio, 1.0; (*c*) deposition temperature, 1600 K, $CH_4/TiCl_4$ inlet molar ratio, 0.5; (*d*) deposition temperature, 1600 K, $CH_4/TiCl_4$ inlet molar ratio, 1.0; (*e*) deposition temperature, 1600 K, $CH_4/TiCl_4$ inlet molar ratio, 3.0; (*f*) deposition temperature, 1600 K, $CH_4/TiCl_4$ inlet molar ratio, 4.0.

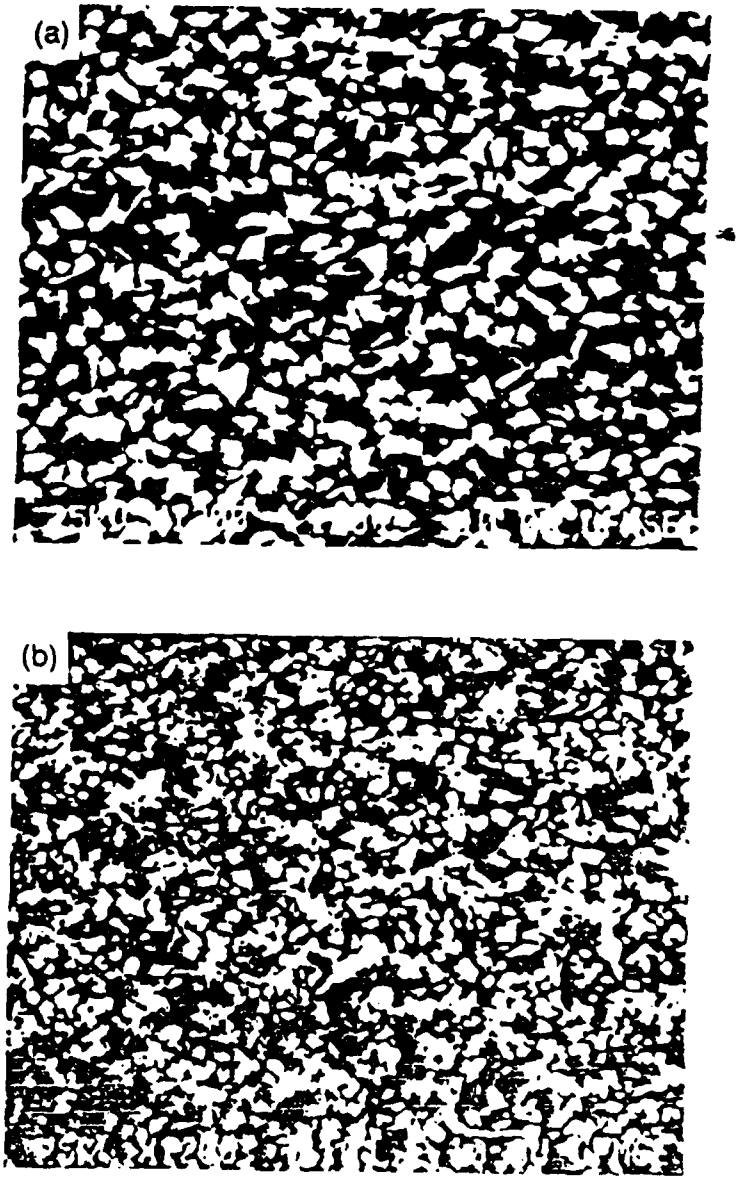

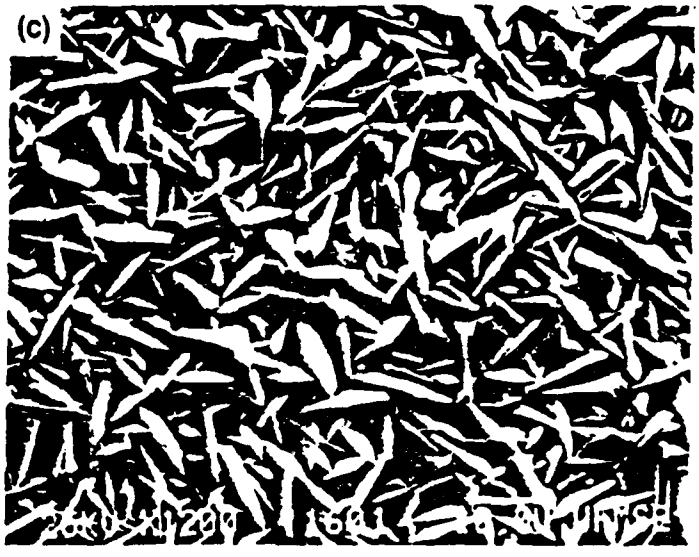
(c)

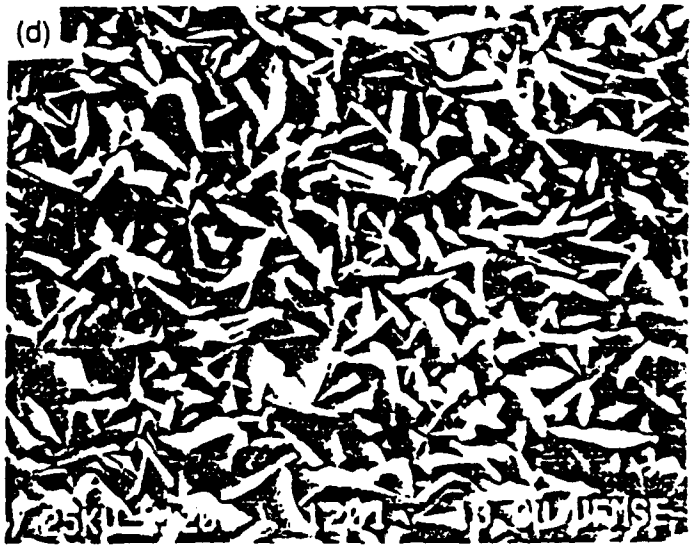
(d)

(e)

(f)

CVD OF TiC_x ON REFRACTORY MATERIALS

M.S. Dariel[1], R. Aparicio[2], T.J. Anderson[2] and M.D. Sacks[1]

[1] Materials Science and Engineering Department
[2] Chemical Engineering Department
University of Florida
Gainesville, FL 32611

Chemical vapor deposition of TiC_x from $TiCl_4$ and CH_4 sources in a H_2 carrier gas was studied on a variety of substrates. Values of apparent activation energies were determined to be 81 kJ/mol for a Ta substrate, 110 kJ/mol for graphite, 121 kJ/mol for Al_2O_3 and 210 kJ/mol for Nicalon. Deposition was reaction limited in the temperature range 1300 to 1500 K. Different preferred grain orientations and surface morphologies were observed on each substrate. The properties of the deposited films were characterized by SEM, XRD and EMPA.

A. INTRODUCTION

TiC_x has been proposed as a matrix phase in hybrid carbon/carbon composites because of its hardness, high melting temperature and resistance to wear (1). These same properties have made TiC_x attractive for applications such as bulk ceramic tools used in industrial cutting technology and, in combination with oxidation resistant Al_2O_3 films, first coatings of fusion reactors (2,3).

Deposition of TiC_x films on refractory materials is of particular interest as a potential reinforcing phase for high temperature ceramic matrix composites. In the present study, the growth rate of TiC_x is reported as a function deposition temperature on a variety of substrates including Si-C-O (Nicalon) fibers, polycrystalline graphite, SiO_2, Al_2O_3, Mo and Ta. The influence of the inlet gas composition on the elemental composition of the films deposited on Nicalon, graphite and Al_2O_3 was measured by EMPA. The surface morphology and grain orientations were characterized as a function of deposition temperature and substrate type.

B. EXPERIMENTAL

TiC_x was deposited on planar substrates in a vertical pedestal type reactor using $TiCl_4$ and CH_4 in H_2 as reactant sources. The pedestal susceptor was made of graphite, and was

heated by a 7.5 kW rf generator. The substrate temperature was measured by both a sheathed type S thermocouple placed in the center of the susceptor and a two-color optical pyrometer focused on the top surface of the substrate through a gas-swept quartz viewport. The reactor was enclosed by a 76 mm diameter quartz tube which was sealed at both ends by water-cooled flanges. The reaction chamber was purged before each deposition by sequential pumping and back-filling with Ar.

Deposition of TiC_x on stacked Nicalon fiber weaves was accomplished by the temperature gradient, forced flow CVI method. The stacks, consisting of 3 weave discs were packed together with a graphite holder and separated from the top of the pedestal susceptor with a graphite ring. Radiation absorption by the stack from the susceptor provided a temperature gradient of approximately 200°C across the stack. As a result, the top layers of the stack (gas inlet) were at a lower average temperature than the bottom layers, thus allowing a reaction front to move in a direction opposite to that of the gas flow. Passage of the gases through weaves was ensured by plugging the reactor wall-susceptor annulus with graphite felt and providing an exit through an axisymetric hole in the susceptor.

All depositions were performed at atmospheric pressure and reactant partial pressures were in the range $7x10^{-3}$ to $2x10^{-2}$ atm for $TiCl_4$ and $1x10^{-2}$ to $2.8x10^{-2}$ atm for CH_4. The H_2 carrier gas flow rate range was 570 to 970 sccm. The deposition temperature was varied in the range 950 to 1270°C and the deposition time varied from 1 to 12 hrs. Substrates consisted of Nicalon 12-harness satin weave cloth preforms, polished graphite, alumina or silica, and high purity Mo or Ta foils.

SEM observations were made on as-deposited coatings, on fracture planes, and on polished cross sections of infiltrated weaves or coated plates, cast in acrylic or epoxide resins. In addition, the coatings were analyzed by XRD and EPMA to obtain information on crystallinity, preferred orientation and elemental composition. For EPMA measurements special care was taken to avoid surface contamination from carbon containing materials used in polishing or other preparation steps.

C. RESULTS AND DISCUSSION

Deposition Rates

The growth rate of TiC_x on various substrates was determined as a function of growth temperature at constant reactant inlet compositions (10 sccm $TiCl_4$, 20 sccm CH_4 and

970 sccm H_2). Since the surface was nonplanar, growth rates were determined by measuring the weight change of the substrate and normalizing by the exposed surface area. The measured weight gain expressed in mg/hr is shown as a function of reciprocal temperature in Figure 1. For all substrates examined, the growth rate was a linear function of inverse temperature. Values of the apparent activation energies were calculated from the results of a linear regression analysis and found to be 81 kJ/mol for Ta, 110 kJ/mol for graphite, 121 kJ/mol for Al_2O_3 and 210 kJ/mol for Nicalon. An apparent activation energy for deposition on Mo was not determined since only 2 growths were performed. No rate data were obtained for SiO_2. Of the substrates used in this study, only graphite has a previously reported atmospheric pressure activation energy (159 kJ/mol) (1,4).

Previous studies on a variety of other substrates as well as the results of this study suggest that deposition of TiC_x is limit[illegible] by heterogeneous reaction (5). An increase in the CH_4 partial pressure was found to increase the TiC_x deposition rate, consistent with previous studies(6). Stjernberg et al. have suggested that deposition occurs by the Langmuir-Hinshelwod adsorption mechanism[6]. In their model $TiCl_4$ undergoes rapid homogeneous thermal decomposition to yield subchlorides which adsorp on one type of site. The decomposition product HCl and CH_4 compete for the available adsorption sites of the second type. Differences in the observed activation energies are attributed to differences in the surface chemistry of different grain orientations (as discussed below) which affect the nucleation mechanism and are determined by substrate type.

Composition of TiC_x Films

The elemental composition of TiC_x films on Al_2O_3, Nicalon and graphite was determined by EMPA. No data was obtained for the films on SiO_2, Ta and Mo.

For both Nicalon and graphite substrates, the C/Ti elemental ratio in the films was in the range 0.91-0.93 at a $CH_4/TiCl_4$ input gas ratio of 2, (partial pressure of $TiCl_4$ = 1 x 10^{-2}) and temperature of 1200°C. Increasing the $CH_4/TiCl_4$ ratio to 3.5 at 1200°C resulted in an C/Ti elemental ratio of 1.07, indicating the formation of free carbon. At 1050°C, the films become richer in Ti, with an elemental ratio of 0.82 at an input gas ratio of 2. As for the TiC_x films on Al_2O_3, the C/Ti ratio remained constant at 0.6 as the input gas ratio and the temperature varied from 0.1 to 1.5 and 1000°C to 1200°C, respectively. Comparison of the experimentally measured compositions with theoretical equilibrium values show

excellent agreement for deposition of TiC_x films on Nicalon and graphite at 1200°C(7). However, neither of the compositions on Nicalon and graphite at 1050°C nor those on Al_2O_3 agree with the equilibrium diagrams.

Surface Morphology and Grain Orientation

The substrates examined in this work have a wide range of chemical compatibility with TiC_x. Graphite is a semimetal and C is a component of the TiC_x solid solution, thus providing a carbon source in addition to the gas phase. Mo and Ta are metals which can form stable compounds with C during the initial stages of growth. Al_2O_3 and SiO_2 are insulators which should be relatively inert in the presence of TiC_x. The properties of Nicalon (Si-C-O) are close to those of SiC and thus similar to TiC_x. As expected, quite dissimilar grain orientations and surface morphologies were observed for different substrates.

The reactor geometry for growth of TiC_x on Nicalon was different than that for other substrates. In this system a temperature gradient was imposed across the stack and significant mass transfer limitations were present in the inner portions of the stack. As the deposition temperature increased from 1000°C to 1200°C, the structure of TiC_x grown on Nicalon fibers changed (Figure 2 a-d) from pyramidal needles 0.2 - 1 μm in size to more rounded, equiaxed grains smaller than 0.2 μm. Fracture sections of coatings showed the grains grown at the lower temperature were columnar and aligned perpendicularly away from the fiber surface (Figure 3). X-ray patterns of all TiC_x films on Nicalon show a random orientation of the crystals despite the variety of microstructures.

Nodular growths were observed on fibers directly facing the gas inlet orifice. In these growths, locally accelerated deposition occurs in spite of the overall lower growth temperature of the fibers on which the gas stream is impinging. Features of these growths are markedly different from the regular type of growth observed on most of the fiber surface, and they consist of blocky crystals with step-ledge like features as shown in Figure 4 a-b. Since no mass transfer limitation was believed to exist on this exposed plane, these growth features are not attributed to local gas phase disturbances but rather to a nucleation phenomenon(8). A possible explanation is related to deposition of powdery, purplish colored titanium subchloride particles on the cold reactor walls in depositions with a $CH_4/TiCl_4$ ratio of 2. Particles above the sample apparently became dislodged and settled onto the upper layer of the stack, thus providing

different nucleation sites that develop into the nodular growths. This explains why no such growths were found when very little subchloride deposition was observed on the reactor walls ($CH_4/TiCl_4$ inlet molar ratio was increased to 7/2).

At deposition temperatures above 1200°C, a third type of growth feature was observed on the fibers located in between the graphite holders. In this region the gas flow was greatly restricted. While the fine grained TiC_x structure on the Nicalon surface was retained (Figure 5), whiskers, 10-15 microns long with an aspect ratios of about 10, were also grown. In their study of Ni-catalyzed TiC_x deposition, Wukulski et al. have reported whisker growth to occur at low reactant concentrations and system pressures (9). Apparently TiC_x whisker growth on Nicalon is promoted by reactant depletion effects within the restricted regions inside the graphite holder. Despite these marked dissimilarities in surface morphology, the X-ray diffraction spectra of both the low and the high temperature forms of TiC_x grown on Nicalon are identical and correspond to that of randomly oriented TiC_x, (Figure 6a).

For CVD of TiC_x on graphite more conventional dome-shaped structures were obtained. Magnification of films grown below 1000°C showed small needle-like aggregates 0.1 by 1 μm in size (Figure 7a). X-ray diffraction results indicated these needles were of random orientation (Figure 6b). TEM analysis of the needle showed them to be composed of grains with very diffuse, weakly defined boundaries, less than 30 nm in size. As the temperature of deposition was increased, their shape became more rounded and equiaxed grains appear (Figure 7b). As the growth temperature was further increased to 1200°C, the crystal edges grew sharper, forming blocky, faceted stacks 5-15 μm in size (Figure 7c,d). Simultaneously, the (220) diffraction line became much stronger (Figure 6c). Lee and Chun studied the deposition of TiC_x on WC-12Co substrates using the same deposition chemistry as this study. They reported the preferred orientation of the films to be independent of deposition time and gas phase composition (10). In addition, they observed a very similar trend in orientation; a random orientation at 1050°C changing to (220) between 1100°C and 1150°C.

TiC_x films deposited on fused silica at 1000°C were weakly adhered to the substrate. SEM analysis of the films revealed heaps of knobby, small (< 0.1 μm) amorphous-like particles covering larger, faceted crystallites (Figure 8). The X-ray diffraction peaks were broader, indicating amorphous areas (Figure 6d). Preliminary TEM measurements showed randomly oriented grains, up to several microns in size, with well developed boundaries. The randomness of grain orientation is

also confirmed by the XRD pattern.

The effect of growth temperature on the morphology of the TiC_x grown on alumina tended to be the reverse as that observed on other substrates. As the temperature increased from 1200°C (Figure 9a) to 1300°C (Figure 9c) the TiC_x grains change from a round, faceted shape to a more elongated form. The reactant composition, however, had the opposite effect. Figure 9b-d shows the microstructure of TiC_x grown at different values of $CH_4/TiCl_4$ gas inlet ratios. The grains changed in the previously observed pattern from a needle-shaped to round, equiaxed crystals. X-ray analysis showed (111) preferred orientation.

CVD of TiC_x on the metals Mo and Ta produced wedge shaped, sharply defined crystallinities at a lower growth rate than on the other substrates (Figure 10a,b). X-ray diffraction results for TiC_x grown on Mo at 1150°C (Figure 6e) show that the (220) line is enhanced; the ratio of peak intensities (220)/(220) has the value of 7 compared to the value 0.6 for the random powder (Figure 6h). At 1200°C growth temperature, the ratio of peak intensities decreased to a value of 0.2 (Figure 6f). This behavior is opposite to that observed for deposition on graphite. The x-ray diffraction spectrum at 1200°C also shows weak Mo_2C lines which is formed during the initial stages of deposition by reaction between the substrate and CH_4. Similar behavior was observed for deposition on Ta substrates with the reaction product TaC forming adjacent to the substrate. The X-ray diffraction analysis shows the (220) lines as dominant, suggesting random orientation, though the (311) line was also strongly enhanced (Figure 6g).

D. SUMMARY

The deposition of TiC_x on a variety of refractory substrates using a chloride chemistry was limited by heterogeneous reaction at a temperature near 1200°C. Values of the apparent activation energies ranged from 81 kJ/mol for Ta to 210 kJ/mol for Nicalon. Under identical growth conditions the morphology and grain orientations were strongly influenced by substrate type and growth temperature. Random grain orientations were deposited on Nicalon, SiO_2 and at low temperature, on graphite. A preferred orientation was observed on Al_2O_3 (111), Ta (311), Mo (220) at low temperature, and graphite (220) at high temperature.

ACKNOWLEDGEMENTS

This work was supported by the Defense Advanced Research Project Agency under Navy grant No. MDA972-88-J-1006.

REFERENCES

1. J.Y. Rossignol, F. Langlais and R. Naslain, Proc. 9th Int. Conf. on CVD, 596 (1985)

2. D.G. Kim, J.S. Yoo and J.S. Chun, Thin Solid Films, 165, 149(1988).

3. M. Okada, Thin Solid Films, 108, 373(1983).

4. L. Agour, E. Fitzer and J. Schlichting, Proc. 5th Int. Conf. on CVD, 600(1975).

5. J.N. Lindstrom and S. Aubrey, Proc. 4th Int. Conf. on CVD, 115(1973).

6. K.G. Stjernberg, Thin Solid Films, 40, 81(1977).

7. C. Bernard, M. Ducarrior and F. Teyssandier, J. Less-Common Metals, 78, 269-274(1981).

8. W.R. Holman and F.J. Huegel, J. Vac. Sci. Technol., 11, 701(1974).

9. L. Wokulski and, K. Wokulska, J. Crystal Growth, 62, 439 (1983).

10. C.W. Lee and J.S. Chun, Proc. 8th Int. Conf. on CVD, 563(1981).

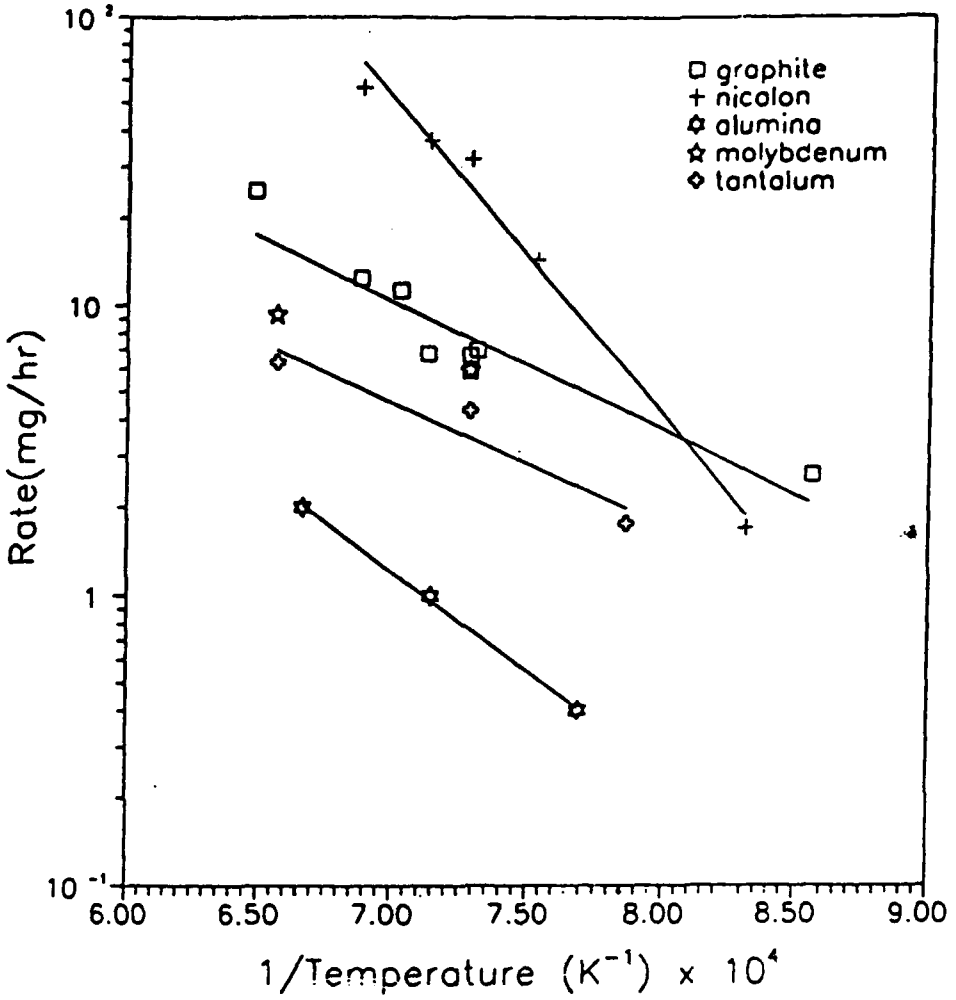

Fig. 1. Growth rate of TiC_x on various substrates as a function of reciprocal temperature.

Fig. 2. Effect of temperature on the microstructure of TiC_x on Nicalon (Si-C-O) fibers. Temperature varied from 1000°C to 1200°C.

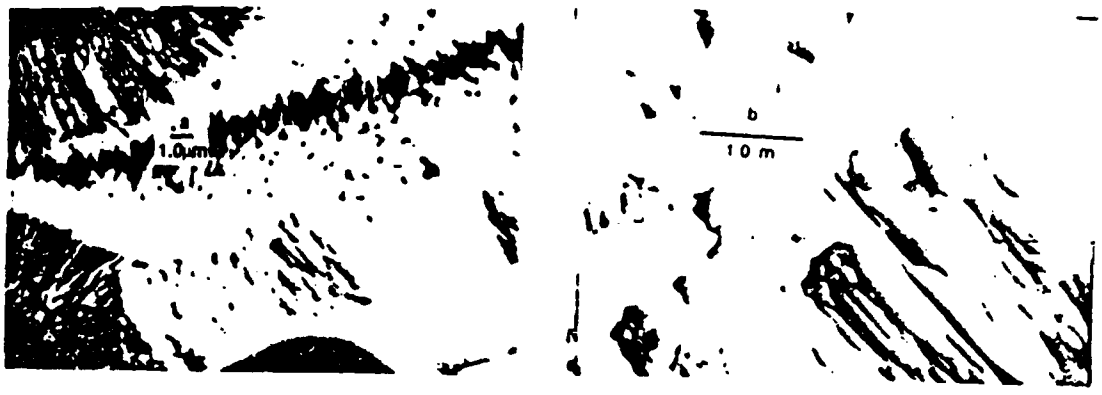

Fig. 3. Microstructure of TiC_x on Nicalon at 1000°C.

Fig. 4. Nucleation nodes of TiC_x on Nicalon.

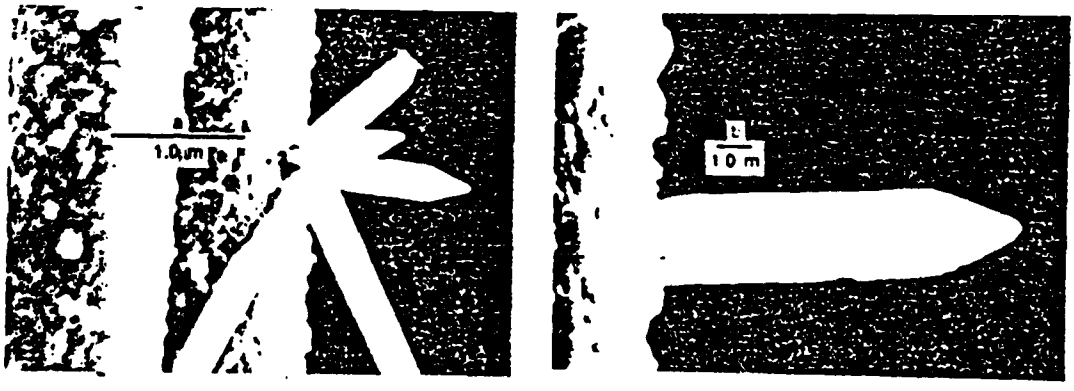

Fig. 5. TiC_x whiskers resulting from reactant depletion.

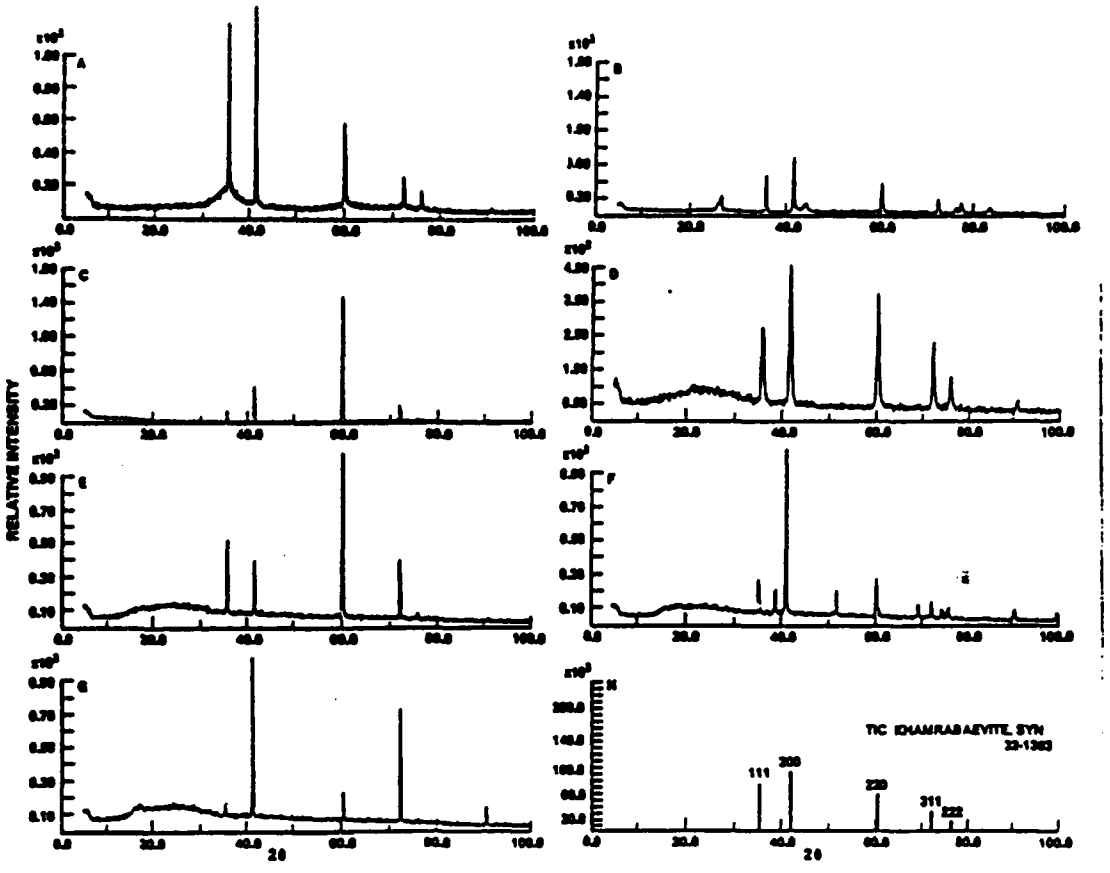

Fig. 6. X-ray diffraction patterns of TiC_x on: a) Nicalon (1000-1200°C), b) Graphite (1000°C), c) Graphite (1200°C), d) Silica (1000°C), e) Molybdenum (1150°C), f) Molybdenum (1200°C), g) Tantalum (1150°C), h) Standard powder pattern.

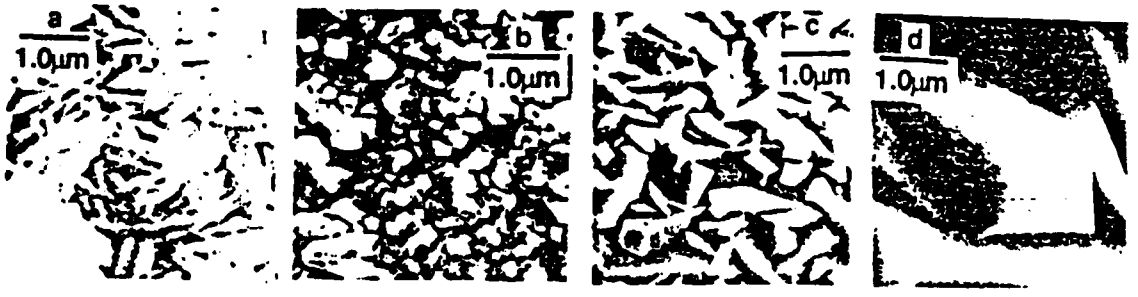

Fig. 7. Microstructure of TiC_x on Graphite at: a) 1000°C, b) 1100°C and c) and d) 1200°C.

Fig. 8. Microstructure of TiC_x on Silica.

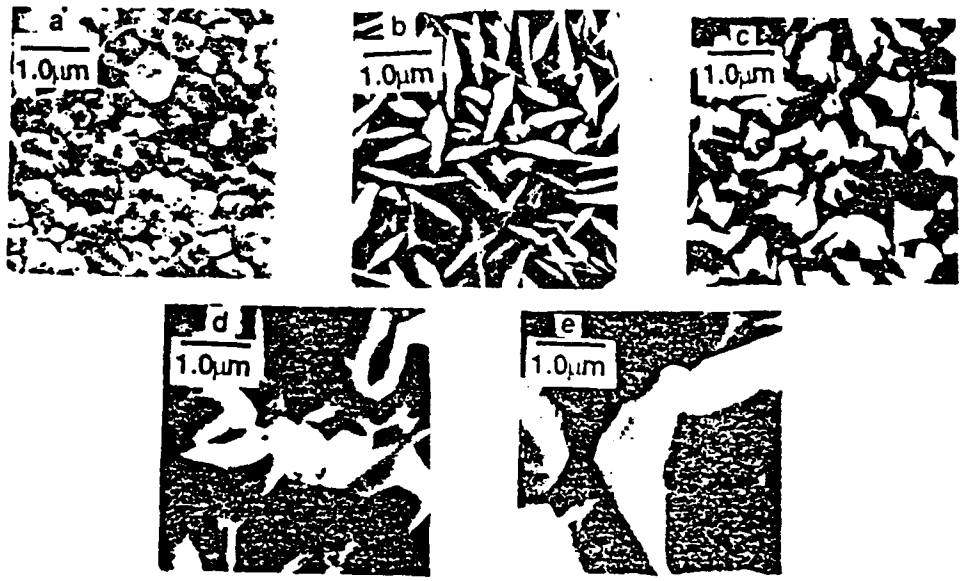

Fig. 9. Microstructure of TiC_x on Alumina at: a) 1200°C and $CH_4/TiCl_4$= 1.0, b) 1300°C and $CH_4/TiCl_4$= 0.5, c) 1300°C and $CH_4/TiCl_4$=1.0, d) 1300°C and $CH_4/TiCl_4$=3, e) 1300°C and $CH_4/TiCl_4$=4.0.

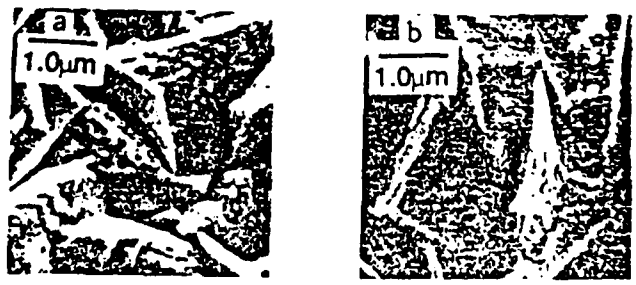

Fig. 10. Microstructure of TiC_x on a) Molybdenum, b) Tantalum.

CVD OF TiC_x ON SINGLE CRYSTAL Al_2O_3

R.A. Aparicio[1], E.F. Allen[1], T.J. Anderson[1], and M.D. Sacks[2], [1]Department of Chemical Engineering and [2]Department of Materials Science and Engineering, University of Florida, Gainesville, FL 32611

ABSTRACT

The kinetics of chemical vapor deposition of TiC_x from CH_4 and $TiCl_4$ sources on single crystal Al_2O_3 were investigated. Experimental growth rates show an Arrhenius dependence on deposition temperature, with apparent activation energies of 296 KJ/mol on (0001) Al_2O_3 and 328 KJ/mol on $(1\bar{1}02)$ Al_2O_3. The growth rate was also found to have a linear dependence on the CH_4 partial pressure. Various grain orientations were observed in the films depending on the deposition temperature, deposition thickness, and substrate orientation. The measured grain orientations, however, were independent of the CH_4 partial pressure.

INTRODUCTION

TiC_x is a material with high strength and hardness, high melting temperature, and good resistance to wear and oxidation. These properties make TiC_x an attractive candidate as a matrix phase in ceramic-ceramic composites. The use of TiC_x in such applications has, however, received only recent attention.[1] Chemical vapor infiltration (CVI) is a useful technique to densify ceramic composites, particularly for systems such as fiber reinforced composites. CVI of TiC_x into ceramic preforms should also be feasible given the similarity of deposition chemistry and recent successes demonstrated for SiC.[2,3,4]

Successful CVI requires that reaction-limited deposition conditions be approached. Thus, an understanding of the kinetics regulating the deposition process, particularly in isolation from mass transfer effects, would be useful in designing suitable CVI reactors and in specifying appropriate operating conditions. In this study, the kinetics of TiC_x deposition on flat Al_2O_3 substrates were investigated in the reaction-limited regime. The influence of the temperature, substrate orientation, and CH_4 partial pressure on the deposition rate is reported. In addition, the coatings were characterized by X-ray diffraction (XRD), electron microprobe analysis (EMPA), and scanning electron microscopy (SEM) to determine the effect of the above parameters on the grain orientation, composition, and surface morphology.

EXPERIMENTAL

The experimental system used to deposit the TiC_x films has been previously described.[5] The films were deposited simultaneously on flat single crystal (0001) and (1$\bar{1}$02) Al_2O_3 substrates.* All depositions were carried out at atmospheric pressure. The methane (CH_4) partial pressure varied from 250 to 4050 Pa, while the titanium tetrachloride ($TiCl_4$)** partial pressure was held constant at 1010 Pa. Hydrogen was used as the carrier and diluent gas in the atmospheric pressure reactor. The total gas flow rate ranged from 4 to 250 std. cm^3/s, and deposition time varied from 1 to 4 hours. Experiments were performed in the temperature range of 1278-1383 K. The deposition temperature was measured with a dual-wavelength (ratio) optical pyrometer focused on the surface of the substrate.

RESULTS AND DISCUSSION

Effect of Deposition Parameters on the Deposition Rate

The influence of the total flow rate on the growth rate was investigated at 1383 K. The rate was observed to increase with flow rate to approximately the one-half power, up to 17 std. cm^3/s. For higher flows, the rate remained constant at values determined by the temperature and reactant gas partial pressures. This result indicates that the boundary between the mass-transfer and reaction-controlled regimes is somewhat less than 17 std. cm^3/s total flow rate. The growth of TiC_x should therefore be reaction-limited for temperatures less than 1383 K and total flow rates greater than or equal to the above value.

The temperature dependence of the deposition rate was determined at constant reactant partial pressures of 2030 Pa for CH_4 and 1010 Pa for $TiCl_4$ and a total flow rate of 17 std. cm^3/s. In order to quantify the apparent rate of deposition, the weight increase of the substrates was measured as a function of time for various temperatures (Fig. 1) and the growth rate was obtained from the slope of the weight change curve. For both substrate orientations, the growth rate followed an Arrhenius dependence on temperature (Fig. 2). The calculated apparent activation energies were 296 KJ/mol (±142 KJ/mol) for (0001) Al_2O_3 and 328 KJ/mol (±128 KJ/mol) for (1$\bar{1}$02) Al_2O_3. These activation energies are nearly 2.5 times higher than those reported for hot pressed polycrystalline Al_2O_3.[5]

The effect of CH_4 partial pressure is shown in Fig. 3. The deposition temperature and the $TiCl_4$ partial pressure were held constant at 1383 K and 1010 Pa, respectively. The slope of the curve is 1.06, indicating first-order

---

* Commercial Crystal Laboratories, Inc., Naples, Florida.

** Fisher Scientific, Fair Lawn, NJ. 98.0% purity reported by the manufacturer.

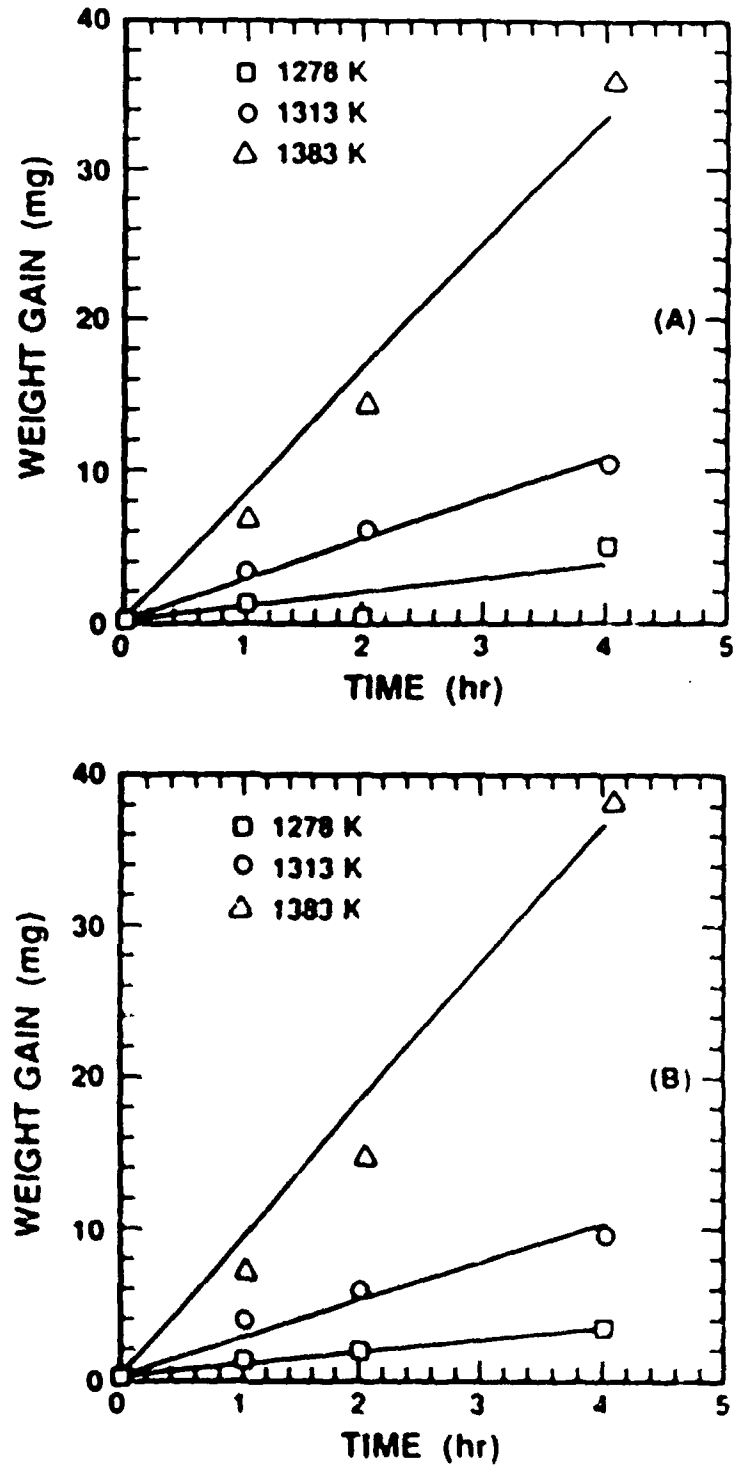

FIG 1 Weight of TiC, deposited on (A) (0001) and (B) $(1\bar{1}02)$ Al_2O_3 as a function of deposition time.

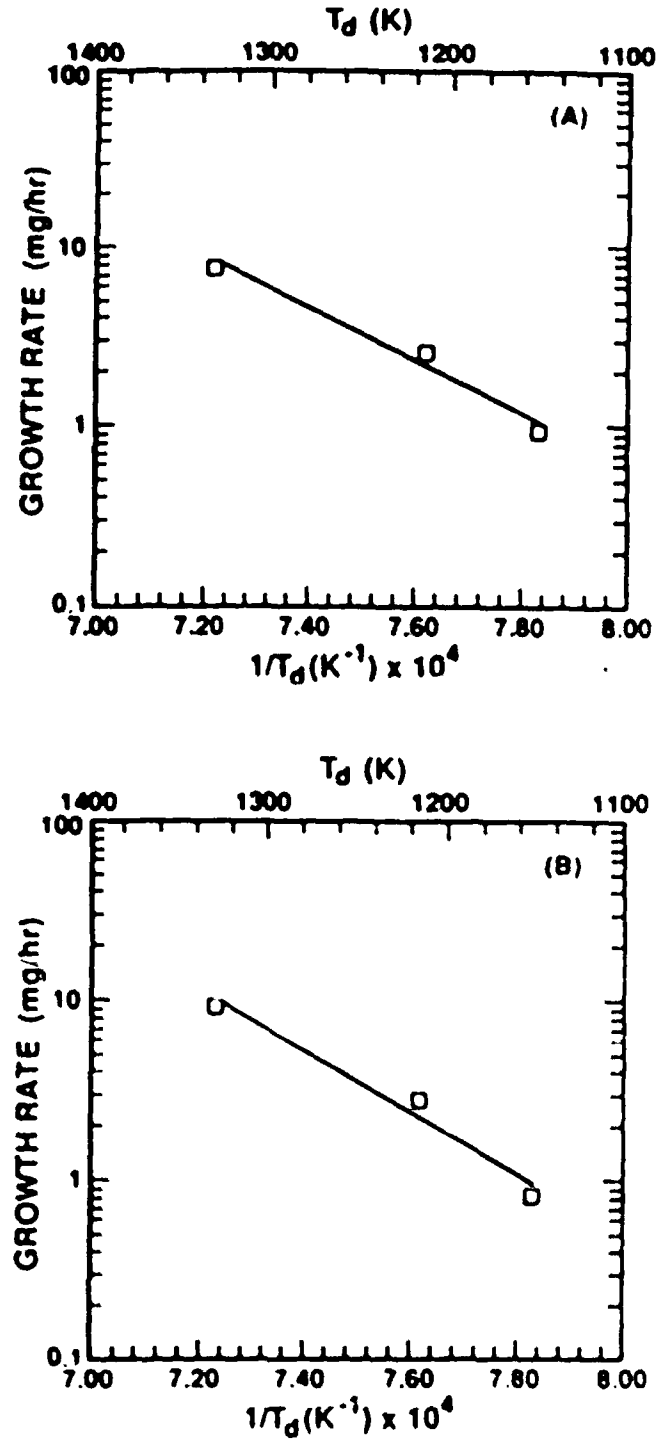

FIG. 2. Arrhenius plots of the TiC$_x$ growth rate on (A) (0001) and (B) (1$\bar{1}$02) Al_2O_3 as a function of temperature

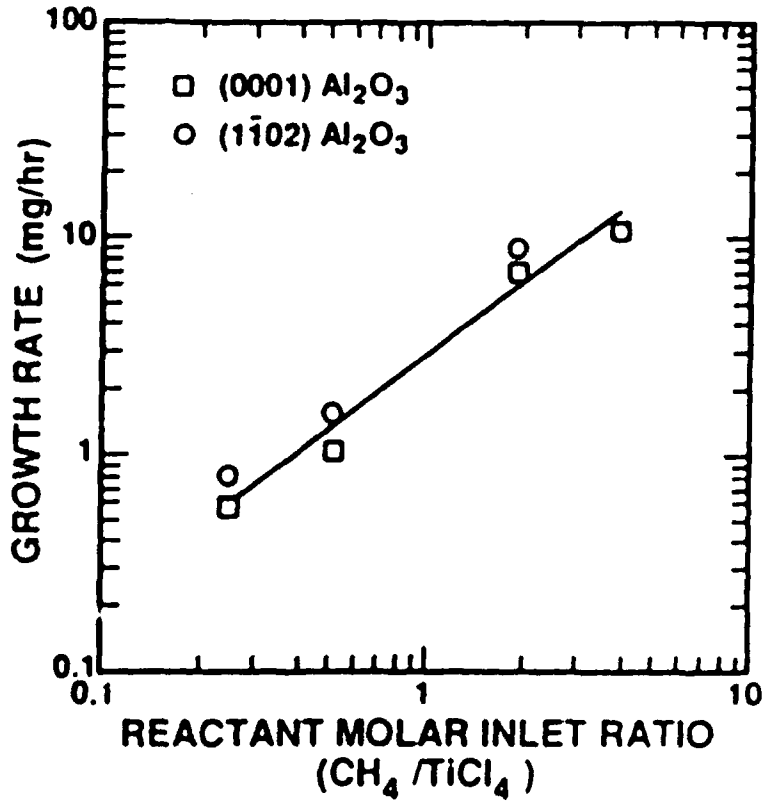

FIG. 3. TiC_x growth rate as a function of the ratio of CH_4 to $TiCl_4$ in the inlet gas. The $TiCl_4$ partial pressure was held constant at 1010 Pa.

dependence of the deposition rate on the CH_4 partial pressure. This result is consistent with work by Stjernberg et al.,[8] who proposed a Langmuir-Hinshelwood mechanism in which the growth rate also follows a first order dependence on the CH_4 partial pressure. Because of this trend, CH_4 decomposition has been postulated as the rate-limiting step in the deposition of TiC_x. For comparison, the above activation energies are in agreement with the activation energy of homogeneous CH_4 pyrolysis at 2273 K (312 KJ/mol).[7]

Surface Morphology, Grain Orientation, and Film Composition

Figure 4 shows the morphological evolution of the coatings on (0001) Al_2O_3 as the temperature was varied from 1278 to 1383 K. The grain size increased with temperature and the grain shape changed from a globular to a faceted structure, presumably caused by an increase in growth rate. A similar trend was observed for the coatings on (1$\bar{1}$02) Al_2O_3.

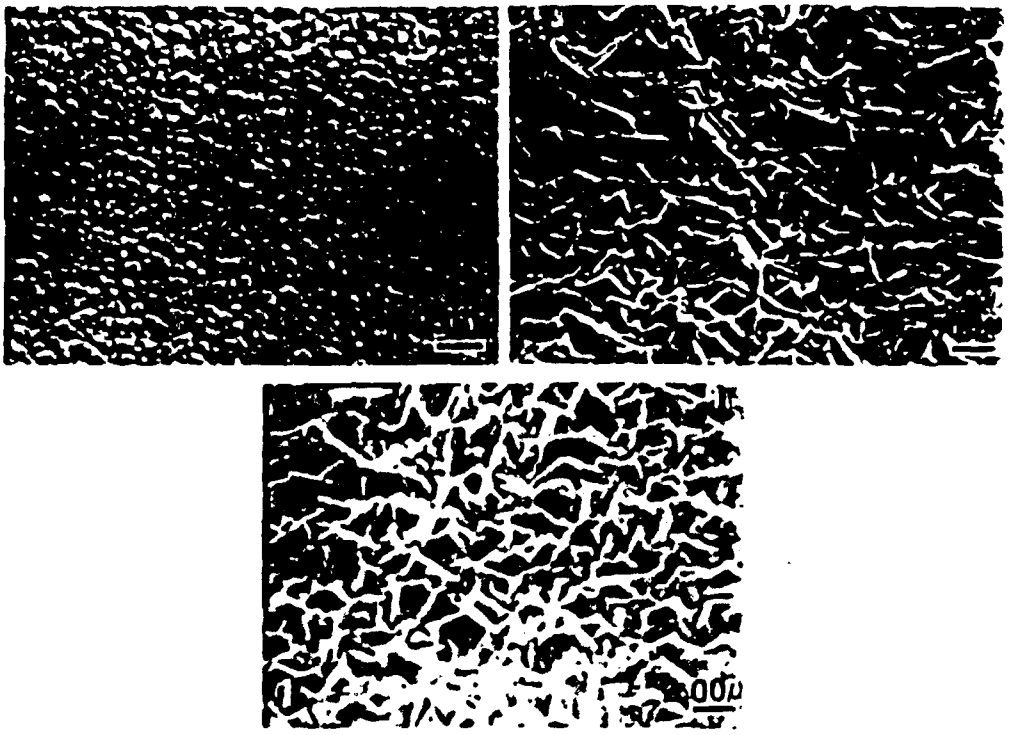

FIG. 4. Microstructure of TiC_x on (0001) Al_2O_3 at: (A) 1273 K, (B) 1323 K, and (C) 1373 K.

The effect of the CH_4 partial pressure on the surface morphology of the films (Fig. 5) is similar to the temperature effect (Fig. 4). There is an increase in grain size; however, the grain shape remains unchanged. Once again, this trend is the same for both Al_2O_3 substrate orientations.

Each film displayed a strong preferred orientation which varied with substrate orientation, deposition time, and deposition temperature (Table 1). For long deposition times and higher growth temperatures, the coatings appeared to be oriented in directions of highest atomic packing. Grain orientations did not, however, vary with CH_4 partial pressure.

The measured film composition remained constant (C/Ti = 0.52 ±0.05) as the ratio of CH_4 to $TiCl_4$ partial pressures in the inlet gas was varied from 0.25 to 4.0. The apparent independence of the film composition on the inlet gas concentration ratio is attributed to the errors in the EMPA measurement, caused by the film surface roughness. Improvement in the measurement could not be achieved by polishing due to poor adhesion of the film to the substrate.

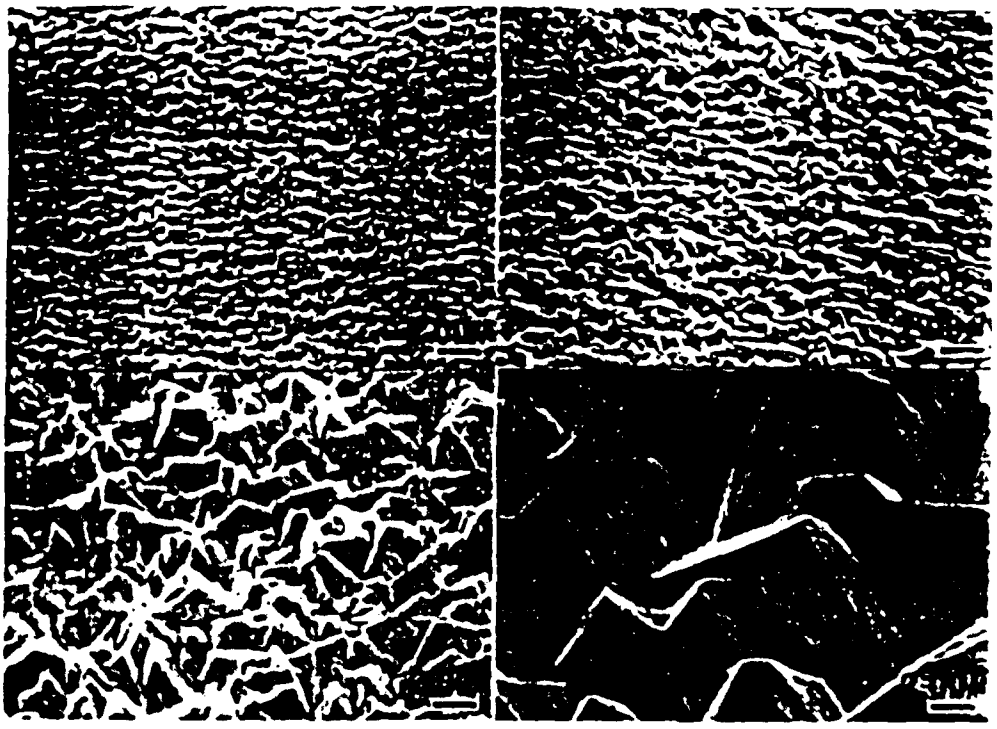

FIG. 5. TiC, microstructures on $(1\bar{1}02)$ Al_2O_3 for various $CH_4/TiCl_4$ ratios: (A) 0.25, (B) 0.50, (C) 2.00, (D) 4.00. $TiCl_4$ partial pressure was constant (1010 Pa)

TABLE 1. Preferred Orientation of TiC, Films as a Function of Substrate Orientation, Deposition Time and Temperature

Substrate Orientation: (0001)

Deposition Temperature (K)	Deposition Time (hr)		
	1	2	4
1278	(200)	(200)	(111)
1313	(111)	(111)	(220)
1383	(111)	(111)	(111), (220)

Substrate Orientation: $(1\bar{1}02)$

Deposition Temperature (K)	Deposition Time (hr)		
	1	2	4
1278	(200), (111)	(200), (111)	(111)
1313	(200), (311)	(200), (311)	(200)
1383	(200)	(220)	(220)

SUMMARY

The deposition rate of TiC_x on single crystal Al_2O_3 from CH_4 and $TiCl_4$ sources followed an Arrhenius dependence on growth temperature, with activation energies of 296 KJ/mol to 328 KJ/mol for (0001) and (1$\bar{1}$02) substrate orientations, respectively. The deposition rate was also a linear function of the CH_4 partial pressure. Reaction-limited growth could be achieved at flow rates greater than or equal to 17 std. cm^3/s, below which the rate depended on the total gas velocity. Grain orientations were affected strongly by the substrate orientation, deposition time, and deposition temperature. As the thickness of the film increased, orientations along planes of highest atomic packing, i.e., (111) and (220), became dominant.

ACKNOWLEDGEMENTS

This work was supported by the Defense Advanced Research Projects Agency under Navy grant No. MDA972-88-J-1006. The authors would also like to thank Pete Axson, Juan Casero, and Amy Hoelzer for their assistance.

REFERENCES

1. J.Y. Rossingnol, F. Langlais, and R. Naslain, "A Tentative Modelization of Titanium Carbide C.V.I. Within the Pore Network of Two-Dimensional Carbon-Carbon Composite Preforms," Electrochem. Soc. Proc. 9th Int. Conf. on Chemical Vapor Deposition, 596-614 (1984).

2. D.P. Stinton, A.J. Caputo, R.A. Lowden, and T.M. Besmann, "Improved Fiber-Reinforced SiC Composites Fabricated by Chemical-Vapor Infiltration," Ceram. Eng. Sci. Proc., 7 (7-8) 983-989 (1986).

3. D.P. Stinton, A.J. Caputo, and R.A. Lowden, "Synthesis of Fiber-Reinforced Silicon Carbide Composites by Chemical Vapor Infiltration," Am. Ceram. Soc Bull., 65 (2) 347-350 (1986).

4. W.J. Lackey, "Review, Status, and Future of the Chemical Vapor Infiltration Process for Fabrication of Fiber-Reinforced Ceramic Composites," Ceram Eng. Sci. Proc., 10 (7-8) 577-584 (1989).

5. R. Aparicio, J.L. Ponthenier, F. Hong, T.J. Anderson, M.D. Sacks and G. Johnson, "Chemical Vapor Deposition of TiC, on Al_2O_3 Substrates," Ceram Eng. Sci. Proc., 10 (9-10) 1462-1471 (1989).

6. K.G. Stjernberg, "The Rate of Chemical Vapor Deposition of TiC," Thin Solid Films, 40 81-88 (1977).

7. W.C. Gardiner, Jr., J.H. Owen, T.C. Clark, J.E. Dove, S.H. Bauer, J.A. Miller, and W.J. McLean, "Rate and Mechanism of CH_4 Pyrolysis from 2000°C to 2700°C," Symp. Int. Combust. Proc., 15 857-868 (1975).